Mathematical Model of the Forced Cooling of Anodes used in the Aluminium Industry

A thesis presented in partial fulfilment of
the requirements for the degree of
Master of Science
in Mathematics
at Massey University

Christopher Charles Palliser
May 1994

ABSTRACT

The aluminium industry consumes large amounts of electrodes, especially anodes, to operate the smelters. These anodes must be baked at high temperatures in order to give them certain mechanical and electrical properties, after which they are cooled. Baking is done in large furnaces made up of pits inside which the anodes are placed in layers and surrounded by packing coke. The furnaces are of two types - open and closed. In a closed furnace, the pits are lined with refractory bricks inside which flues run vertically and large covers are used to close over parts of the furnace.

This thesis presents a mathematical model of part of a forced cooling section of a closed furnace, where air is being sucked or blown through the flues by fans, so that the anodes cool more rapidly. Both one- and two-dimensional models are developed in order to calculate the transient temperature distribution in the anodes, packing coke and side flue wall. For the two-dimensional model, the transient temperature and pressure distributions of the air in the side wall flues and fire shafts are also calculated. After exploring an analytical method for the one-dimensional case, numerical techniques are used thereafter.

Given initial block and air temperatures, the two-dimensional model allows calculation of the appropriate temperature and pressure distributions for various mass flows of air in the side wall flues and fire shafts. The results show that for a sufficiently high mass flow, the anodes can be cooled enough so that they can be safely removed from the pits after three fire cycles (the length of time the anodes are exposed to forced cooling).

ACKNOWLEDGEMENTS

This thesis is dedicated to my wife, Alataua. Without her love, patience, encouragement, hard work and prayers over the last five years, none of this would have been possible. Fa'afetai lava la'u pele.

My love and thanks to my parents, Ray and Trixie, who never lost faith in me and have given me so much. Lots of alofa and kisses for my children, Matthew, Carissa, Joshua, Susan and Samuel.

My special thanks to my supervisor, Dr R. McKibbin, for his expertise, guidance and patience.

I am also grateful to Professor G. C. Wake and other colleagues in the Department of Mathematics for their encouragement and support.

I thank New Zealand Aluminium Smelters Ltd for the scholarship. Thanks to Mr R. Braithwaite and his colleagues for their assistance and hospitality.

This thesis script has been typed by Mrs G. Tyson, whose skill and care I gratefully acknowledge.

Thank you to my sisters, brothers-in-law and families: Ruth and Ian Campbell, Claire and Peter Bruin, Catherine and Peter Kelly and Keneti Faulalo. Thanks Peter Bruin for your expert assistance with the computer.

I also thank my friends who have supported and prayed for me, especially Haig and Pam Thomson, Bill and Felicity Kimberley, Tony and Maraia Statham.

CONTENTS

NOMENCLATURE

Alternative uses are separated by a semi-colon. Dimensions are in square brackets.

A, B	defined functions
A_n , B_n, C_n, D_n	constants
a, b, c, d, e, f	lengths associated with a flue and a flue wall [m]
Bi	Biot number [–]
c_m, m = 1 to 9	constants
c_p, cf_p	specific heat capacity at constant pressure of the block and the fluid or air [J/kg K]
ca_p, cp_p, cw_p	specific heat capacity at constant pressure of the anode, packing coke and flue wall [J/kg K]
E, e	total and internal energy per unit mass of the block [J/kg]
ea, ep, ew	internal energy per unit mass of the anode, packing coke and flue wall [J/kg]
estTf	estimated fluid temperature [K]
F, f	defined functions
Fo, $\hat{Fo}$	Fourier [–] and 'hatted' Fourier number of the block [1/K]
Foa, Fop, Fow	Fourier number of the anode, packing coke and flue wall [–]
G	defined function
h	enthalpy per unit mass of the block [J/kg]; heat transfer coefficient [W/m^2K]
hc, hr	heat transfer coefficient for convection and radiation [W/m^2K]
k	thermal conductivity of the block [W/mK]; real constant
ka, kp, kw	thermal conductivity of the anode, packing coke and flue wall [W/mK]
kf	thermal conductivity of the fluid [W/mK]

ℓ	characteristic length [m]
L_x	width of the block [m]
L_y	depth of the block [m]
$\dot{m}$	mass flow of the fluid [kg/s]
max.	maximum
min.	minimum
Nu	Nusselt number [–]
p	pressure in the block; pressure of the fluid or air [N/m^2]
percentdiff	percentage difference between fluid temperatures
pfl, pfs	pressure of the fluid in a flue and a fire shaft [N/m^2]
Pr	Prandtl number [–]
$\dot{Q}$	rate of heat flow per unit area of the block [J/sm^2]
$\dot{Q}w$	rate of heat flow per unit area at the flue wall [J/sm^2]
Re	Reynolds number [–]
S	surface of an elemental volume in the block [m^2]
T	temperature of the block [K]
t	time [s]
Ta, Tp, Tw	temperature of the anode, packing coke and flue wall [K]
Tf	fluid or air temperature [K]
V	elemental volume in the block or a flue [m^3]
v	velocity of the fluid [m/s]
W	width of a 'large' flue [m]
X	defined function
x, y, z	spatial coordinates

Greek

α, $\hat{\alpha}$	thermal diffusivity [m^2/s] and 'hatted' thermal diffusivity of the block [m^2/sK]
αa, αp, αw	thermal diffusivity of the anode, packing coke and flue wall [m^2/s]
Γ_1 , Γ_2	defined functions
Δp	change in the pressure of the fluid; pressure difference across a fan [N/m^2]
ΔQ	heat transferred from the block in time Δt [J]
ΔQa, ΔQp, ΔQw	heat transferred from the anode, packing coke and flue wall in time Δt [J]
ΔQf	heat gained by the fluid or air in time Δt [J]
Δt	overall time step length [s]
Δta, Δtp, Δtw	length of time step in the anode, packing coke and flue wall [s]
Δx	distance between mesh points in the x-direction [m]
Δxa, Δxp, Δxw	distance between mesh points in the anode, packing coke and flue wall [m]
Δy	distance between mesh points in the y-direction [m]
ε	emissivity of the flue wall [–]; roughness of the flue wall [m]
Θ_1 , Θ_2 , Θ_3, θ	defined functions
Λ_1, Λ_2, Λ_3	defined functions
λ	real constant; defined function; friction factor [–]
μ	dynamic viscosity of the fluid [kg/ms]
ρ	density of the block [kg/m^3]
ρa, ρp, ρw	density of the anode, packing coke and flue wall [kg/m^3]
ρf	density of the fluid [kg/m^3]

σ	Stefan-Boltzmann constant [W/m^2K^4]
τ	integration variable
ψ	defined function

Subscripts

i, i = 1 to Nx	mesh points in the x-direction
j, j = 1 to Ny	mesh points in the y-direction
p	constant pressure [N/m^2]
q, q = 1 to Nxa	mesh points in the x-direction in the anode
r, r = 1 to Nxp	mesh points in the x-direction in the packing coke
s, s = 1 to Nxw	mesh points in the x-direction in the flue wall
w	flue wall
n	natural number

Superscripts

n	time steps, n = 1 to Nt

CHAPTER 1 INTRODUCTION

1.1 Background

The aluminium industry consumes large amounts of electrodes, especially anodes, to operate the smelters. These carbon anodes are made of petroleum coke held together by a pitch binder. They must be baked to a given temperature, approximately 1200 °C, following a given temperature profile (no more than 10 -15 °C/hour) in order to end up with the required mechanical and electrical properties. Baking is done in large furnaces made up of pits inside which the unbaked anodes are placed in layers and surrounded by packing coke. These furnaces are of two types, one of which is the Riedhammer (vertical ring, or closed) furnace, a schematic of which is shown in Figure 1.1.

In the Riedhammer furnace, the pits are lined with refractory bricks inside which flues run vertically and large covers are used to close over parts of the furnace. A typical Riedhammer furnace consists of two or three fire trains grouped together on a rectangular shaped ring. As shown in Figure 1.1, each fire train comprises about fourteen sections, or sets of pits, and consists of three zones - preheat, fire and cooling zone. Hot combustion gases flow through the flues in the fire and preheat zones, whilst air flows through the flues in the cooling zone.

The cooling zone is divided into two parts - natural and forced cooling. In the natural cooling part, the anodes are just left to cool. The forced cooling sections have big fans which either blow or suck air through the flues to increase the rate of cooling of the anodes (see Figure 1.1). There is one fan per section. The rate of cooling is not constrained and may be done as quickly as possible. The fans, fire ramps and exhaust manifold are moved in the fire direction by one section every 32 or 36 hours. This time period is called the fire cycle.

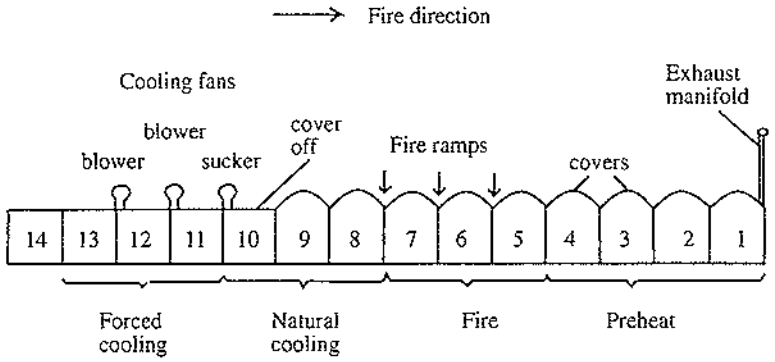

Figure 1.1
A schematic longitudinal view of a typical fire train arrangement in a Riedhammer furnace at NZ Aluminium Smelters Ltd (see Bourgeois *et al.*, 1990).

1.2 Previous work

Mathematical modelling of ring furnaces started seriously in 1980 with Furman and Martirena (1980). Since then others have developed different aspects of ring furnace (open and closed) mathematical modelling. The advent of computational fluid dynamics packages has enabled the development of more elaborate models. Due to the ring furnace's large dimensions and time constant ($2\frac{1}{2}$ - 3 weeks), experimentation on a real furnace is not only impractical, but also risky, lengthy and costly. Hence the need for mathematical models in order to analyse and predict performance.

Furman and Martirena (1980) used a three-dimensional finite difference model. The total duration of the baking cycle was simulated. Therefore the time period was long, 300 - 400 hours. In order to save computation time, most of the time steps used were correspondingly long. The first 10 hours were divided in steps of 0.1, 0.2, 0.5, 2.2, 3.0 and 4.0 hours, all further steps were 7.0 hours long. To ensure the stability of the calculations with these long temporal steps, an implicit Crank-Nicholson scheme was used. The equations were solved using successive relaxation. 960 nodes were used - 4 in the y-direction (x-direction in this thesis), 20 in the z-direction (y-direction in this thesis) and 12 in the x-direction (z-direction in this thesis). A 'sensitivity' analysis was performed. This involved introducing a significant variation of a

given property and observing the corresponding temperature calculations. It was found that the thermal conductivity of the packing coke and the vertical gradient of the gases' temperature along the flues were the parameters which decisively influenced the calculations. It was claimed, therefore, that these were the only parameters which needed to be known accurately. The temperature-dependent thermal properties of the anodes, packing coke, flue walls and gases were not adjusted as the temperature varied.

The paper by de Fernández *et al.* (1983) used the identical set of nodes as used in the paper of the previous paragraph, so it was a three-dimensional model. However, no mention was made of the solution method. Initially the temperature difference between the top and bottom layer of anodes in a pit was calculated. It was found that this difference was in much closer agreement with the experimental difference, when the thermal properties of the anodes, packing coke and flue walls were adjusted according to the temperature reached at the end of the last time step. The 'negative' image of the heating temperature distribution was used to try and model the cooling temperature distribution. It did not work and this was attributed to two factors, one of which was the occurrence of natural convection. It was suggested that a battery of fans be used on uncovered sections in order to overcome this natural convection. Clearly, fans were not being used at this particular smelter when this paper was written.

The transient two-dimensional model presented by Bourgeois *et al.* (1990) neglected the heat transfer in the longitudinal direction, that is, from the fire shaft to head wall. This helped to simplify the model and keep CPU time down. It was claimed that experimental studies had shown that this longitudinal temperature variation was small compared with the flue wall to anode-centre and vertical variation. Unlike the models from the earlier papers, this one incorporated pressure measurements, namely the draught profile along a fire train. One of the limitations of the model was that it could not determine the temperatures in the forced cooling sections (they were considered disconnected from the main fire train). There was fairly good agreement between calculated and experimental results.

Bui *et al.* (1992) divided a furnace section into four zones - fire shaft, under-lid, pit and under-pit. For gas flow distribution, it was stated that the

underlid zone was the most important; whereas for heat transfer to, and therefore presumably from, the anodes, the pit zone was the most important. A three-dimensional model of heat transfer and fluid flow for the under-lid zone of any section of the fire train was developed. For the purposes of validation, the under-lid zone of the first covered cooling section was simulated. The solution procedure was not discussed in detail, but the general purpose computational fluid dynamics PHOENICS code was used as a solver. A larger number of nodes was used, namely 23180. The calculated results followed reasonably well the trend of the measured ones.

1.3 This work - an outline

A heat transfer and pressure distribution model of part of a forced cooling section (from now on called section) of the Riedhammer furnace is presented in this thesis. The cover has been removed, the packing coke is still in place and a blowing or sucking fan (blower or sucker) is positioned over the fire shafts - see Figure 1.2. Each uncovered section is a separate entity disconnected from the main fire train.

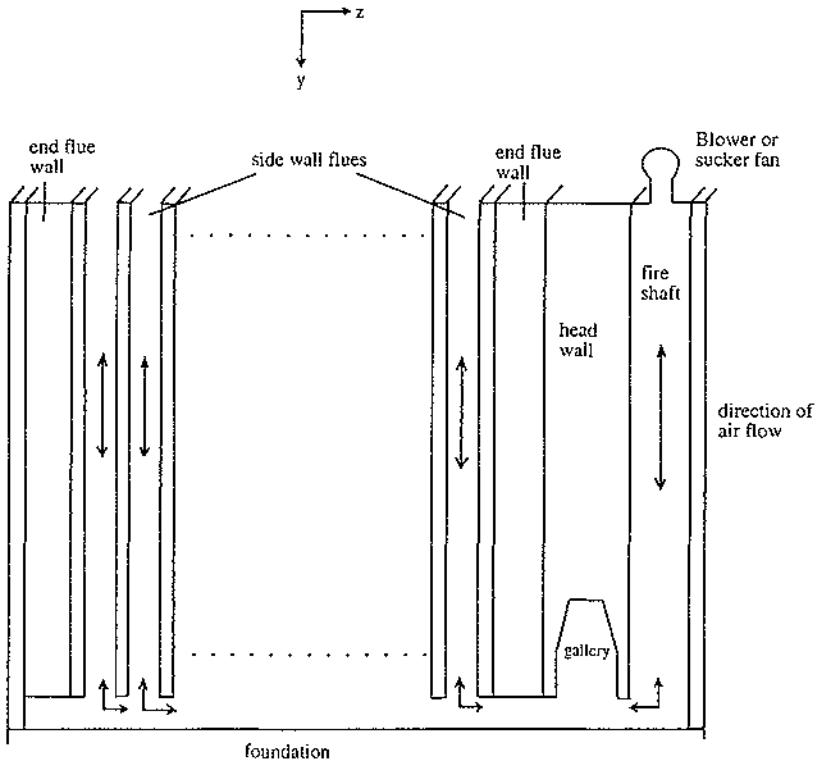

Figure 1.2
Schematic longitudinal view of a flue wall in a forced cooling section

The model presented here is used to determine the effect that different mass flows of air have on:

(a) the block (anodes, packing coke and side flue wall) temperature,
(b) the air temperature in the side wall flues, and
(c) the air pressure in the side wall flues and the fire shafts.

Heat is transferred from the anodes into the air in the side wall flues via the packing coke and the side flue wall. The transfer of heat is taken to be by conduction in the anodes and flue wall, and is assumed to be by conduction in the packing coke. The heat is then transferred into the air by convection and radiation from the surface of the flue wall.

The section is three-dimensional. Simplified one-dimensional and two-dimensional models are studied in Chapter 2. This is done by concentrating on the anodes, packing coke, side flue walls and side wall flues part of the section. Simplifications involved in developing the models are justified by a result from Bui *et al.* (1992) and dimensional considerations.

In Chapter 3, the heat conduction equation is derived in the present context, to give a partial differential equation. The consequences of assuming constant thermal conductivities or otherwise is examined. Using the models from Chapter 2, boundary conditions are then added to the partial differential equations to give boundary value problems.

The thermal properties of the anodes, packing coke and side flue walls are discussed and calculated in Chapter 4.

The one-dimensional heat equation is solved analytically for three different sets of boundary conditions in Chapter 5. The last set are those of the model developed in Chapter 2.

In Chapter 6, explicit numerical methods are used to solve the boundary value problem. Using these, the problem is solved for the case where the thermal conductivities are constant within the anodes, packing coke and side flue wall, to give the transient temperature distribution in the block. In this constant

thermal conductivities case, the thermal conductivities are the only thermal property that is not being adjusted as the temperature varies with time; whereas in the non-constant case all thermal properties are being adjusted as the temperature varies with time (it is assumed these properties are dependent on temperature). For the non-constant thermal conductivities case, the boundary value problem is set up, but not solved due to the introduction of non-linear terms. For this one-dimensional case, the air temperature in the side wall flues is assumed to be constant.

The two-dimensional model is developed in Chapter 7. Only the constant thermal conductivities case is considered. This builds on the work done in the previous chapter on the one-dimensional model. Unlike the one-dimensional model, the temperature of the air in the side wall flues is changing with time and space as heat is transferred into it from the block. This is modelled using an implicit numerical method and combined with the two-dimensional heat equation for the block to give the transient one-dimensional temperature distribution of air along the flues and the transient temperature distribution in the block. As a check on the working, the heat given out by the block and the heat gained by the air in the flues is calculated. Because of the set-up of the model, these should be approximately equal if the calculations are done correctly.

The transient one-dimensional pressure distribution in the side wall flues and fire shafts is calculated in Chapter 8.

CHAPTER 2 DEVELOPMENT OF THE MODELS

2.1 Introduction

Ideally the model should be three-dimensional and provide the temperature distribution that is calculated throughout the section, starting from the fire shafts, moving into the head wall, then the gallery, then the area between the foundation and the bottom of the anodes and finishing in the flues, flue walls, packing coke and anodes. However, this would be too complicated and time consuming, so the model is simplified by:

(i) restricting it to the flues, flue walls, packing coke and anodes zone, which is the most important one for anode cooling (see Bui *et al.*, 1992);

(ii) making it one- and two-dimensional.

Most of the cooling of the anodes occurs through them transferring heat into nearby air. Therefore (ii) of the model simplification is done by finding which sides of the anodes have the most exposure to air. It is then assumed that the anodes transfer most of their heat from these sides. Heat transfer from the remaining sides is then ignored, enabling the development of a two-dimensional model. In order to understand and solve this two-dimensional model, a one-dimensional model is developed first.

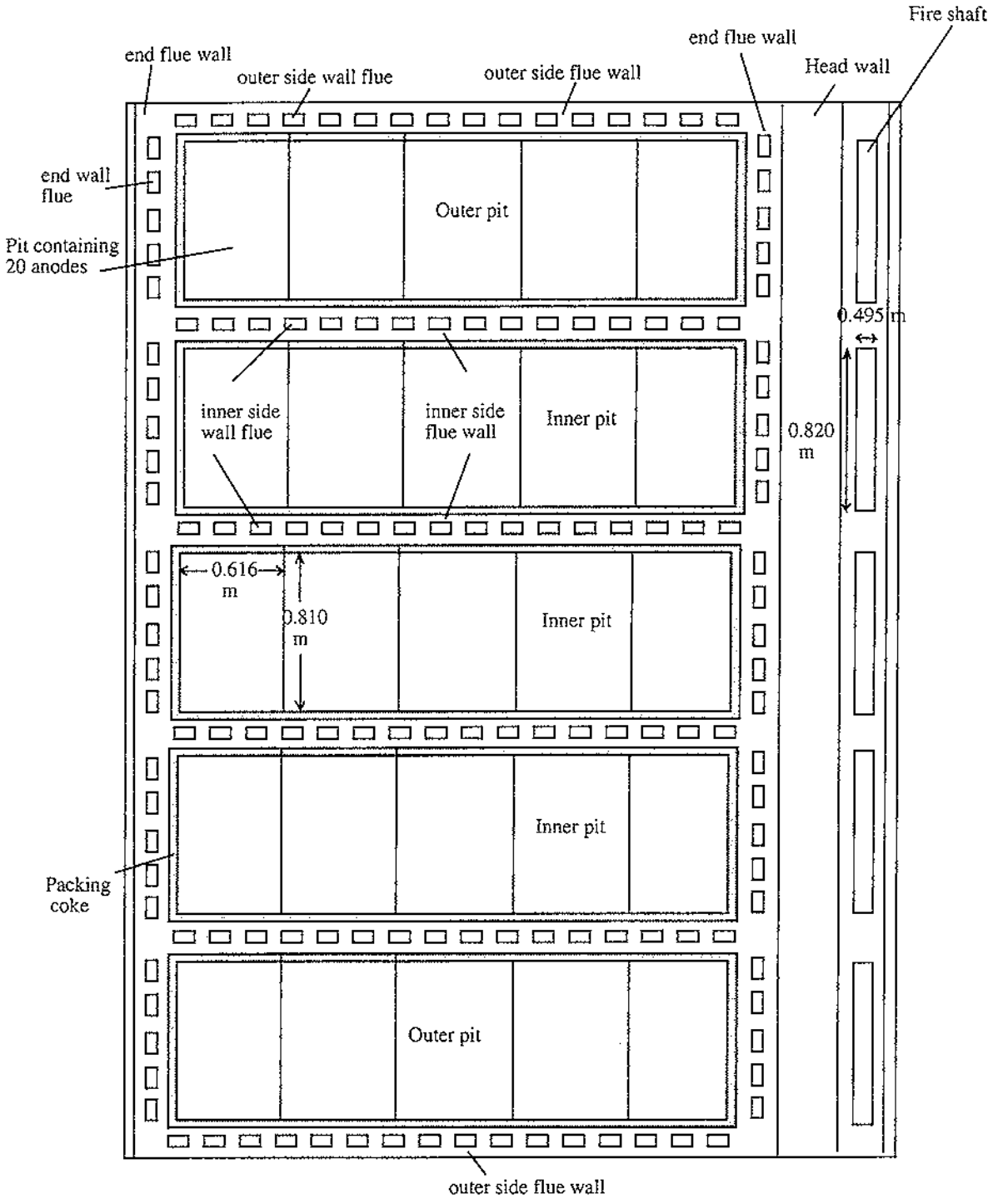

Figure 2.1

Schematic plan view of a section with the packing coke removed from the top to expose the top row of anodes.

(The flues are assumed to be rectangular, whereas in fact the corners of each flue are rounded.)

2.2 Calculation of cooling areas around the anodes

The anodes are rectangular blocks. There are twenty anodes stacked in a pit - five rows of four. For the purposes of modelling, these twenty anodes are treated as one big anode. This big anode has six sides, each of which is adjacent to air via packing coke and/or a flue wall:

(a) one side is adjacent to the air which is above the anode;

(b) one side is adjacent to the air which is flowing between the bottom surface of the anode and the foundation;

(c) two sides are adjacent to the air flowing in the end wall flues;

(d) two sides are adjacent to the air flowing in the inner/outer side wall flues. (As can be seen from Figure 2.1, if the pit is an inner one, then these two sides are adjacent to the inner side wall flues; whereas if the pit is an outer one, then one of these sides is adjacent to the inner side wall flues and the other side is adjacent to the outer side wall flues.)

The areas of these different sides of the anode that are adjacent to air are now calculated. Since most of the anode cooling occurs through heat transfer into nearby air, the area between flues is ignored. A line of symmetry, an adiabatic boundary, is assumed to run through the centre of each flue, see Figure 2.3, so the appropriate areas are calculated on half flue measurements. Since the dimensions of each pit/flue wall are identical, the calculations are done for one pit/flue wall area (for measurements refer to Figures 2.1 - 2.3).

(a) The area of the side that is adjacent to the air which is above the anode

$$= \text{(length of anode)} \times \text{(width of anode)}$$
$$= (0.616 \times 5) \times 0.810$$
$$= 2.5\ \text{m}^2.$$

(b) The area of the side that is adjacent to the air which is moving between the bottom surface of the anode and the foundation

$$= \text{area as in (i)}$$
$$= 2.5\ \text{m}^2.$$

(c) The area of the two sides that are adjacent to the air flowing in the end wall flues

= (length of one end wall flue + 2 × $\frac{1}{2}$ width of one end wall flue) × (depth of anode) × (number of flues in one end wall) × (number of end walls)

= (0.120 + 2 × 0.06) × (1.166 × 4) × (5) × (2)

= 11.2 m^2

(d) The area of the two sides that are adjacent to the air flowing in the inner/outer side wall flues

= (length of one inner/outer side wall flue + 2 × $\frac{1}{2}$ width of one inner/outer wall flue) × (depth of anode) × (number of flues in one inner/outer side wall) × (number of inner/outer side walls)

= (0.178 + 2 × 0.074) × (1.166 × 4) × (16) × (2)

= 48.7 m^2.

Therefore total area of the sides **not** adjacent to the air in the inner/outer side wall flues

= (a) + (b) + (c)

= 16.2 m^2

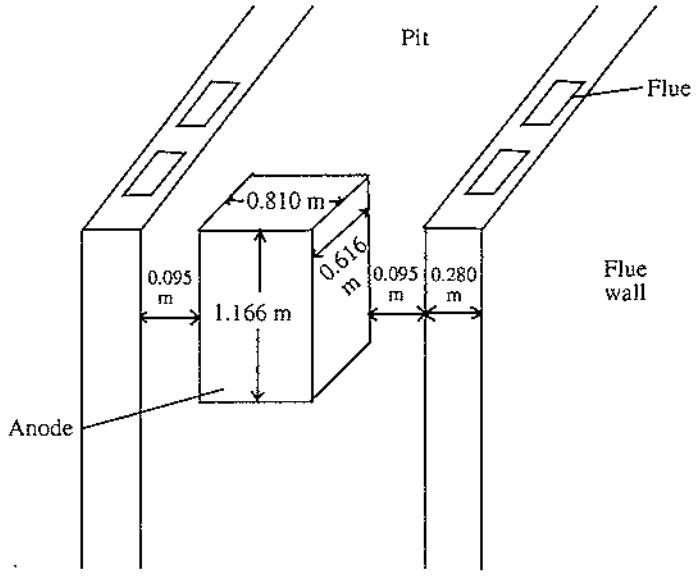

Figure 2.2
Schematic cross section of an anode in a pit

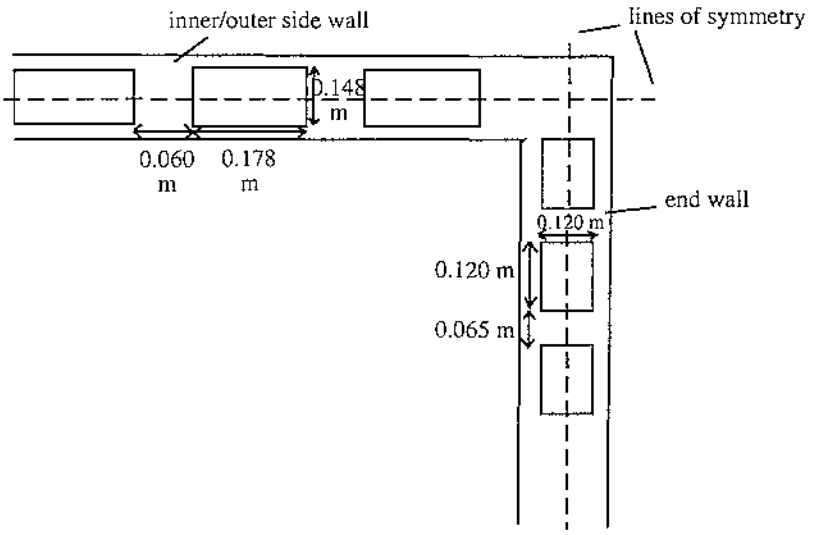

Figure 2.3
Schematic plan view of a pit corner and flues

Comparing this figure with that of (d), namely 48.7 m^2, it is clear that the greatest areas of the anode adjacent to the air are the two sides adjacent to the air flowing in the inner/outer side wall flues. It is therefore assumed that the anode transfers most of its heat into the air flowing in the inner/outer side wall flues. It is further assumed that there is no heat transfer into the air which is:

(a) above the anode;
(b) flowing between the bottom surface of the anode and the foundation;
(c) flowing in the end wall flues.

This last assumption allows modelling in two dimensions rather than three.

This agrees with experimental studies mentioned in Bourgeois *et al.* (1990). The studies found that longitudinal (from fire shaft to head wall) temperature variation was small compared with the flue wall to anode-centre and vertical variation.

The x-direction is taken to be across the pits, and the vertical as the y-direction. (The z-direction is taken to be along the pits - see Figure 1.2.) This is developed further in §2.3 and §2.4.

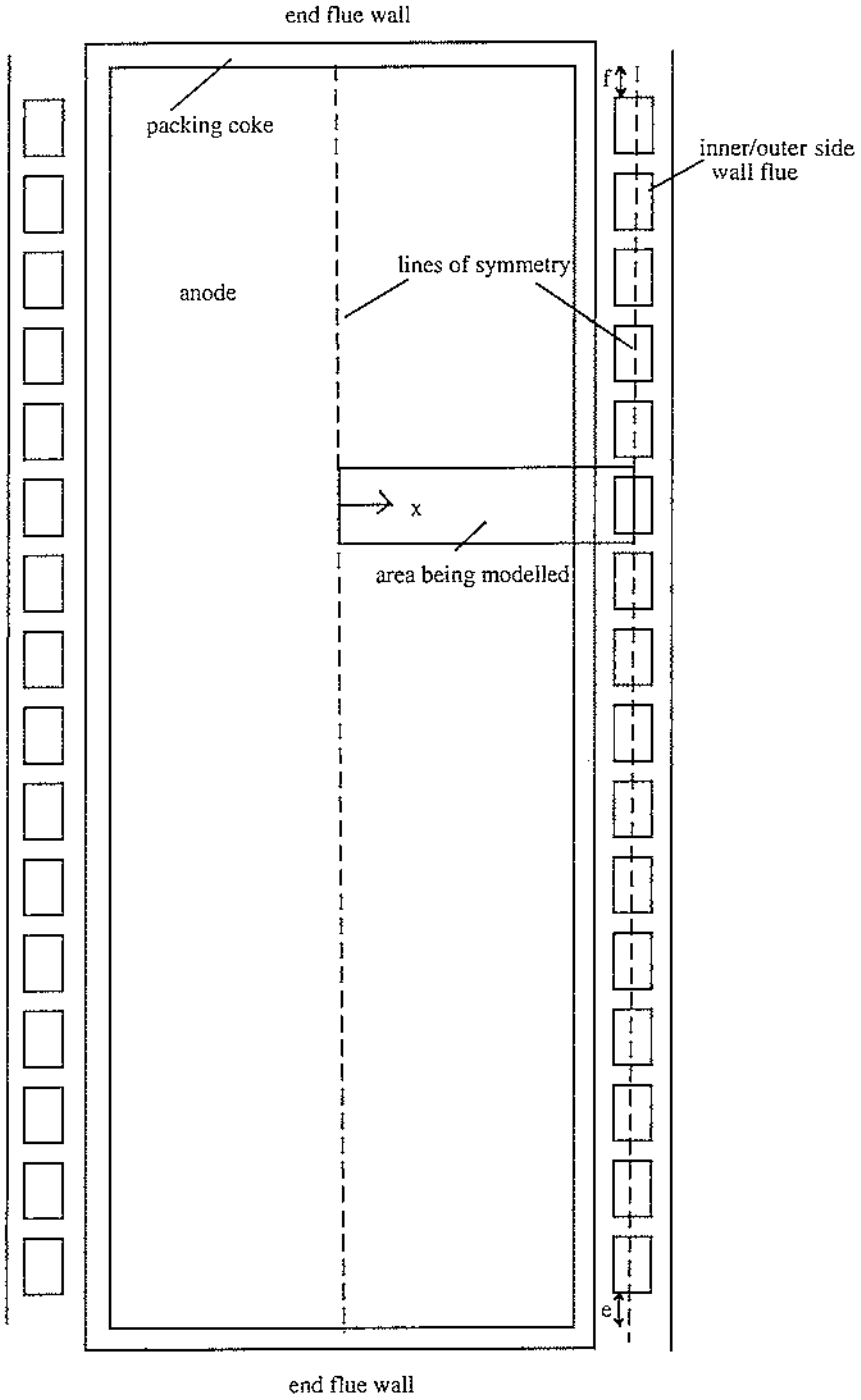

Figure 2.4
Schematic plan view of one pit with anode, packing coke, flue walls and flues

2.3 One-dimensional model

It is assumed that lines of symmetry, which denote adiabatic boundaries, run through the centre line of each pit and flue, as shown in Figure 2.4. All pits are treated alike, that is, there is no difference between outer and inner pits [although it is realized that there is heat loss through the outer side flue walls on either side of the section - see Bui *et al.* (1992)].

From now on, inner/outer side flue walls are referred to as the flue walls and inner/outer side wall flues as flues.
A representative slice of anode, packing coke, flue wall and flue is selected. This slice is adjacent to one flue, as shown in Figure 2.4.

As in §2.2, it is assumed that the anode transfers heat into the air in the flue not only along a (= 0.178 m) but also along b and c too (both = 0.074 m) see Figure 2.5. This poses a difficulty in regard to the thickness of the flue wall. For example, from the outer edge of the packing coke, d, to the flue wall at a, distance = 0.140 - 0.074 = 0.066 m. But what about the distance from d to the flue wall at b or c?

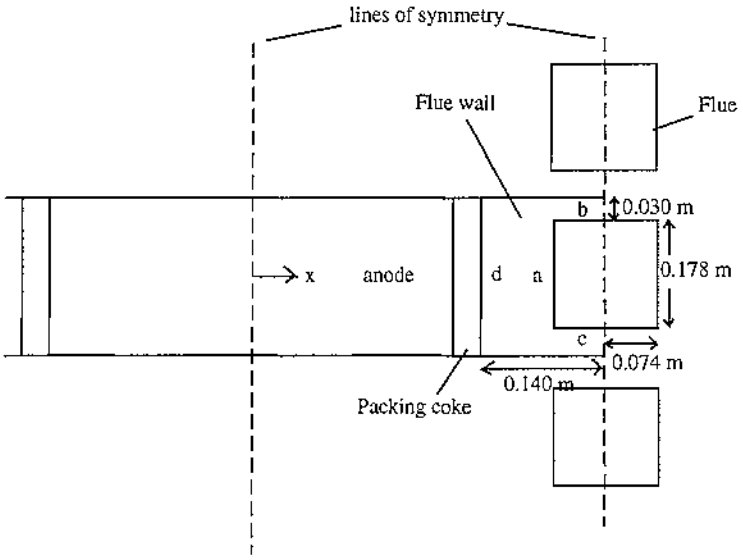

Figure 2.5
Schematic plan view of the representative slice showing anode, packing coke, flue wall and flue.

In order to overcome this difficulty, each flue is thought of being stretched or elongated, as illustrated in Figure 2.6, so that the sixteen flues in a flue wall become one 'large' flue. This large flue, amongst other things, must have the same cross-sectional area as the sixteen individual flues (for measurements refer to Figures 2.3 and 2.5).

Cross-sectional area of sixteen individual flues

$= (\text{cross-sectional area of one flue}) \times 16$

$= (0.178 \times 0.148) \times 16$

$= 0.421504 \text{ m}^2$

Cross-sectional area of 'large' flue

$= (\text{length of 'large' flue}) \times (\text{width of 'large' flue})$

$= (\text{length of one individual flue} \times 16 + \text{distance between two individual flues} \times 15 + \text{distance e} + \text{distance f}) \times W,$

where $W \equiv$ the width of 'large' flue,

$= (0.178 \times 16 + 0.060 \times 15 + 0.030 + 0.030) \times W$

$= 3.808 \times W \text{ m}^2,$

and this has to equal 0.421504 m^2,

$\Rightarrow W = 0.111 \text{ m}.$

Therefore the thickness of the flue wall in the case of the 'large' flue is $0.140 - \frac{0.111}{2} = 0.085$ m (rounded) see Figure 2.6.

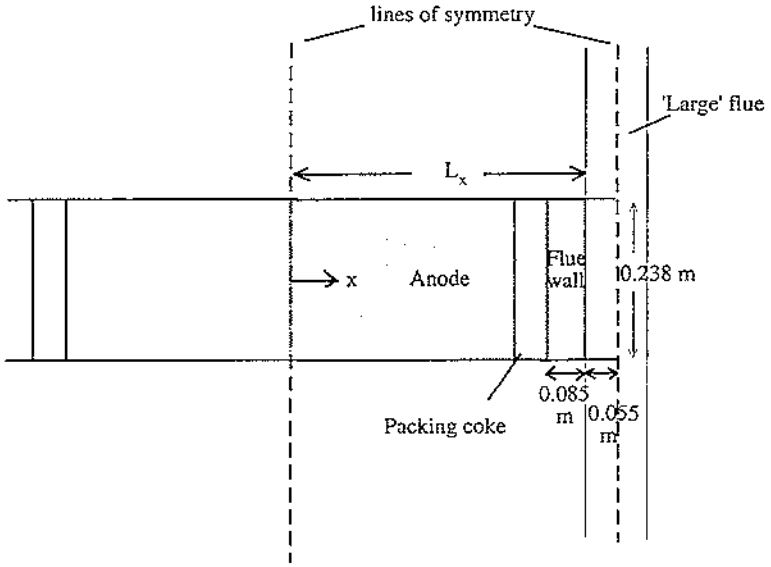

Figure 2.6

Schematic plan view of 'large' flue and surroundings.

The block is defined to be the shaded area in Figure 2.6.

L_x = width of block
= (width of anode) + (width of packing coke) + (width of flue wall)
= 0.585 m.

Note: In evaluating the Reynolds number and the heat transfer coefficient in Chapters 6, 7 and 8, the flue dimensions of Figure 2.5 are used, that is the 'real' flue dimensions.

2.4 Two-dimensional model

The one-dimensional model developed in §2.3 is extended by introducing a vertical or y component as shown in Figure 2.7.

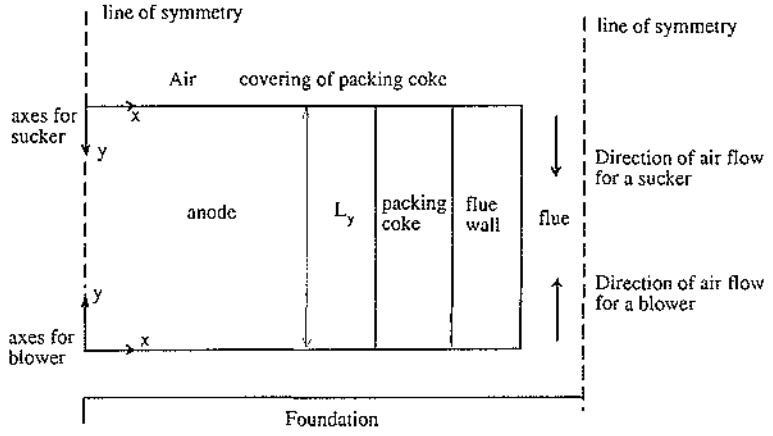

Figure 2.7
Schematic cross section of the two-dimensional block and flue

The same representative slice is taken as for the one-dimensional case, except that here the slice has a y component. In fact the slice extends vertically from the top surface of the anode to the bottom surface of the anode.

L_y = depth of anode
= 1.166×4
= 4.664 m.

The x and y axes are positioned differently according to whether a blower

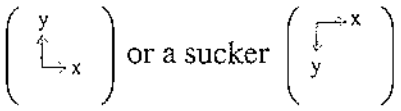

Blower versus sucker

In reality, in the case of a blower operating, the air has to pass through the fire shafts, the gallery and into the area between the bottom of the anode and the foundation prior to it flowing up through the flues. This is not the case if a sucker is operating, since the air has no 'history' like this prior to it flowing down the flues. The air here is drawn from the air above the top surface of the anode (see Figure 1.2). Hence for a blower, the inlet air temperature is determined at the top of the fire shafts, whereas for a sucker it is determined at the top of the flues.

But given an inlet air temperature for a blower (air temperature at the top of the fire shafts, which is atmospheric temperature) the two-dimensional model for a blower is unable to determine what the air temperature will be when the air arrives at the bottom of the flues - the inlet air temperature for the model. It is assumed that the inlet air temperature for the model in the case of a blower is atmospheric temperature. Atmospheric temperature is assumed to be 20 ^{o}C. There is no such difficulty for a sucker, since the inlet air temperature in reality (atmospheric temperature) is the same as that for the two-dimensional model for a sucker.

Therefore for the purpose of the two-dimensional model, it makes no difference to the temperature distribution as to whether a blower or a sucker is operating except that the block temperature distribution is reversed, since $y = 0$ for a blower corresponds to $y = L_y$ for a sucker and $y = L_y$ for a blower corresponds to $y = 0$ for a sucker (see Figure 2.7).

CHAPTER 3 DERIVATION OF THE HEAT EQUATION IN THE BLOCK

3.1 The heat equation

The rate at which heat accumulates in an elemental volume (V) of block material is given by $\frac{d}{dt}\iiint_V \rho E \, dV$ where ρ is the density, t is time and E is the total energy (internal, kinetic and potential) per unit mass of the system.

This must be balanced by the rate of heat leaving V. This is given by $\iint_S -\dot{Q} \, d\mathbf{S}$, where $\dot{Q} = dQ/dt$ is the rate of heat flow (conductive, convective and radiative) per unit area at the surface (S) of V.

First consider $\frac{d}{dt}\iiint_V \rho E \, dV$.

Since V is closed (mass does not enter or leave V) and stationary then E = e, where e ≡ internal energy per unit mass, and

$$\frac{d}{dt}\iiint_V \rho E \, dV = \iiint_V \frac{\partial}{\partial t}(\rho e)\, dV$$
$$= \iiint_V \rho \frac{\partial e}{\partial t} dV$$

since ρ is constant with respect to time - see Chapter 4.

Introducing the enthalpy $h = e + \frac{p}{\rho}$, where p ≡ pressure (Currie, 1993) and using the fact that p and ρ are constant with respect to time gives:

$$\frac{d}{dt}\iiint_V \rho E \, dV = \iiint_V \rho \frac{\partial h}{\partial t} dV$$
$$= \iiint_V \rho \frac{\partial h}{\partial T}\frac{\partial T}{\partial t} dV \quad (T \equiv \text{temperature})$$
$$= \iiint_V \rho c_p \frac{\partial T}{\partial t} dV$$

since $\frac{\partial h}{\partial T}$ at constant pressure $= c_p \equiv$ the specific heat capacity at constant pressure.

Now consider $\iint_S -\dot{Q}\, d\mathbf{S}$. Since there is no convective or radiative effect, by Fourier's Law (Rogers and Mayhew, 1992)

$$\dot{Q} = -k\,\nabla T \quad (k \equiv \text{thermal conductivity})$$

Therefore
$$\begin{aligned}\iint_S -\dot{Q}\, d\mathbf{S} &= \iint_S k\,\nabla T\, d\mathbf{S} \\ &= \iint_S k\,\nabla T\cdot\mathbf{n}\, dS \\ &= \iiint_V \nabla\cdot(k\nabla T)\, dV \text{ by Gauss' Divergence Theorem.}\end{aligned}$$

Therefore
$$\iiint_V \rho\, c_p \frac{\partial T}{\partial t}\, dV = \iiint_V \nabla\cdot(k\nabla T)\, dV$$
$$\Rightarrow \quad \rho\, c_p \frac{\partial T}{\partial t} = \nabla\cdot(k\nabla T) \qquad (3.1)$$

If k is constant, then Equation (3.1) becomes

$$\rho c_p \frac{\partial T}{\partial t} = k\,\nabla^2 T$$

i.e. $$\boxed{\frac{\partial T}{\partial t} = \alpha\nabla^2 T}$$ where $\alpha = k/\rho c_p \equiv$ thermal diffusivity.

If k is not constant and varies with temperature, then in the one-dimensional case Equation (3.1) becomes

$$\rho c_p \frac{\partial T}{\partial t} = \frac{\partial}{\partial x}\left(k\frac{\partial T}{\partial x}\right)$$
$$= \frac{\partial k}{\partial x}\frac{\partial T}{\partial x} + k\frac{\partial^2 T}{\partial x^2}$$

$$= \frac{dk}{dT}\left(\frac{\partial T}{\partial x}\right)^2 + k\frac{\partial^2 T}{\partial x^2}$$

Therefore $$\boxed{\frac{\partial T}{\partial t} = \hat{\alpha}\left(\frac{\partial T}{\partial x}\right)^2 + \alpha\frac{\partial^2 T}{\partial x^2}} \quad \text{where } \hat{\alpha} = \frac{dk}{dT}/\rho c_p .$$

In the two-dimensional case Equation (3.1) becomes

$$\rho c_p \frac{\partial T}{\partial t} = \frac{\partial}{\partial x}\left(k\frac{\partial T}{\partial x}\right) + \frac{\partial}{\partial y}\left(k\frac{\partial T}{\partial y}\right)$$

$$= \frac{\partial k}{\partial x}\frac{\partial T}{\partial x} + k\frac{\partial^2 T}{\partial x^2} + \frac{\partial k}{\partial y}\frac{\partial T}{\partial y} + k\frac{\partial^2 T}{\partial y^2}$$

Therefore $$\boxed{\frac{\partial T}{\partial t} = \hat{\alpha}\left[\left(\frac{\partial T}{\partial x}\right)^2 + \left(\frac{\partial T}{\partial y}\right)^2\right] + \alpha\left[\frac{\partial^2 T}{\partial x^2} + \frac{\partial^2 T}{\partial y^2}\right]}$$

3.2 The boundary conditions

Referring to (a) and (b) on p.11 of §2.2,

(a) No heat transfer into the air which is above the anode

$$\Rightarrow \quad \text{adiabatic boundary on } \begin{cases} y = 0, & \text{sucker} \\ y = L_y, & \text{blower} \end{cases}.$$

$$\Rightarrow \quad \frac{\partial T}{\partial y} = 0 \text{ on } \begin{cases} y = 0, & \text{sucker} \\ y = L_y, & \text{blower} \end{cases}.$$

(b) No heat transfer into the air which is flowing between the bottom surface of the anode and the foundation

$$\Rightarrow \quad \text{adiabatic boundary on } \begin{cases} y = L_y, & \text{sucker} \\ y = 0, & \text{blower} \end{cases}$$

$$\Rightarrow \quad \frac{\partial T}{\partial y} = 0 \text{ on } \begin{cases} y = L_y, & \text{sucker} \\ y = 0, & \text{blower.} \end{cases}$$

Referring to the assumption made in §2.3, that is, it is assumed that an adiabatic boundary runs through the centre line of the pit

$$\Rightarrow \qquad \frac{\partial T}{\partial x} = 0 \quad \text{on } x = 0.$$

Suppose the block has some initial temperature, T_1,

$$\Rightarrow \qquad T = T_1 \quad \text{when } t = 0.$$

Clearly the temperature at $x = L_x$ (on the flue wall) is decreasing with time because of the air flowing past and heat being transferred from here into the air. Let this decreasing temperature be $T_w(t)$, where $w \equiv$ wall and (t) denotes dependence on time

Then $\qquad T = T_w(t)$ on $x = L_x$.

3.3 Summary

The boundary value problem for the heat conduction in the block is now specified, both for the one- and two-dimensional models.

One dimension

$$\left.\begin{aligned} \frac{\partial T}{\partial t}(x, t) &= \alpha \frac{\partial^2 T}{\partial x^2}, && \text{constant } k \\ \frac{\partial T}{\partial t}(x, t) &= \hat{\alpha}\left(\frac{\partial T}{\partial x}\right)^2 + \alpha \frac{\partial^2 T}{\partial x^2}, && \text{non-constant } k \end{aligned}\right\} 0 \le x \le L_x, \quad t > 0$$

with $\quad \frac{\partial T}{\partial x}(0, t) = 0, \qquad t > 0,$

$\qquad T(L_x, t) = T_w(t), \qquad t > 0 \qquad$ and

and $\quad T(x, 0) = T_1, \qquad 0 \le x \le L_x.$

Two dimensions

$$\left.\begin{aligned} \frac{\partial T}{\partial t}(x, y, t) &= \alpha\left(\frac{\partial^2 T}{\partial x^2} + \frac{\partial^2 T}{\partial y^2}\right) && \text{constant } k \\ \frac{\partial T}{\partial t}(x, y, t) &= \hat{\alpha}\left[\left(\frac{\partial T}{\partial x}\right)^2 + \left(\frac{\partial T}{\partial y}\right)^2\right] \\ &\quad + \alpha\left[\frac{\partial^2 T}{\partial x^2} + \frac{\partial^2 T}{\partial y^2}\right] && \text{non-constant } k \end{aligned}\right\} \begin{aligned} &0 \le x \le L_x \\ &0 \le y \le L_y \\ &t > 0 \end{aligned}$$

with $\frac{\partial T}{\partial x}(0, y, t) = 0, \qquad 0 \le y \le L_y, \quad t > 0,$

$T(L_x, y, t) = T_w(t), \qquad 0 \le y \le L_y, \quad t > 0,$

$T(x, y, 0) = T_i, \qquad 0 \le x \le L_x, \quad 0 \le y \le L_y,$

and $\frac{\partial T}{\partial y}(x, 0, t) = \frac{\partial T}{\partial y}(x, L_y, t) = 0, \qquad 0 \le x \le L_x, \quad t > 0.$

CHAPTER 4 THERMAL PROPERTIES OF THE BLOCK

4.1 Introduction

The thermal properties of interest are of course those that appear in the heat equation, namely k, ρ and c_p. Once these are found, $\alpha = \frac{k}{\rho c_p}$ and $\hat{\alpha} = \frac{dk}{dT}/\rho\, c_p$ can be calculated.

This chapter is included since in the readings for this thesis, values or formulae for the values of k, ρ and c_p were rarely given. The non-referenced values and formulae given here were obtained from Braithwaite (private communication, 1993).

In order to simplify expressions and save computing time, linear approximations are used for formulae when approximations are deemed necessary. As most of the block temperatures in the section ≥ 400 K (127 °C), linear approximations seem reasonable.

For the linear approximations, the equation $p(T) = p(T_0) + (T - T_0)p[T_0, T_1]$ is used (Burden and Faires, 1989) where $p[T_0, T_1] = \frac{p(T_1) - p(T_0)}{T_1 - T_0}$.

4.2 Carbon Anode

Thermal conductivity, ka (W/mK)

From Log and Oye (1990),

$$ka = ka_0 + 0.274\sqrt{ka_0}\,(\sqrt{T} - \sqrt{T_0}) - 2.8 \times 10^{-3}(ka_0)^{0.77}\,(T - T_0)$$

where $T_0 \equiv$ room temperature 293 K say, and

$ka_0 \equiv$ thermal conductivity of anode at room temperature, in W/mK.

ka_0 is given by the equation,

$$ka_0 = -1.2105 + 0.1744\, L_c = 4.1959,$$

since L_c (crystallite height) = 31 Å for anodes.

ka is approximated using the points (400, 4.91) and (970, 6.35) - see Figure 4.1.

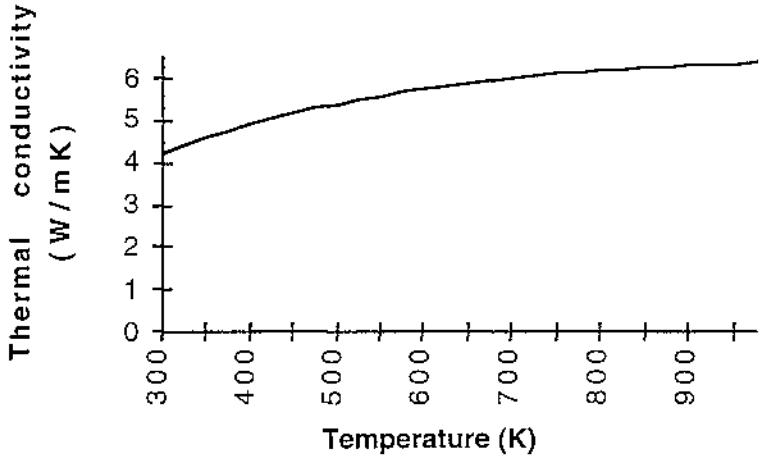

Figure 4.1
Thermal conductivity of the anode [from Log and Oye (1990)]

$$ka = (2.53 \times 10^{-3})T + 3.90 \qquad (4.1)$$

$$\frac{d(ka)}{dT} = 0.137\sqrt{ka_0}\,\frac{1}{\sqrt{T}} - 2.8 \times 10^{-3}\,(ka_0)^{0.77}\ W/mK^2$$

is approximated using the points $(400, 5.58 \times 10^{-3})$ and $(970, 5.63 \times 10^{-4})$ – see Figure 4.2.

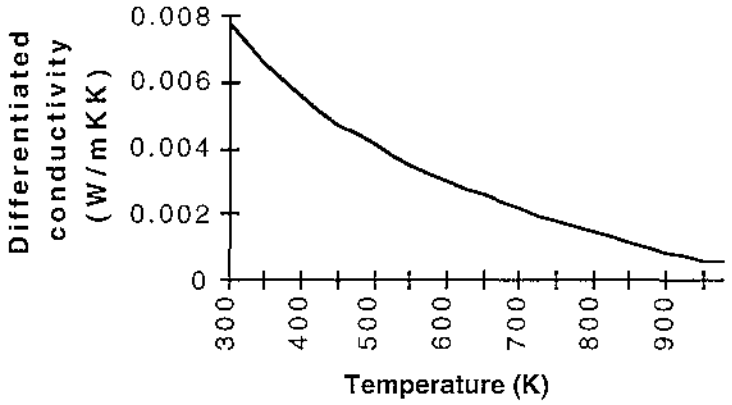

Figure 4.2
The rate of change with respect to temperature of the thermal conductivity of the anode

$$\frac{d(ka)}{dT} = (-8.80 \times 10^{-6})T + 9.10 \times 10^{-3} \qquad (4.2)$$

The equations for ka and d(ka)/dT are valid for temperatures ≤ 973 K (700 °C), as most of the anode temperatures in the section are. If any anode temperature > 973 K, then Equations (4.1) and (4.2) are still used.

Specific heat capacity, ca_p (J/kgK)

$$ca_p = (-0.13374402 \times 10^{-8})T^4 + (0.64604614 \times 10^{-5})T^3 - (0.11572658 \times 10^{-1})T^2 + (0.95663719 \times 10^{1})T - 0.13731392 \times 10^{4}$$

This is approximated using the points $(400, 9.81 \times 10^2)$ and $(970, 1.73 \times 10^3)$ - see Figure 4.3.

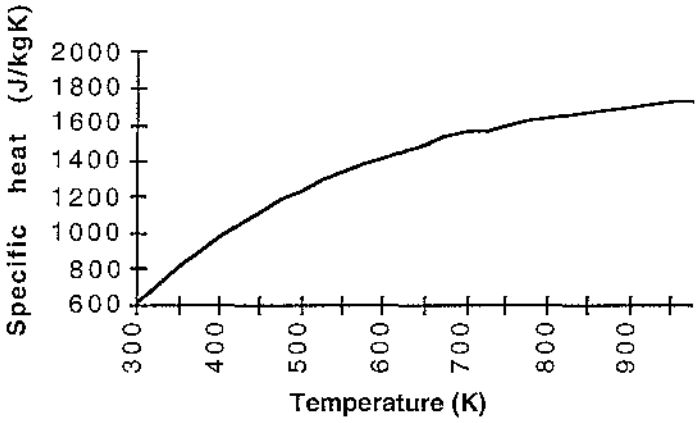

Figure 4.3
Specific heat capacity at constant pressure of the anode

$$ca_p = (1.31)T + 4.55 \times 10^2 \qquad (4.3)$$

Density, ρa (kg/m^3)

The density of the anode is approximated by 1550.

4.3 Packing Coke

Thermal conductivity, kp (W/mK)

Using data supplied by Braithwaite (private communication, 1993), the average packing coke particle size is found to be 5.7 mm. This is then used in de Fernández *et al.* (1983) to approximate kp using the points $(473, 4.00 \times 10^{-1})$ and (1073, 1.16) - see Figure 4.4.

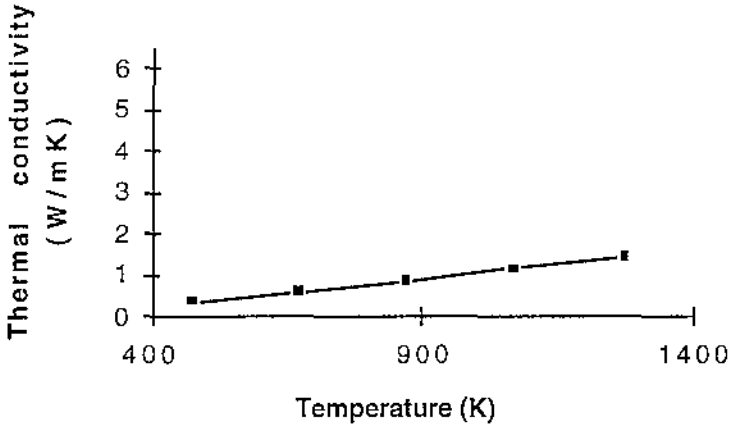

Figure 4.4
Thermal conductivity of the packing coke (interpolated from data supplied by Braithwaite, 1993)

$$kp = (1.27 \times 10^{-3})T - 1.99 \times 10^{-1} \qquad (4.4)$$

$$\frac{d(kp)}{dT} = 1.27 \times 10^{-3} \ \ W/mK^2 \qquad (4.5)$$

Specific heat capacity, cp_p (J/kgK)

$$cp_p = 933.0 + (0.916)T - \frac{4.08 \times 10^7}{T^2} .$$

This is approximated using the points $(400, 1.04 \times 10^3)$ and $(1000, 1.81 \times 10^3)$ - see Figure 4.5.

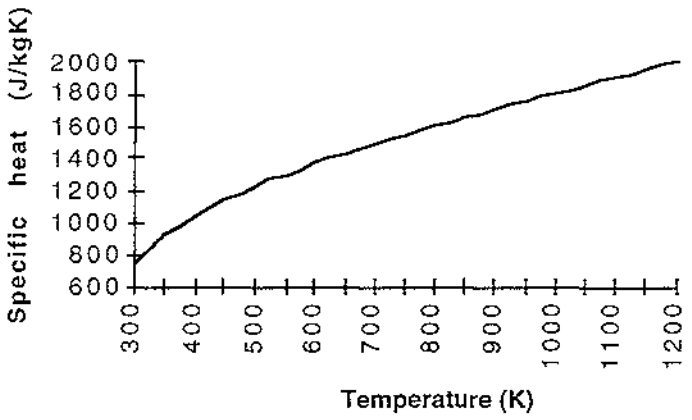

Figure 4.5
Specific heat capacity at constant pressure of the packing coke

$$cp_p = (1.28)T + 5.27 \times 10^2 \qquad (4.6)$$

Density, ρp (kg/m^3)

The density of the packing coke is approximated by 670.

4.4 Flue Wall

Thermal Conductivity, kw (W/mK).

This is approximated using the points (657, 1.35) and (1265, 1.77) - see Figure 4.6.

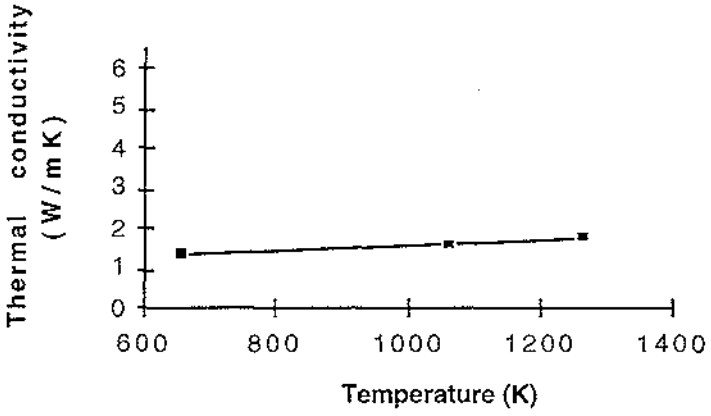

Figure 4.6
Thermal conductivity of the flue wall (interpolated from data supplied by Braithwaite, 1993)

$$kw = (6.91 \times 10^{-4})T + 8.96 \times 10^{-1} \quad (4.7)$$

$$\frac{d(kw)}{dT} = 6.91 \times 10^{-4} \ W/mK^2 \quad (4.8)$$

Specific heat capacity, cw_p (J/kgK)

The specific heat capacity at constant pressure of the flue wall is approximated by 1250.

Density, ρw (kg/m^3)

The density of the flue wall is approximated by 2440.

CHAPTER 5 ONE-DIMENSIONAL ANALYTICAL SOLUTION

5.1 Introduction

k is assumed to be constant, so the boundary value problem is (from §3.3)

$$\left.\begin{aligned} &\frac{\partial T}{\partial t} = \alpha \frac{\partial^2 T}{\partial x^2}, && 0 \le x \le L_x, \quad t > 0 \\ \text{with} \quad &\frac{\partial T}{\partial x}(0, t) = 0, && t > 0, \\ &T(L_x, t) = T_w(t), && t > 0, \\ &T(x, 0) = T_1, && 0 \le x \le L_x . \end{aligned}\right\} \qquad (5.1)$$

Instead of trying to solve (5.1) straightaway, initially boundary value problems with simpler boundary conditions are solved analytically. Using the knowledge gained from solving these simpler problems, (5.1) is then solved.

5.2 Solution with different boundary conditions

(a) The ends of the block are maintained at constant temperature, T_0, for all time, $t > 0$, and the block is initially at temperature T_1 for $0 \le x \le L_x$.

$$\frac{\partial T}{\partial t} = \alpha \frac{\partial^2 T}{\partial x^2}, \qquad 0 \le x \le L_x, \quad t > 0$$

with $T(0, t) = T(L_x, t) = T_0, \qquad t > 0,$

$T(x, 0) = T_1, \qquad 0 \le x \le L_x.$

Let $T(x, t) = \theta(x, t) + \psi(x)$

Homogeneous boundary conditions are obtained for a differential equation involving θ, if $\psi = T_0$.

With this choice of ψ, the problem becomes

$$\left.\begin{aligned} &\frac{\partial\theta}{\partial t} = \alpha\frac{\partial^2\theta}{\partial x^2}, && 0 \le x \le L_x,\ t > 0 \\ \text{with}\quad &\theta(0, t) = \theta(L_x, t) = 0, && t > 0, \\ &\theta(x, t) = T_1 - T_0, && 0 \le x \le L_x \end{aligned}\right\} \quad (5.2)$$

(5.2) can be solved using separation of variables.

Let $\theta(x, t) = X(x)\,G(t)$

$\therefore$ Equation (5.2) becomes $G'(t)\,X(x) = \alpha X''(x)G(t)$

$$\Rightarrow \quad \frac{G'(t)}{\alpha G(t)} = \frac{X''(x)}{X(x)} = -\lambda \text{ say.}$$

$$\Rightarrow \quad X'(x) + \lambda X(x) = 0 \qquad (5.3)$$

$$\text{with} \quad X(0) = X(L_x) = 0$$

$$\text{and} \quad G'(t) + \lambda\alpha G(t) = 0 \qquad (5.4)$$

Solving Equation (5.3), with $\lambda < 0, \lambda = 0, \lambda > 0$ in turn:

(i) If $\lambda = -k^2$

then $X = c_1 \cosh kx + c_2 \sinh kx$

Now, $X(0) = 0 \Rightarrow c_1 = 0$

and $X(L_x) = 0 \Rightarrow c_2 = 0$

$\therefore$ $\lambda = -k^2$ gives a trivial solution.

(ii) If $\lambda = 0$

then $X = c_3 x + c_4$

Now, $X(0) = 0 \Rightarrow c_4 = 0$

and $X(L_x) = 0 \Rightarrow c_3 = 0$

$\therefore$ $\lambda = 0$ gives a trivial solution.

(iii) Take $\lambda = k^2$

then $X = c_5 e^{ikx} + c_6 e^{-ikx}$

or $X = c_7 \cos\sqrt{\lambda}\,x + c_8 \sin\sqrt{\lambda}\,x$

Now $X(0) = 0 \Rightarrow c_7 = 0$

and $X(L_x) = 0 \Rightarrow c_8 \sin\sqrt{\lambda}\,L_x = 0$

$$\Rightarrow \sqrt{\lambda}\,L_x = n\pi,\ n \in N$$

$$\Rightarrow \lambda = \frac{n^2\pi^2}{L_x^2},\ n \in N,$$

which are the eigenvalues.

$$\therefore \quad X \in \left\{ A_n \sin\frac{n\pi x}{L_x} : n \in N \right\}$$

which are the eigenfunctions; these are orthogonal on $[0, L_x]$.

Now, solving Equation (5.4)

$$G = c_9 e^{-\lambda\alpha t}$$

$$\therefore \quad \theta \in \left\{ B_n \sin\left(\frac{n\pi x}{L_x}\right) e^{-n^2\pi^2\alpha t/L_x^2} : n \in N \right\}$$

The most general solution of this form is

$$\theta(x, t) = \sum_{n=1}^{\infty} B_n \sin\left(\frac{n\pi x}{L_x}\right) e^{-n^2\pi^2\alpha t/L_x^2}$$

where $$\theta(x, 0) = T_1 - T_0 = \sum_{n=1}^{\infty} B_n \sin\frac{n\pi x}{L_x}$$

Using the orthogonality of the eigenfunctions gives

$$B_n = \frac{2}{L_x}\int_0^{L_x} (T_1 - T_0) \sin\left(\frac{n\pi x}{L_x}\right)dx = \frac{T_1 - T_0}{n\pi}[1 - (-1)^n]$$

$$\therefore \quad \theta(x,t) = \frac{T_1 - T_0}{\pi} \sum_{n=1}^{\infty} \frac{1}{n}[1 - (-1)^n] \sin\left(\frac{n\pi x}{L_x}\right) e^{-n^2\pi^2\alpha t/L_x^2}$$

Now θ is known, T is obtained as $T = \theta + T_0$.

(b) A boundary value problem is now solved that is almost the same as (5.1) except that here $T(L_x, t) = T_0$ = a constant, whereas the boundary condition in (5.1) is $T(L_x, t) = T_w(t)$ - varies (decreases) with time.

$$\frac{\partial T}{\partial t} = \alpha \frac{\partial^2 T}{\partial x^2}, \qquad 0 \le x \le L_x, \quad t > 0$$

with

$$\frac{\partial T}{\partial x}(0, t) = 0, \qquad t > 0,$$

$$T(L_x, t) = T_0, \qquad t > 0,$$

$$T(x, 0) = T_1, \qquad 0 \le x \le L_x.$$

As in (a), let $T(x, t) = \theta(x, t) + \psi(x)$, and $\psi = T_0$ gives homogeneous boundary conditions, so the problem becomes

$$\left.\begin{aligned} &\frac{\partial \theta}{\partial t} = \alpha \frac{\partial^2 \theta}{\partial t^2}, && 0 \le x \le L_x, \quad t > 0 \\ \text{with} \quad &\frac{\partial \theta}{\partial x}(0, t) = 0, && t > 0, \\ &\theta(L_x, t) = 0, && t > 0, \\ &\theta(x, 0) = T_1 - T_0, && 0 \le x \le L_x. \end{aligned}\right\} \quad (5.5)$$

Solving (5.5) using separation of variables gives

$$\theta(x,t) = \sum_{n=1}^{\infty} C_n \cos\left[\left(\frac{(2n-1)\pi x}{2L_x}\right)\right] e^{-(2n-1)^2\pi^2\alpha t/4L_x^2}$$

where

$$\theta(x, 0) = T_1 - T_0 = \sum_{n=1}^{\infty} C_n \cos\left[\frac{(2n-1)\pi x}{2L_x}\right]$$

Using the orthogonality of the eigenfunctions gives

$$C_n = \frac{2}{L_x}\int_0^{L_x} (T_1 - T_0) \cos\left[\frac{(2n-1)\pi x}{2L_x}\right] dx = \frac{4}{\pi}\frac{(T_1 - T_0)}{(2n-1)} (-1)^{n-1}$$

$$\therefore\ \theta(x,t) = \frac{4}{\pi}(T_1 - T_0)\sum_{n=1}^{\infty} \frac{(-1)^{n-1}}{(2n-1)} \cos\left[\frac{(2n-1)\pi x}{2L_x}\right] e^{-(2n-1)^2\pi^2\alpha t/4L_x^2}$$

Now θ is known, T is obtained as $T = \theta + T_0$.

(c) See (5.1).

Let $T(x, t) = \theta(x, t) + \psi(t)$.

Homogeneous boundary conditions are obtained for a differential equation involving θ if $\psi = T_w(t)$. With this choice of ψ, the problem becomes

$$\frac{\partial\theta}{\partial t} + \frac{d}{dt}T_w(t) = \alpha\frac{\partial^2\theta}{\partial x^2},\quad 0 \le x \le L_x,\ t > 0 \qquad (5.6)$$

with $\dfrac{\partial\theta}{\partial x}(0, t) = 0, \qquad t > 0,$

$\theta(L_x, t) = 0, \qquad t > 0,$

$\theta(x, 0) = T_1 - T_w(t), \qquad 0 \le x \le L_x$

From (b),

$$\theta(x, t) = \sum_{n=1}^{\infty} D_n(t) \cos\left[\frac{(2n-1)\pi x}{2L_x}\right]$$

where $D_n(0) = \dfrac{4}{\pi}\dfrac{(T_1 - T_w(0))}{(2n-1)}(-1)^{n-1}$

Therefore Equation (5.6) becomes

$$\sum_{n=1}^{\infty} \frac{d}{dt}D_n(t) \cos\left[\frac{(2n-1)\pi x}{2L_x}\right] + \frac{d}{dt}T_w(t)$$

$$= -\alpha\sum_{n=1}^{\infty} D_n(t)\left[\frac{(2n-1)\pi}{2L_x}\right]^2 \cos\left[\frac{(2n-1)\pi x}{2L_x}\right]$$

Using the orthogonality of the eigenfunctions gives

$$\frac{d}{dt}D_n(t)\ \frac{L_x}{2} + \int_0^{L_x}\frac{d}{dt}\,T_w(t)\,\cos\left[\frac{(2n-1)\pi x}{2L_x}\right]dx$$

$$= -\alpha\,D_n(t)\left[\frac{(2n-1)\pi}{2L_x}\right]^2\ \frac{L_x}{2} \qquad (5.7)$$

The above integral $= \frac{d}{dt}T_w(t)\ \frac{2L_x}{(2n-1)\pi}(-1)^{n-1}$

Hence Equation (5.7) becomes

$$\frac{d}{dt}D_n(t) + \lambda\,D_n(t) = f(t)$$

where $\lambda = \alpha\left[\frac{(2n-1)\pi}{2L_x}\right]^2$

and $f(t) = \frac{d}{dt}T_w(t)\ \frac{4}{(2n-1)\pi}(-1)^n.$

Therefore $D_n(t) - D_n(0) = e^{-\lambda t}\int_0^t e^{\lambda\tau}\,f(\tau)d\tau$

i.e. $D_n(t) = D_n(0) + e^{-\lambda t}\int_0^t e^{\lambda\tau}\,f(\tau)d\tau$

θ can now be determined and hence $T = \theta + T_w(t)$ can be calculated.

The difficulty with this analytical solution is knowing $T_w(t)$.
Numerical methods enable it to be calculated.

CHAPTER 6 ONE-DIMENSIONAL NUMERICAL SOLUTION

6.1 Introduction

This chapter finds the solution to the one-dimensional boundary value problem with constant thermal conductivities using explicit numerical methods. All the thermal properties, except for the thermal conductivities of the anode, packing coke and flue wall are adjusted according to the temperature reached at the end of the last time step. The non-constant thermal conductivities case is also examined, but not solved due to the introduction of non-linear terms.

6.2 Constant thermal conductivities

Recall from §3.3 that the boundary value problem is

$$\left.\begin{aligned} &\frac{\partial T}{\partial t} = \alpha \frac{\partial^2 T}{\partial x^2}, && 0 \le x \le L_x, \quad t > 0 \\ \text{with} \quad &\frac{\partial T}{\partial x}(0, t) = 0, && t > 0, \\ &T(L_x, t) = T_w(t), && t > 0, \\ &T(x, 0) = T_1, && 0 \le x \le L_x. \end{aligned}\right\} \quad (6.1)$$

$\frac{\partial T}{\partial t}$ and $\frac{\partial^2 T}{\partial x^2}$ are approximated by using Taylor series expansions.

$$T(x, t + \Delta t) = T(x, t) + \Delta t \frac{\partial T}{\partial t} + O(\Delta t)^2 \ ...$$

$$\therefore \quad \frac{\partial T}{\partial t} = \frac{T(x, t + \Delta t) - T(x, t)}{\Delta t} + O(\Delta t) \ ...$$

$$T(x + \Delta x, t) = T(x, t) + \Delta x \frac{\partial T}{\partial x} + \frac{(\Delta x)^2}{2!} \frac{\partial^2 T}{\partial x^2} + O(\Delta x)^3 + ...$$

$$T(x - \Delta x, t) = T(x, t) - \Delta x \frac{\partial T}{\partial x} + \frac{(\Delta x)^2}{2!} \frac{\partial^2 T}{\partial x^2} - O(\Delta x)^3 + ...$$

$$\therefore \quad \frac{\partial^2 T}{\partial x^2} = \frac{T(x + \Delta x, t) + T(x - \Delta x, t) - 2T(x, t)}{(\Delta x)^2} + O(\Delta x)^2 \ \ldots$$

So $$\frac{\partial T}{\partial t} = \alpha \frac{\partial^2 T}{\partial x^2}$$

is approximated by

$$\frac{T(x, t + \Delta t) - T(x, t)}{\Delta t} = \alpha \left[\frac{T(x + \Delta x, t) + T(x - \Delta x, t) - 2T(x, t)}{(\Delta x)^2} \right] \quad (6.2)$$

where the error of the left hand side is of order Δt, and the error of the right hand side is of order $(\Delta x)^2$.

T_i^n is defined as the block temperature in Kelvin at mesh point i, $i \in \mathbb{Z}^+$, at time step n, $n \in \mathbb{Z}^+$. i runs from 1 to Nx where $i = 1$ is the mesh point on $x = 0$ and $i = Nx$ is the mesh point on $x = L_x$.

Δx is the distance between mesh points in metres. n runs from 1 to the end of the time period, where $n = 1$ corresponds to $t = 0$ and $n = Nt$ corresponds to the end of the time period. Δt is the length between time steps in seconds.

Rewriting Equation (6.2) using the subscript/superscript notation gives:

$$\frac{T_i^{n+1} - T_i^n}{\Delta t} = \alpha_i^n \left[\frac{T_{j+1}^n + T_{i-1}^n - 2T_i^n}{(\Delta x)^2} \right]$$

i.e. $$T_i^{n+1} = Fo_i^n \left[T_{i+1}^n + T_{i-1}^n + \left(\frac{1}{Fo_i^n} - 2 \right) T_i^n \right] \quad (6.3)$$

where $Fo_i^n = \frac{\alpha_i^n \Delta t}{(\Delta x)^2} \equiv$ the Fourier number of the block at mesh point i at time step n and it is dimensionless; $\alpha_i^n \equiv$ the thermal diffusivity of the block at mesh point i at time step n, in m^2/s.

If $Fo_i^n > \frac{1}{2}$, then the higher the value of T_i^n, the lower will be the resulting value of T_i^{n+1}. It can be shown that this may lead to difficulties in regard to the Law of Conservation of Energy (Rogers and Mayhew, 1992).

If $i = Nx$, then the value of $T_{i+1} = T_{Nx+1}$ in Equation (6.3) is not known. On the flue wall, the rate of heat flow per unit area (J/sm^2) at time step $n \equiv \dot{Q}w^n$ say $= \frac{dQw^n}{dt} = -k_{Nx}^n \frac{\partial T_{Nx}^n}{\partial x}$, by Fourier's Law.

But by conservation of heat flow at the flue wall, the rate of heat per unit area flowing out through the wall by conduction = the rate of heat per unit area flowing into the fluid or air by convection and radiation.

i.e. $$-k_{Nx}^n \frac{\partial T_{Nx}^n}{\partial x} = h^n \left(T_{Nx}^n - Tf\right) \qquad (6.4)$$

where $h^n \equiv$ the heat transfer coefficient at the flue wall at time step n, in W/m^2K,

$Tf^n \equiv$ the fluid or air temperature at time step n, in K,

(Tf^n is assumed to be constant for all n, so Tf^n is denoted as Tf)

and $k_{Nx}^n \equiv$ the thermal conductivity of the block at mesh point Nx at time step n, in W/mK.

$$\therefore \quad \frac{\partial T_{Nx}^n}{\partial x} = \frac{-h^n}{k_{Nx}^n} \left(T_{Nx}^n - Tf\right) \qquad (6.5)$$

Now imagine that the side of the flue wall is increased by Δx to $L_x + \Delta x$, which corresponds to the mesh point Nx + 1. Suppose that the temperature here varies in such a way that the temperature at i = Nx is always what it should be under the conditions of the actual problem.

Using a Taylor series expansion gives

$$\frac{\partial T^n_{Nx}}{\partial x} = \frac{T^n_{Nx+1} - T^n_{Nx-1}}{2\Delta x} + O(\Delta x)^2 \ ...$$

$$= \frac{-h^n}{k^n_{Nx}} \left(T^n_{Nx} - Tf\right) \quad \text{from Equation (6.5)}$$

$$\therefore \qquad T^n_{Nx+1} = \frac{-2\Delta x h^n}{k^n_{Nx}} \left(T^n_{Nx} - Tf\right) + T^n_{Nx-1}$$

where the error of this approximation is $(\Delta x)^2$.

Substituting this into Equation (6.3) gives at $i = Nx$,

$$T^{n+1}_{Nx} = Fo^n_{Nx} \left[2Bi^n Tf + 2T^n_{Nx-1} + \left(\frac{1}{Fo^n_{Nx}} - 2(1 + Bi^n) \right) T^n_{Nx} \right],$$

where $Bi^n = \frac{\Delta x h^n}{k^n_{Nx}} \equiv$ the Biot number of the block at time step n and it is dimensionless.

As before, in order to satisfy the Law of Conservation of Energy, it is required that

$$\frac{1}{Fo^n_{Nx}} - 2(1 + Bi^n) \geq 0$$

$$\Rightarrow \qquad Fo^n_{Nx} \leq \frac{1}{2(1 + Bi^n)}$$

At $i = 1$, the value of $T_{i-1} = T_{1-1} = T_0$ in Equation (6.3) is not known. A Taylor series expansion gives

$$\frac{\partial T^n_1}{\partial x} = \frac{T^n_2 - T^n_0}{2\Delta x} + O(\Delta x)^2 \ ...$$

The adiabatic boundary condition is $\frac{\partial T^n_1}{\partial x} = 0$

$$\therefore \qquad \frac{T_2^n - T_0^n}{2\Delta x} = 0 \text{ where the error of the left hand side is of order } (\Delta x)^2.$$

$$\therefore \qquad T_2^n = T_0^n .$$

Substituting this into Equation (6.3) gives at $i = 1$,

$$T_1^{n+1} = Fo_1^n \left[2T_2^n + \left(\frac{1}{Fo_1^n} - 2 \right) T_1^n \right],$$

where $Fo_1^n \leq \frac{1}{2}$.

Determining Fo_i^n

$$Fo_i^n = \frac{\alpha_i^n \Delta t}{(\Delta x)^2}$$

(a) Obtaining α_i^n

$$\alpha_i^n = \frac{k_i}{\rho_i (c_p)_i^n}$$

k_i is constant within each of the anode, packing coke and flue wall, and equals ka, kp or kw depending on whether the calculations are occurring in the anode, packing coke or flue wall. k_i is calculated using the temperature midway between the initial and assumed final average temperature of the block. Suppose this final average block temperature is Tf.

For example, suppose the initial block temperature is 873 K and Tf is 373 K.

So k_i is calculated using $373 + \frac{873 - 373}{2} = 623$ K.

ka $= (2.53 \times 10^{-3})\, 623 + 3.90,$ see Equation (4.1)
kp $= (1.27 \times 10^{-3})\, 623 - 1.99 \times 10^{-1},$ see Equation (4.4)
kw $= (6.91 \times 10^{-4})\, 623 + 8.96 \times 10^{-1},$ see Equation (4.7)

ρ_i = ρa, ρp or ρw and $(c_p)_i^n$ = $(ca_p)_i^n$, $(cp_p)_i^n$ or $(cw_p)_i^n$ depending on whether the calculations are occurring in the anode, packing coke or flue wall.

For example, suppose the initial and assumed final block temperatures are as before, and the temperature at mesh point i which is in the packing coke at time step n is 685 K.

Then $kp = (1.27 \times 10^{-3})623 - 1.99 \times 10^{-1}$

$= 5.92 \times 10^{-1}$ W/mK

$\rho p = 670$ kg/m^3

and $(cp_p)_i^n = (1.28)685 + 5.27 \times 10^2$, see Equation (4.6)

$= 1.40 \times 10^3$ J/kgK

Therefore

$$\alpha p_i^n = \frac{5.92 \times 10^{-1}}{(670)(1.40 \times 10^3)} \text{ m}^2/\text{s}$$

(αp_i^n is the thermal diffusivity of the packing coke at mesh point i at time step n.)

(b) Obtaining Δx

Depending on whether the calculations are occurring in the anode, packing coke or flue wall, Δxa, Δxp or Δxw are used respectively. To obtain Δxa, the number of spatial steps in the anode, Nxa, are specified and then the width of the anode is divided by Nxa–1.

That is, $$\Delta xa = \frac{\text{width of the anode}}{Nxa - 1} .$$

Similarly for Δxp and Δxw.

(c) Obtaining Δt

See later

Determining Bi^n

$$Bi^n = \frac{\Delta x\, h^n}{k^n_{Nx}} = \frac{(\Delta x w)h^n}{kw}$$

(a) Obtaining kw

See (a) on p. 38.

(b) Obtaining h^n

h^n has two components - radiation and convection, that is

$h^n = hr^n + hc^n$,

where $hr^n \equiv$ the heat transfer coefficient for radiation at time step n

and $hc^n \equiv$ the heat transfer coefficient for convection at time step n

(both in $W/m^2 K$).

hc^n is a function of Tf^n, and Tf^n is assumed it to be constant for all n. Therefore hc^n is denoted as hc.

$$hr^n = \varepsilon \sigma \left(T^n_{Nx} - Tf\right) \left(\left(T^n_{Nx}\right)^2 - (Tf)^2\right)$$

where $\varepsilon \equiv$ wall surface emissivity and is dimensionless

$= 0.97$ [Braithwaite (private communication, 1993)]

and $\sigma \equiv$ Stefan-Boltzmann constant

$= 5.67 \times 10^{-8}\ W/m^2 K^4$.

$$hc = \frac{(kf)Nu}{\ell}$$

where $kf \equiv$ thermal conductivity of the fluid or air, in W/mK,

$Nu \equiv$ the Nusselt number (dimensionless)

and $\ell \equiv$ the characteristic length

$$= \frac{4 \times \text{area}}{\text{perimeter}} \text{ m.}$$

See Figure 2.3 for the dimensions of a flue.

Note: Since the air in the flue is being blown or sucked past the end of the block, it is assumed that forced convection is occurring rather than natural or free convection. Buoyancy forces, which are associated with natural convection, are ignored here.

$$Nu = 0.023\ Re^{0.8}\, Pr^{0.4}. \qquad (6.6)$$

where $Re \equiv$ Reynolds number (dimensionless)

and $Pr \equiv$ Prandtl number (dimensionless)

This equation for Nu assumes that:

(i) the flow is turbulent, i.e. Re > 4000 (this is checked in the program);

(ii) the flow is fully developed, i.e. the ratio of channel length to ℓ is greater than 20, which it is since

$$\frac{\text{length of flue}}{\ell} = \frac{L_y}{\ell} = \frac{4.664}{\frac{4 \times 0.026344}{0.652}} \approx 29;$$

(iii) the physical properties are constant, which they are.

$$Re = \frac{(\rho f) v \ell}{\mu}$$ ($v \equiv$ the velocity of the air, m/s, $\rho f \equiv$ the density of the fluid or air, kg/m^3, and $\mu \equiv$ the dynamic viscosity of the air, kg/ms)

or $$Re = \frac{\dot{m}\ell}{\mu(\text{area})}$$ ($\dot{m} \equiv$ the mass flow, kg/s)

$$= \frac{4\dot{m}}{\mu(\text{perimeter})} \qquad (6.7)$$

Note: There are 5 fire shafts in a section and the centre one is blocked off. So if the total mass flow through all 4 fire shafts is x kg/s, then the mass flow through one flue is x/96 kg/s, since there are 96 flues in a section, and x/4 kg/s per fire shaft.

$$\dot{m} = \frac{(\rho f) L}{\Delta p}$$

where $L \equiv$ the connected load of the drive motor of a fan (1500 W for a blower, 3000 W for a sucker),

$\Delta p \equiv$ the total pressure difference across a fan
(200 N/m^2 for a blower or sucker),

and $\rho f \approx 0.75$ kg/m^3 - see §8.2, Figure 8.1.

Therefore

$$\dot{m} \approx \begin{cases} 5.6 \text{ kg/s for a blower} \\ 11.3 \text{ kg/s for a sucker} \end{cases}$$

$$Pr = \frac{cf_p \mu}{kf},$$

where $cf_p \equiv$ the specific heat capacity at constant pressure of the fluid or air, in J/kgK.

cf_p, μ and kf all vary according to the temperature of the air, so hc = hc(Tf)

Values for kf, Pr and cf_p were obtained from Perry *et al.* (1984). Then

$$\mu = \frac{(kf)\, Pr}{cf_p} \qquad (6.8)$$

can be determined.

Linear approximations are used for kf and cf_p and a quadratic approximation for Pr. See Figures 6.1 - 6.3 respectively.

For the quadratic approximation, the equation
$p(T) = p(T_0) + (T - T_0)p[T_0, T_1] + (T - T_0)(T - T_1)\, p[T_0, T_1, T_2]$ is used (Burden and Faires, 1989) where

$$p[T_0, T_1, T_2] = \frac{p[T_1, T_2] - p[T_0, T_1]}{T_2 - T_0}$$

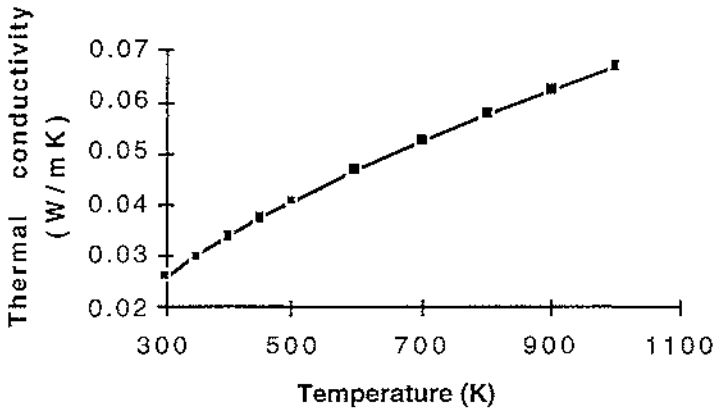

Figure 6.1
Thermal conductivity of air [interpolated from data from Perry *et al.* (1984)]

$$kf = (5.65 \times 10^{-5})\,Tf + 1.02 \times 10^{-2} \qquad (6.9)$$

using the points $(350, 3.00 \times 10^{-2})$ and $(1000, 6.67 \times 10^{-2})$.

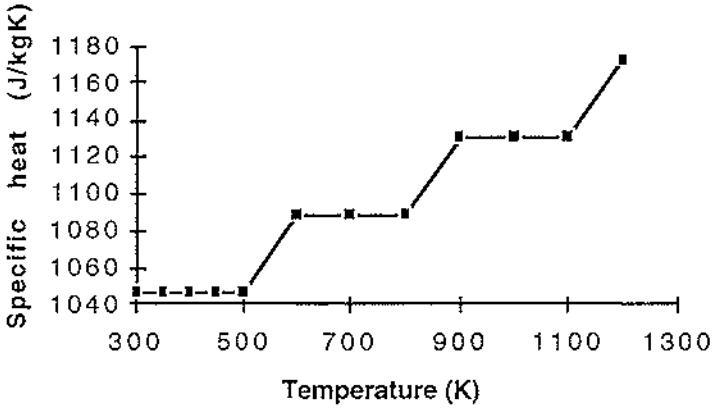

Figure 6.2
Specific heat of air at 1 atmosphere [interpolated from data from Perry *et al.* (1984)]

$$cf_p = (1.38 \times 10^{-1})\,Tf + 9.92 \times 10^{2} \qquad (6.10)$$

using the points $(400, 1.047 \times 10^{3})$ and $(1000, 1.130 \times 10^{3})$.

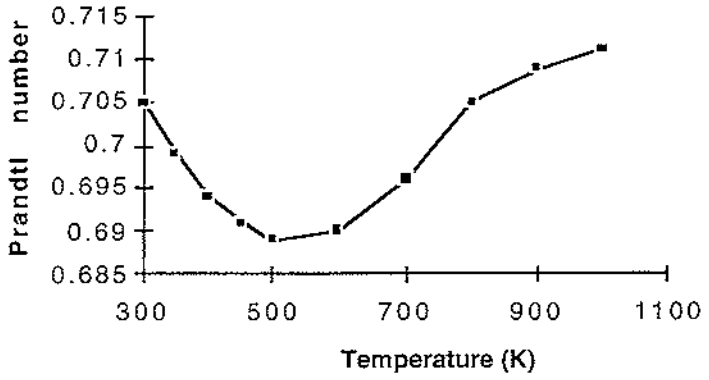

Figure 6.3
Prandtl number of air at 1 bar [interpolated from data from Perry *et al.* (1984)]

$$Pr = (1.89 \times 10^{-7})\,Tf^2 - (2.20 \times 10^{-4})\,Tf + 7.54 \times 10^{-1} \qquad (6.11)$$

using the points $(300, 7.05 \times 10^{-1})$, $(600, 6.90 \times 10^{-1})$ and $(900, 7.09 \times 10^{-1})$.

Determining Δt

(a) Obtaining Δta (the length of the time step in the anode)

$$Foa_i^n \leq \frac{1}{2}$$

(Foa_i^n is the Fourier number of the anode at mesh point i at time step n)

i.e. $$\frac{(\alpha a_i^n)(\Delta ta)}{(\Delta xa)^2} \leq \frac{1}{2}$$

(αa_i^n is the thermal diffusivity of the anode at mesh point i at time step n)

$$\therefore \quad \Delta ta \leq \frac{(\Delta xa)^2}{2\alpha a_i^n}$$

The upper bound on Δta is obtained by calculating the maximum value that αa_i^n can take.

$$\max.\ \alpha a_i^n = \frac{ka}{(\rho a)(\min.(ca_p)_i^n)}$$

Suppose the minimum block temperature equals the assumed final average block temperature which equals Tf (see the discussion earlier in this section).

$$\text{min. } (ca_p)_i^n = (1.31)Tf + 4.55 \times 10^2, \text{ see Equation (4.3)}$$

(b) Obtaining Δtp (the length of the time step in the packing coke).

Similarly $\Delta tp \leq \dfrac{(\Delta xp)^2}{2\alpha p_i^n}$ and the upper bound on Δtp is obtained by calculating the maximum value that αp_i^n can take.

$$\text{max. } \alpha p_i^n = \frac{kp}{(\rho p)(\text{min.}(cp_p)_i^n)}$$

and $\text{min. } (cp_p)_i^n = (1.28)Tf + 5.27 \times 10^2$, see Equation (4.6).

(c) Obtaining Δtw (the length of the time step in the flue wall)

$$Fow_i^n \leq \text{min. } \left(\frac{1}{2}, \frac{1}{2(1+Bi^n)}\right)$$ (Fow_i^n is the Fourier number of the flue wall at mesh point i at time step n)

$$= \frac{1}{2(1 + Bi^n)}, \qquad \text{since } Bi^n > 0 \text{ for all n.}$$

i.e. $$\frac{(\alpha w_i^n)(\Delta tw)}{(\Delta xw)^2} \leq \frac{1}{2(1 + Bi^n)}$$ (αw_i^n is the thermal diffusivity of the flue wall at mesh point i at time step n)

$$\therefore \quad \Delta tw \leq \frac{(\Delta xw)^2}{2\alpha w_i^n (1 + Bi^n)}$$

The upper bound on Δtw is obtained by calculating the maximum values that αw_i^n and Bi^n can take.

$$\max.\ \alpha w_i^n = \alpha w = \frac{kw}{(\rho w)(cw_p)}, \quad \text{see §4.4.}$$

Since $Bi^n = \frac{(\Delta xw)h^n}{kw}$, the maximum value of Bi^n is obtained by calculating the maximum value of h^n.

$$\max.\ h^n = \max.\ hr^n + \max.\ hc^n$$

$$\begin{aligned}
\max.\ hr^n &= \varepsilon\sigma\left[\max.\ T_{Nx}^n - Tf\right]\left[(\max.\ T_{Nx}^n)^2 - (Tf)^2\right] \\
&= \varepsilon\sigma\left[\text{initial } T_{Nx} - Tf\right]\left[(\text{initial } T_{Nx})^2 - (Tf)^2\right] \\
&= \varepsilon\sigma\left[T_{Nx}^1 - Tf\right]\left[(T_{Nx}^1)^2 - (Tf)^2\right] \\
&= hr^1
\end{aligned}$$

$$\begin{aligned}
\max.hc^n &= \frac{(\max.kf)(\max.Nu)}{\ell} \\
&= \frac{(kf)(Nu)}{\ell}, \text{ since Tf is assumed to be constant} \\
&= hc
\end{aligned}$$

(d) Obtaining the overall Δt

The upper bound on the overall Δt = minimum (max. Δta, max. Δtp, max. Δtw).

Temperature on the anode/packing coke boundary

The temperature on the anode/packing boundary needs to satisfy the equations for temperature distribution in both the anode and packing coke.

Ta_q^n and Foa_q^n are defined as the anode temperature (in Kelvin) and Fourier number respectively at mesh point q, $q \in Z^+$, at time step n, $n \in Z^+$. q runs from 1 to Nxa, where $q = 1$ is the mesh point on $x = 0$, and $q = Nxa$ is the mesh point on the anode/packing coke boundary.

Similarly, Tp_r^n and Fop_r^n are defined as the packing coke temperature (in Kelvin) and Fourier number respectively at mesh point r, $r \in Z^+$, at time step n, $n \in Z^+$. r runs from 1 to Nxp, where $r = 1$ is the mesh point on the

anode/packing coke boundary, and r = Nxp is the mesh point on the packing coke/flue wall boundary.

At q = Nxa.

From Equation (6.3)

$$Ta_{Nxa}^{n+1} = Foa_{Nxa}^{n}\left[Ta_{Nxa+1}^{n} + Ta_{Nxa-1}^{n} + \left(\frac{1}{Foa_{Nxa}^{n}} - 2\right)Ta_{Nxa}^{n}\right] \quad (6.12)$$

Ta_{Nxa+1}^{n} is an imaginary mesh point outside the anode, which coincides with Tp_2^n only if $\Delta xa = \Delta xp$.

At r = 1.

From Equation (6.3)

$$Tp_1^{n+1} = Fop_1^{n}\left[Tp_2^{n} + Tp_0^{n} + \left(\frac{1}{Fop_1^{n}} - 2\right)Tp_1^{n}\right] \quad (6.13)$$

Tp_0^n is an imaginary point outside the packing coke, which coincides with Ta_{Nxa-1}^{n} only if $\Delta xa = \Delta xp$.

By Fourier's Law, on the anode/packing coke boundary

$$\dot{Q}(t) = dQ/dt = -k\nabla T = -k\frac{\partial T}{\partial x} \approx -k\left(\frac{T(x+\Delta x, t) - T(x-\Delta x, t)}{2\Delta x}\right),$$

$\dot{Q}(t) \equiv$ the rate of heat flow per unit area, in J/sm^2.

i.e. $$-ka\left(\frac{Ta_{Nxa+1}^{n} - Ta_{Nxa-1}^{n}}{2\Delta xa}\right) = -kp\left(\frac{Tp_2^{n} - Tp_0^{n}}{2\Delta xp}\right) \quad (6.14)$$

Equations (6.12) - (6.14) involve three unknowns: Ta_{Nxa+1}^{n}, Tp_0^n and $Ta_{Nxa}^{n+1} = Tp_1^{n+1}$. These equations are solved for Tp_1^{n+1}, the temperature at time step n + 1 on the anode/packing coke boundary, using the fact that $Ta_{Nxa}^{n} = Tp_1^{n}$.

$$Tp_1^{n+1} = \frac{Fop_1^n}{\Gamma_1}\left\{2Tp_2^n + 2\left[\frac{ka}{kp}\frac{\Delta xp}{\Delta xa}\right]Ta_{Nxa-1}^n + \left[\frac{ka}{kp}\frac{\Delta xp}{\Delta xa}\left(\frac{1}{Foa_{Nxa}^n} - 2\right) + \left(\frac{1}{Fop_1^n} - 2\right)\right]Tp_1^n\right\} \quad (6.15)$$

where $\Gamma_1 = 1 + \frac{Fop_1^n}{Foa_{Nxa}^n}\frac{ka}{kp}\frac{\Delta xp}{\Delta xa}$.

In order to satisfy the Law of Conservation of Energy it is required that the coefficients of Tp_2^n, Ta_{Nxa-1}^n and $Tp_1^n \geq 0$.

Since ka, kp, αa_{Nxa}^n and $\alpha p_1^n > 0$ for all possible temperatures of interest and $Foa_{Nxa}^n \leq \frac{1}{2}$, $Fop_1^n \leq \frac{1}{2}$ (the restrictions determined earlier), then the coefficients ≥ 0.

Temperature on the packing coke/flue wall boundary

This case is similar to the anode/packing coke boundary one. Therefore

$$Tw_1^{n+1} = \frac{Fow_1^n}{\Gamma_2}\left\{2Tw_2^n + 2\left[\frac{kp}{kw}\frac{\Delta xw}{\Delta xp}\right]Tp_{Nxp-1}^n + \left[\frac{kp}{kw}\frac{\Delta xw}{\Delta xp}\left(\frac{1}{Fop_{Nxp}^n} - 2\right) + \left(\frac{1}{Fow_1^n} - 2\right)\right]Tw_1^n\right\} \quad (6.16)$$

where $\Gamma_2 = 1 + \frac{Fow_1^n}{Fop_{Nxp}^n}\frac{kp}{kw}\frac{\Delta xw}{\Delta xp}$.

Tw_s^n and Fow_s^n are the flue wall temperature (in Kelvin) and Fourier number respectively at mesh point s, $s \in Z^+$, at time step n, $n \in Z^+$. s runs from 1 to Nxw where s = 1 is the mesh point on the packing coke/flue wall boundary and s = Nxw is the mesh point on $x = L_x$.

As in the previous case, the coefficients of Tw_2^n, Tp_{Nxp-1}^n and $Tw_1^n \geq 0$, so the Law of Conservation of Energy is satisfied.

Summary

The numerical solution of (6.1) requires the solution of

1 $$Ta_1^{n+1} = Foa_1^n \left[2Ta_2^n + \left(\frac{1}{Foa_1^n} - 2 \right) Ta_1^n \right],$$

2 $$Ta_q^{n+1} = Foa_q^n \left[Ta_{q+1}^n + Ta_{q-1}^n + \left(\frac{1}{Foa_q^n} - 2 \right) Ta_q^n \right],$$

$$q = 2 \text{ to } Nxa-1,$$

3 $$Ta_{Nxa}^{n+1} = Tp_1^{n+1}$$, see Equation (6.15),

4 $$Tp_r^{n+1} = Fop_r^n \left[Tp_{r+1}^n + Tp_{r-1}^n + \left(\frac{1}{Fop_r^n} - 2 \right) Tp_r^n \right]$$

$$r = 2 \text{ to } Nxp-1,$$

5 $$Tp_{Nxp}^{n+1} = Tw_1^{n+1}$$, see Equation (6.16),

6 $$Tw_s^{n+1} = Fow_s^n \left[Tw_{s+1}^n + Tw_{s-1}^n + \left(\frac{1}{Fow_s^n} - 2 \right) Tw_s^n \right]$$

$$s = 2 \text{ to } Nxw-1,$$

7 $$Tw_{Nxw}^{n+1} = Fow_{Nxw}^n \left[2Bi^n Tf + 2Tw_{Nxw-1}^n + \left(\frac{1}{Fow_{Nxw}^n} - 2\left(1 + Bi^n\right) \right) Tw_{Nxw}^n \right]$$

provided $$Foa_q^n \leq \frac{1}{2}, \qquad q = 1 \text{ to } Nxa,$$

$$Fop_p^n \leq \frac{1}{2}, \qquad r = 1 \text{ to } Nxp,$$

$$Fow_s^n \leq \frac{1}{2}, \qquad s = 1 \text{ to } Nxw - 1,$$

$$Fow_{Nxw}^n \leq \frac{1}{2(1 + Bi^n)}, \qquad n > 1.$$

6.3 Non-constant thermal conductivities

Here the boundary value problem is (see §3.3)

$$\left.\begin{aligned} &\frac{\partial T}{\partial t} = \hat{\alpha}\left(\frac{\partial T}{\partial x}\right)^2 + \alpha \frac{\partial^2 T}{\partial x^2}, \quad 0 \le x \le L_x, \ t > 0 \\ \text{with} \quad &\frac{\partial T}{\partial x}(0, t) = 0, \qquad t > 0, \\ &T(L_x, t) = T_w(t), \qquad t > 0, \\ &T(x, 0) = T_1, \qquad 0 \le x \le L_x. \end{aligned}\right\} \quad (6.17)$$

$\left(\frac{\partial T}{\partial x}\right)^2$ has to be approximated as well as $\frac{\partial T}{\partial t}$ and $\frac{\partial^2 T}{\partial x^2}$. As in §6.2, $\frac{\partial T}{\partial x}$ is approximated by using a Taylor series expansion.

$$T(x + \Delta x, t) = T(x, t) + \Delta x \frac{\partial T}{\partial x} + \frac{(\Delta x)^2}{2!} \frac{\partial^2 T}{\partial x^2} + O(\Delta x)^3 + \ldots$$

$$T(x - \Delta x, t) = T(x, t) - \Delta x \frac{\partial T}{\partial x} + \frac{(\Delta x)^2}{2!} \frac{\partial^2 T}{\partial x^2} - O(\Delta x)^3 + \ldots$$

$$\therefore \quad \left(\frac{T(x + \Delta x, t) - T(x - \Delta x, t)}{2\Delta x}\right)^2 = \left(\frac{\partial T}{\partial x} + O(\Delta x)^2 + \ldots\right)^2$$

$$= \left(\frac{\partial T}{\partial x}\right)^2 + O(\Delta x)^2 \ldots$$

$$\therefore \quad \left(\frac{\partial T}{\partial x}\right)^2 = \left[\frac{T(x + \Delta x, t) - T(x - \Delta x, t)}{2\Delta x}\right]^2$$

This approximation for $\left(\frac{\partial T}{\partial x}\right)^2$ has error of order $(\Delta x)^2$.

If $\frac{\partial T}{\partial t}$ and $\frac{\partial^2 T}{\partial x^2}$ are approximated as in §6.2, then the partial differential equation

$$\frac{\partial T}{\partial t} = \hat{\alpha}\left(\frac{\partial T}{\partial x}\right)^2 + \alpha \frac{\partial^2 T}{\partial x^2} \quad \text{is approximated}$$

by $$\frac{T(x, t+\Delta t) - T(x, t)}{\Delta t} = \hat{\alpha}\left[\frac{T(x+\Delta x, t) - T(x-\Delta x, t)}{2\Delta x}\right]^2 + \alpha\left[\frac{T(x+\Delta x, t) + T(x-\Delta x, t) - 2T(x, t)}{(\Delta x)^2}\right],$$

where the error of the left hand side is of order Δt, and the error of the right hand side is of order $(\Delta x)^2$.

Therefore, in subscript/superscript notation,

$$T_i^{n+1} = \hat{Fo}_i^n\left[T_{i+1}^n - T_{i-1}^n\right]^2 + Fo_i^n\left[T_{i+1}^n + T_{i-1}^n + \left(\frac{1}{Fo_i^n} - 2\right)T_i^n\right] \quad (6.18)$$

where $\hat{Fo}_i^n = \frac{\hat{\alpha}_i^n \Delta t}{4(\Delta x)^2} \equiv$ the 'hatted' Fourier number of the block at mesh point i at time step n, in 1/K,

and $\hat{\alpha}_i^n \equiv$ the 'hatted' thermal diffusivity of the block at mesh point i at time step n, in m^2/sK,

As in §6.2, $Fo_i^n \leq \frac{1}{2}$.

and $$T_{Nx+1}^n = \frac{-2\Delta x h^n}{k_{Nx}^n}\left(T_{Nx}^n - Tf\right) + T_{Nx-1}^n$$

Substituting for T_{Nx+1}^n in Equation (6.18) gives at i = Nx:

$$T_{Nx}^{n+1} = \hat{Fo}_{Nx}^n\left[-2B_i^n\left(T_{Nx}^n - Tf\right)\right]^2 + Fo_{Nx}^n\left[2Bi^n Tf + 2T_{Nx-1}^n + \left(\frac{1}{Fo_{Nx}^n} - 2\left(1+Bi^n\right)\right)T_{Nx}^n\right] \quad (6.19)$$

where $Bi^n = \frac{\Delta x\, h^n}{k^n_{Nx}}$.

As in §6.2, $Fo^n_{Nx} \leq \frac{1}{2(1+Bi^n)}$.

The boundary condition at i = 1 gives $T^n_2 = T^n_0$, as before. Substituting this into Equation (6.18) gives at i = 1:

$$T^{n+1}_1 = \hat{Fo}^n_1 \left[T^n_2 - T^n_2\right]^2 + Fo^n_1 \left[T^n_2 + T^n_2 + \left(\frac{1}{Fo^n_1} - 2\right)T^n_1\right]$$

$$= Fo^n_1 \left[2T^n_2 + \left(\frac{1}{Fo^n_1} - 2\right)T^n_1\right]$$

with $Fo^n_1 \leq \frac{1}{2}$.

Equations (6.18) and (6.19) involve non-linear terms. Because of this, it was decided to leave the non-constant thermal conductivities case at this point.

6.4 Results

As input, the program requires an initial block temperature (Ta^1_q, q = 1 to Nxa, Tp^1_r, r = 1 to Nxp, Tw^1_s, s = 1 to Nxw), an air temperature (Tf), the number of mesh points in the anode (Nxa), packing coke (Nxp) and flue wall (Nxw), the mass flow ($\dot{m}$) and finally the length of the time period. The mass flow is the total mass flow through all 4 fire shafts. The program's output is the transient temperature distribution of the block.

The initial block temperature is assumed to be equal at all mesh points and is chosen as 600 ^{0}C. Tf is chosen to be 20 ^{0}C, Nxa = 15, Nxp = 4, Nxw = 4 and the length of the time period = 96 hours. The length of the overall time step (Δt) is chosen to be 20 seconds. The number of mesh points coupled with the small Δt is sufficient for convergence, that is, more mesh points and a smaller Δt do not alter the temperatures significantly. Mesh point 1 corresponds to x = 0 and mesh point 21 to x = L_x. Δxa, Δxp and Δxw are approximately the same - 0.028 to 0.032 m.

As shown in §1.1, Figure 1.1, the fire trains being used at the New Zealand Aluminium Smelters Ltd have 3 forced cooling sections. Assuming a fire cycle time of 32 hours, the fans are moved in the fire direction by one section every 32 hours. Therefore each section undergoes $3 \times 32 = 96$ hours of forced cooling.

Figures 6.4 - 6.6 show the temperature profile of the block at 32 , 64 and 96 hours for various mass flows.

The arrows in the figures indicate the mesh points on the anode/packing coke and packing coke/flue wall boundaries.

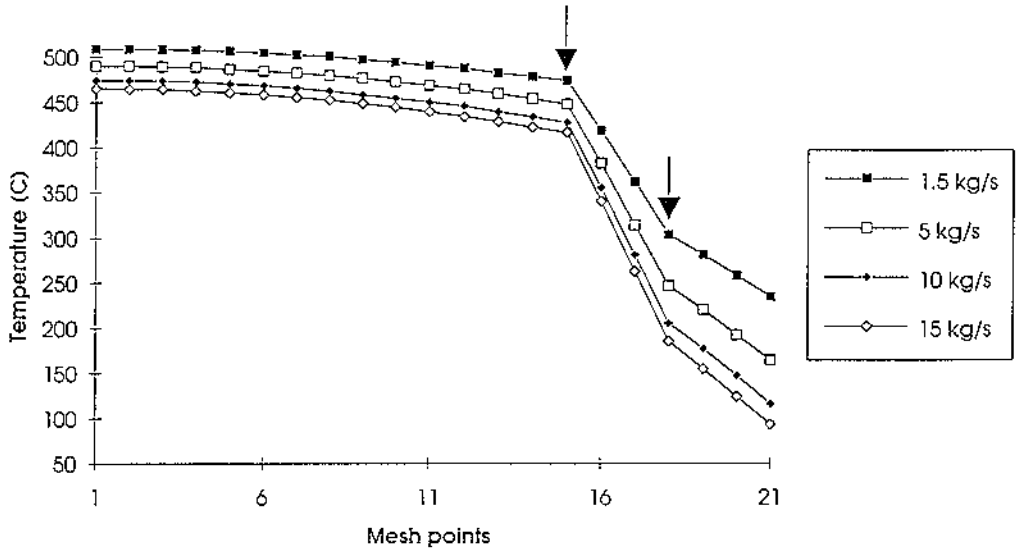

Figure 6.4
Temperature profile of the block at 32 hours (1 fire cycle)

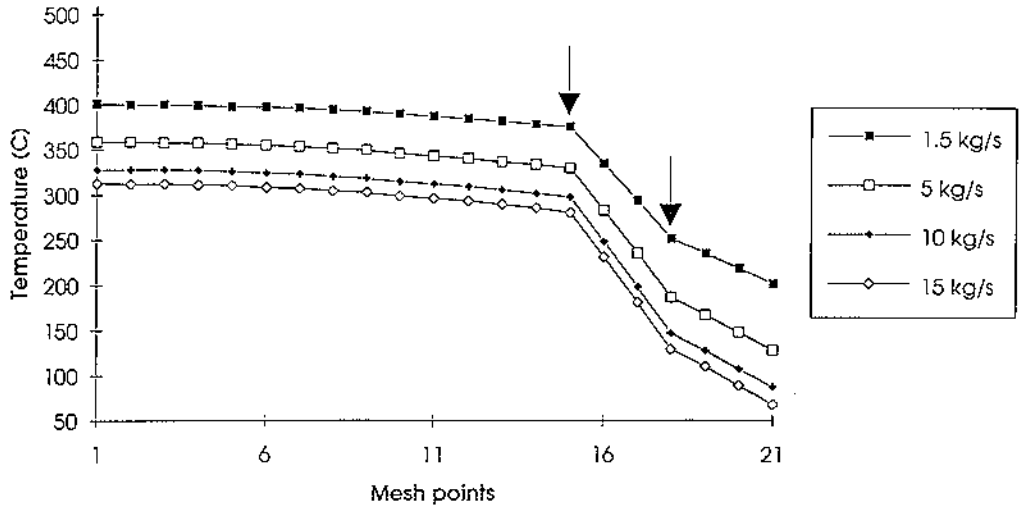

Figure 6.5
Temperature profile of the block at 64 hours (2 fire cycles)

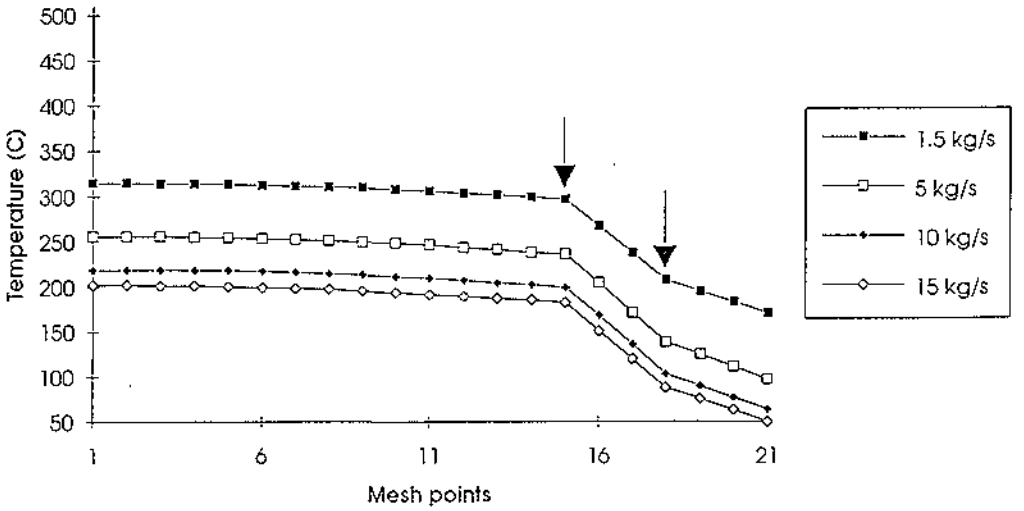

Figure 6.6
Temperature profile of the block at 96 hours (3 fire cycles)

Figure 6.7 shows the temperature profile of the block at 96 hours for different thermal conductivities, but a constant mass flow (5 kg/s). Firstly the thermal conductivities of the three materials (ka, kp and kw) are calculated as discussed in §6.2. Then ka is divided by 2, whilst kp and kw are left unaltered. Then kp is divided by 2, whilst ka and kw are left unaltered. Finally kw is divided by 2, whilst ka and kp are left unaltered.

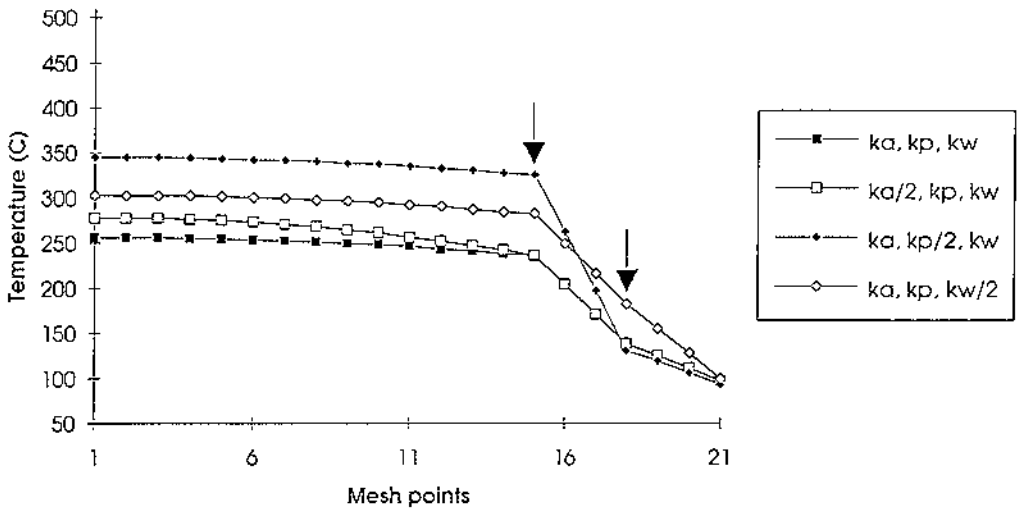

Figure 6.7
Temperature profile of the block at 96 hours with $\dot{m} = 5$ kg/s

6.5 Discussion of results

Figures 6.4 - 6.6 show that when the mass flows increase, the block cools more quickly. They also show that as time goes on and the temperature difference between the block and the air decreases, then the rate of cooling of the block also decreases. These results confirm that the set-up of the model and the calculations are correct.

For this particular set of initial temperatures, it takes a mass flow of 15 kg/s in order for the anodes to reach approximately 200 °C at 96 hours (3 fire cycles) - see Figure 6.6. This is similar to the mass flows used experimentally. At about this temperature, the anodes can be safely removed from the pits and stacked on the floor.

As expected, altering the thermal conductivities effects the cooling rate of the anodes, see Figure 6.7. The greatest effect on anode cooling occurs when kp is altered. Altering ka produces the least effect, whilst altering kw produces an intermediate effect. This result agrees with that of Furman and Martirena (1980). It was found that kp was one of the two parameters which decisively influenced the calculations, see §1.2.

CHAPTER 7 TWO-DIMENSIONAL NUMERICAL SOLUTION

7.1 Introduction

Only the constant thermal conductivities case is examined. The main difference, besides the increase in dimension, between this chapter and the previous one, is that here the fluid or air temperature in the flue is not constant. As mentioned in §1.3, the air temperature (and pressure) is changing as heat is transferred from the block out into the air in the flue.

7.2 Air Flow in the Flue

An elemental volume (V) of air in the 'large' flue is considered, as shown in Figure 7.1.

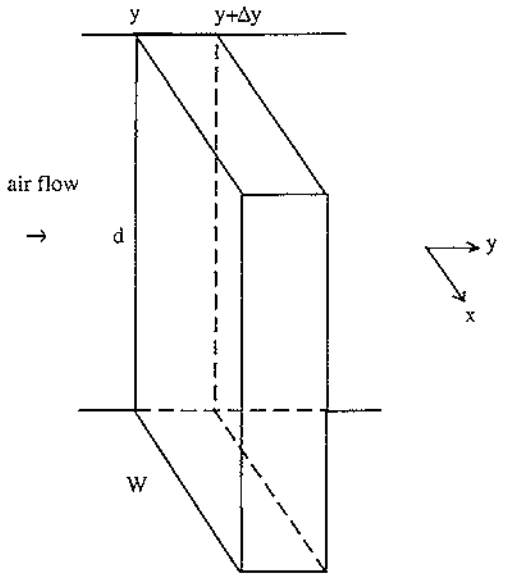

Figure 7.1
Elemental volume of air in the flue

$V = d\,W\,\Delta y\ m^3$, where $d = 0.238$ m and $W = 0.111$ m (see Figure 2.6).

Mass of the air in $V = \rho f \times d \times W \times \Delta y$ kg ($\rho f \equiv$ density of air or fluid in kg/m^3)

Energy of the air in V = mass × specific heat capacity × temperature

$$= ((\rho f) dW\Delta y) \times cf_p \times Tf \ J$$

By the conservation of mass:
The change in the mass of the air in V over time Δt = the mass of the air entering V during time Δt – the mass of the air leaving V during time Δt.

i.e. $\left((\rho f)dW\Delta y\right)_{t+\Delta t} - \left((\rho f)dW\Delta y\right)_t = \left((\rho f)vdW\right)_y \Delta t - \left((\rho f)vdW\right)_{y+\Delta y} \Delta t$

($v \equiv$ the velocity of the air in m/s)

$$\Rightarrow \quad \frac{(\rho f)_{t+\Delta t} - (\rho f)_t}{\Delta t} + \frac{((\rho f)v)_{y+\Delta y} - ((\rho f)v)_y}{\Delta y} = 0$$

$$\Rightarrow \quad \frac{\partial(\rho f)}{\partial t} + \frac{\partial}{\partial y}((\rho f)v) = 0 \qquad (7.1)$$

Similarly by the conservation of energy:
The change in the energy of the air in V over time Δt = the energy or heat gained by the air in V from the block during time Δt + the energy of the air entering V during time Δt – the energy of the air leaving V during time Δt.

i.e. $\left((\rho f)dW\,\Delta y\,(cf_p)Tf\right)_{t+\Delta t} - \left((\rho f)dW\,\Delta y\,(cf_p)Tf\right)_t$
$= (\dot{Q}w)d\ \Delta y\ \Delta t + \left((\rho f)vdW(cf_p)Tf\right)_y \Delta t -$
$\left((\rho f)vdW(cf_p)Tf\right)_{y+\Delta y} \Delta t$

$$\Rightarrow \quad \frac{\left((\rho f)(cf_p)Tf\right)_{t+\Delta t} - \left((\rho f)(cf_p)Tf\right)_t}{\Delta t} + \frac{\left((\rho f)v(cf_p)Tf\right)_{y+\Delta y} - \left((\rho f)v(cf_p)Tf\right)_y}{\Delta y} = \frac{1}{W}(\dot{Q}w)$$

$$\Rightarrow \quad \frac{\partial}{\partial t}\left((\rho f)(cf_p)Tf\right) + \frac{\partial}{\partial y}\left((\rho f)v(cf_p)Tf\right) = \frac{1}{W}(\dot{Q}w)$$

$$\Rightarrow \quad \rho f\frac{\partial}{\partial t}(cf_pTf) + cf_pTf\frac{\partial}{\partial t}(\rho f) + (\rho f)v\frac{\partial}{\partial y}(cf_pTf) + cf_pTf\frac{\partial}{\partial y}\left((\rho f)v\right) = \frac{1}{W}(\dot{Q}w)$$

But $cf_pTf\frac{\partial}{\partial t}(\rho f) + cf_pTf\frac{\partial}{\partial y}\left((\rho f)v\right) = cf_pTf\left(\frac{\partial}{\partial t}(\rho f) + \frac{\partial}{\partial y}((pf)v)\right) = 0,$

see Equation (7.1).

Therefore $\rho f\frac{\partial}{\partial t}(cf_pTf) + (\rho f)v\frac{\partial}{\partial y}(cf_pTf) = \frac{1}{W}(\dot{Q}w)$

and since $(\rho f)v = \frac{\dot{m}}{dW}$

then $\rho f \frac{\partial}{\partial t}(cf_p Tf) + \frac{\dot{m}}{dW}\frac{\partial}{\partial y}(cf_p Tf) = \frac{1}{W}(\dot{Q}w)$ (7.2)

$$\Rightarrow \rho f\left(Tf\frac{\partial(cf_p)}{\partial t} + cf_p\frac{\partial Tf}{\partial t}\right) + \frac{\dot{m}}{dW}\left(Tf\frac{\partial(cf_p)}{\partial y} + cf_p\frac{\partial Tf}{\partial y}\right) = \frac{1}{W}(\dot{Q}w)$$

and since $cf_p = cf_p(Tf)$

$$\rho f\left(Tf\frac{d(cf_p)}{dTf}\frac{\partial Tf}{\partial t} + cf_p\frac{\partial Tf}{\partial t}\right) + \frac{\dot{m}}{dW}\left(Tf\frac{d(cf_p)}{dTf}\frac{\partial Tf}{\partial y} + cf_p\frac{\partial Tf}{\partial y}\right) = \frac{1}{W}(\dot{Q}w)$$

i.e. $\rho f\frac{\partial Tf}{\partial t} + \frac{\dot{m}}{dW}\frac{\partial Tf}{\partial y} = \frac{1}{WF}(\dot{Q}w)$

where $F = Tf\frac{d(cf_p)}{dTf} + cf_p$.

The transient term, $\frac{\partial Tf}{\partial t}$, is neglected since the thermal inertia of the air is very small compared to the thermal inertia of the block, see Thibault *et al.*(1985).

Therefore $\frac{\partial Tf}{\partial y} = \frac{d(\dot{Q}w)}{\dot{m}F}$ (7.3)

From Equation (6.4), $\dot{Q}w = \dot{Q}w(t) = h(t)[T(L_x, t) - Tf(t)]$

But for this two dimensional case,
$\dot{Q}w = \dot{Q}w(y, t) = h(y, t)\,[T(L_x, y, t) - Tf(y, t)]$

Approximating $\frac{\partial Tf}{\partial y}$ using a Taylor series expansion gives

$$\frac{\partial Tf}{\partial y} = \frac{Tf(y + \Delta y, t) - Tf(y - \Delta y, t)}{2\,\Delta y} + O(\Delta y)^2 \ldots$$

Equation (7.3) becomes:

$$\frac{Tf(y + \Delta y, t) - Tf(y - \Delta y, t)}{2\,\Delta y} = \frac{d\,h(y, t)[T(L_x, y, t) - Tf(y, t)]}{\dot{m}\,F(y, t)}$$

where the error of the left hand side is of order $(\Delta y)^2$.

Therefore

$$Tf(y + \Delta y, t) = \frac{2\,\Delta y\,d\,h(y, t)[T(L_x, y, t) - Tf(y, t)]}{\dot{m}\,F(y, t)} + Tf(y - \Delta y, t) \quad (7.4)$$

Tf_j^n is defined as the air temperature (in Kelvin) in the flue at mesh point j at time step n, and h_j^n as the heat transfer coefficient (in W/mK^2) at the flue wall at mesh point j at time step n, j and $n \in \mathbb{Z}^+$. j runs from 1 to Ny, where $j = 1$ is the mesh point in the flue corresponding to $y = 0$ in the block, and $j = Ny$ is the mesh point in the flue corresponding to $y = L_y$ in the block.

Δy is the distance between mesh points (in metres) in the y direction and F_j^n is the value of F at mesh point j in the flue at time step n. $T_{i,j}^n$ is defined as the block temperature (in Kelvin) at mesh point (i, j), where i and n are defined as in §6.2. j runs from 1 to Ny, and $j = 1$ corresponds to $y = 0$ in the block, and $j = Ny$ corresponds to $y = L_y$ in the block.

Rewriting Equation (7.4) using the subscript/superscript notation gives:

$$Tf_{j+1}^n = \frac{2\ \Delta y\ d\ h_j^n\left(T_{Nx,j}^n - Tf_j^n\right)}{\dot{m}\ F_j^n} + Tf_{j-1}^n$$

or $$Tf_j^n = G_{j-1}^n + Tf_{j-2}^n, \quad (7.5)$$

where $$G_{j-1}^n = \frac{2\ \Delta y\ d\ h_{j-1}^n\left(T_{Nx,j-1}^n - Tf_{j-1}^n\right)}{\dot{m}\ F_{j-1}^n}$$

and $$F_{j-1}^n = Tf_{j-1}^n \frac{d(cf_p)_{j-1}^n}{dTf} + (cf_p)_{j-1}^n .$$

It is assumed that the inlet air temperature at time step n, Tf_1^n, remains constant for all n. For the next mesh point, Tf_2^n, Equation (7.5) cannot be

used, since $Tf^{n}_{j-2} = Tf^{n}_{0}$ is an imaginary mesh point outside the flue. In this case, it is necessary to find a Taylor series approximation such that the mesh points are inside the flue. The 3 - 4 - 1 approximation outlined as follows is such an approximation.

$$Tf(y - \Delta y, t) = Tf(y, t) - \Delta y \frac{\partial Tf}{\partial y} + \frac{(\Delta y)^2}{2} \frac{\partial^2 Tf}{\partial y^2} - O(\Delta y)^3 + \ldots \quad (7.6)$$

$$Tf(y - 2\Delta y, t) = Tf(y, t) - 2\,\Delta y \frac{\partial Tf}{\partial y} + \frac{(2\,\Delta y)^2}{2} \frac{\partial^2 Tf}{\partial y^2} - O(\Delta y)^3 + \ldots \quad (7.7)$$

$4 \times$ (7.6) minus (7.7) gives:

$$4Tf(y - \Delta y, t) - Tf(y - 2\Delta y, t) = 3Tf(y, t) - 2\Delta y \frac{\partial Tf}{\partial y} + O(\Delta y)^3 + \ldots$$

$$\Rightarrow \quad \frac{\partial Tf}{\partial y} = \frac{3Tf(y, t) - 4Tf(y - \Delta y, t) + Tf(y - 2\Delta y, t)}{2\Delta y} + O(\Delta y)^2 \ldots$$

Switching to subscript/superscript notation gives:

$$\frac{\partial Tf}{\partial y} = \frac{3Tf^{n}_{j} - 4Tf^{n}_{j-1} + Tf^{n}_{j-2}}{2\Delta y}$$

where the error of the right hand side is of order $(\Delta y)^2$.

So in this case Equation (7.3) becomes:

$$\frac{3Tf^{n}_{j} - 4Tf^{n}_{j-1} + Tf^{n}_{j-2}}{2\Delta y} = \frac{d\ h^{n}_{j}\left(T^{n}_{Nx,j} - Tf^{n}_{j}\right)}{\dot{m}\ F^{n}_{j}}$$

or

$$\frac{3Tf^{n}_{j+1} - 4Tf^{n}_{j} + Tf^{n}_{j-1}}{2\Delta y} = \frac{d\ h^{n}_{j+1}\left(T^{n}_{Nx,j+1} - Tf^{n}_{j+1}\right)}{\dot{m}\ F^{n}_{j+1}}$$

i.e. $$Tf^{n}_{j} = -\frac{1}{4} G^{n}_{j+1} + \frac{3}{4} Tf^{n}_{j+1} + \frac{1}{4} Tf^{n}_{j-1} \quad (7.8)$$

and for j = 2, Equation (7.8) becomes

$$Tf^{n}_{2} = -\frac{1}{4} G^{n}_{3} + \frac{3}{4} Tf^{n}_{3} + \frac{1}{4} Tf^{n}_{1} \quad (7.9)$$

But in Equation (7.5), the G^n_{j-1} are calculated at the previous spatial step. For example, for Tf^n_4, G^n_3 is calculated and for Tf^n_{Ny}, G^n_{Ny-1} is calculated.

But in Equation (7.9), the $G^n_j (= G^n_3)$ is calculated at the next spatial step, since for Tf^n_2, G^n_3 is calculated. Also, note that G^n_3 is used twice, once for calculating Tf^n_4 in Equation (7.5) and again for calculating Tf^n_2 in Equation (7.9).

So in order to be consistent, instead of calculating G^n_3 for Tf^n_2 in Equation (7.9), G^n_1 is calculated.

Therefore $$Tf^n_2 = -\frac{1}{4} G^n_1 + \frac{3}{4} Tf^n_3 + \frac{1}{4} Tf^n_1$$

Summary

1 $$Tf^n_1 = \text{constant} \qquad (7.10)$$

2 $$Tf^n_2 = -\frac{1}{4} G^n_1 + \frac{3}{4} Tf^n_3 + \frac{1}{4} Tf^n_1 \qquad (7.11)$$

3 $$Tf^n_j = G^n_{j-1} + Tf^n_{j-2} \text{ , } j = 3 \text{ to Ny.} \qquad (7.12)$$

where $$G^n_j = \frac{2\ \Delta y\ d\ h^n_j \left(T^n_{Nx,j} - Tf^n_j\right)}{\dot{m}\ F^n_j}$$

and $$F^n_j = Tf^n_j \frac{d(cf_p)^n_j}{dTf} + (cf_p)^n_j .$$

$$\frac{d(cf_p)^n_j}{dTf} = 0.138, \text{ see Equation (6.10).}$$

The calculation of Tf at the next time step

Relaxation is used and this is outlined as follows. Given the air temperatures along the flue at say time step n, that is given Tf^n_j, j = 1 to Ny, the air temperatures along the flue at the next time step are estimated using Equations (7.11) and (7.12). Call these estimates $estTf^n_j$. It is not necessary to estimate Tf^n_1 since Tf^n_1 = constant for all n = atmospheric temperature = 20 °C (see §2.4).

So $\quad \text{estTf}_2^n = -\frac{1}{4} G_1^n + \frac{3}{4} \text{Tf}_3^n + \frac{1}{4} \text{Tf}_1^n$

and $\quad \text{estTf}_j^n = G_{j-1}^n + \text{Tf}_{j-2}^n, \quad j = 3 \text{ to Ny.}$

Next the percentage differences between Tf_j^n and est Tf_j^n relative to Tf_j^n are calculated for $j = 2$ to Ny.

i.e. $\quad \text{percentdiff}_j^n = \dfrac{\left|\text{Tf}_j^n - \text{estTf}_j^n\right|}{\text{Tf}_j^n} \times 100, \quad j = 2 \text{ to Ny.}$

If the maximum percentage difference for all $j \geq 0.1$, then the above process is repeated, replacing the Tf_j^n with est Tf_j^n, $j = 2$ to Ny. New estTf_j^n and hence a new maximum percentage difference is calculated. This process keeps repeating itself until the maximum percentage difference < 0.1. When this inequality is satisfied, then $\text{Tf}_j^{n+1} = \text{estTf}_j^n$, $j = 2$ to Ny.

Once the Tf_j^{n+1} are calculated, then this enables the calculations in the block to be done for time step $n + 1$. After these temperature calculations in the block are completed, then the calculation of the Tf_j at the next time step begins again and so on.

7.3 The heat equation in the block

Recall from §3.3 that the boundary value problem is

$$\left.\begin{aligned}
&\frac{\partial T}{\partial t}(x, y, t) = \alpha\left(\frac{\partial^2 T}{\partial x^2} + \frac{\partial^2 T}{\partial y^2}\right), && 0 \leq x \leq L_x,\ 0 \leq y \leq L_y,\ t > 0 \\
&\text{with} \quad \frac{\partial T}{\partial x}(0, y, t) = 0, && 0 \leq y \leq L_y,\ t > 0, \\
&\qquad T(L_x, y, t) = T_w(t), && 0 \leq y \leq L_y,\ t > 0, \\
&\qquad T(x, y, 0) = T_1, && 0 \leq x \leq L,\ 0 \leq y \leq L_y, \\
&\qquad \frac{\partial T}{\partial y}(x, 0, t) = \frac{\partial T}{\partial y}(x, L_y, t) = 0, && 0 \leq x \leq L_x,\ t > 0.
\end{aligned}\right\} \quad (7.13)$$

Discretising (7.13) as in Chapter 6, gives in subscript/superscript notation:

$$T_{i,j}^{n+1} = Fo_{i,j}^{n} \left\{ \left(\frac{\Delta y}{\Delta x} \right)^2 \left(T_{i+1,j}^{n} + T_{i-1,j}^{n} \right) + T_{i,j+1}^{n} + T_{i,j-1}^{n} + \left[\frac{1}{Fo_{i,j}^{n}} - 2\left(\left(\frac{\Delta y}{\Delta x} \right)^2 + 1 \right) \right] T_{i,j}^{n} \right\} \qquad (7.14)$$

$$i = 1 \text{ to } Nx,\ j = 1 \text{ to } Ny,\ n > 1,$$

where $T_{i,j}^{n}$ and $Fo_{i,j}^{n} = \dfrac{\alpha_{i,j}^{n} \Delta t}{(\Delta y)^2}$ are the temperature and the Fourier number of the block respectively at mesh point (i, j) at time step n,

with $\dfrac{\partial T_{1,j}^{n}}{\partial x} = 0, \quad j = 1 \text{ to } Ny,\ n > 1,$

$$\frac{\partial T_{Nx,j}^{n}}{\partial x} = \frac{-h_{j}^{n}}{k_{Nx,j}^{n}} \left(T_{Nx,j}^{n} - Tf_{j}^{n} \right), \quad j = 1 \text{ to } Ny,\ n > 1,$$

$$T_{i,j}^{1} = T_{1}, \quad i = 1 \text{ to } Nx,\ j = 1 \text{ to } Ny,$$

$$\frac{\partial T_{i,1}^{n}}{\partial y} = \frac{\partial T_{i,Ny}^{n}}{\partial y} = 0, \ i = 1 \text{ to } Nx, \quad n > 1.$$

Using Figure 7.2 as a guide and Equation (7.14), $T_{i,j}^{n+1}$ is now determined for all i and j, with the partial derivatives of the boundary conditions approximated as was done in §6.2.

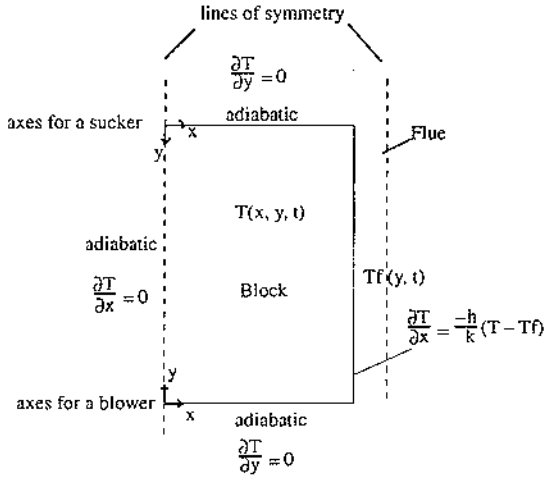

Figure 7.2

Schematic cross-section of the block and flue showing axes and boundary conditions

i = 1, j = 1

The boundary conditions $\frac{\partial T^n_{i,j}}{\partial x} = 0$ and $\frac{\partial T^n_{i,1}}{\partial y} = 0$ give $T^n_{0,1} = T^n_{2,1}$ and $T^n_{1,0} = T^n_{1,2}$ respectively, therefore

$$T^{n+1}_{1,1} = Fo^n_{1,1}\left\{2\left(\frac{\Delta y}{\Delta x}\right)^2 T^n_{2,1} + 2T^n_{1,2} + \left[\frac{1}{Fo^n_{1,1}} - 2\left(\left(\frac{\Delta y}{\Delta x}\right)^2 + 1\right)\right]T^n_{1,1}\right\} \quad (7.15)$$

provided $\quad Fo^n_{1,1} \le \dfrac{1}{2\left(\left(\frac{\Delta y}{\Delta x}\right)^2 + 1\right)}$.

i = 2 to Nx−1, j = 1

The boundary condition $\frac{\partial T^n_{i,1}}{\partial y} = 0$ gives $T^n_{i,0} = T^n_{i,2}$.

Hence
$$T^{n+1}_{i,1} = Fo^n_{i,1}\left\{\left(\frac{\Delta y}{\Delta x}\right)^2\left(T^n_{i+1,1} + T^n_{i-1,1}\right) + 2T^n_{i,2} + \left[\frac{1}{Fo^n_{i,1}} - 2\left(\left(\frac{\Delta y}{\Delta x}\right)^2 + 1\right)\right]T^n_{i,1}\right\} \quad (7.16)$$

provided $\quad Fo^n_{i,1} \le \dfrac{1}{2\left(\left(\frac{\Delta y}{\Delta x}\right)^2 + 1\right)}$.

i = Nx, j = 1

$\frac{\partial T^n_{i,1}}{\partial y} = 0$ gives $T^n_{Nx,0} = T^n_{Nx,2}$ and as in §6.2

$$\frac{\partial T^n_{Nx,j}}{\partial x} = \frac{-h^n_j}{k^n_{Nx,j}}\left(T^n_{Nx,j} - Tf^n_j\right), \quad j = 1 \text{ to } Ny,$$

gives $\quad T^n_{Nx+1,1} = \dfrac{-2(\Delta x)h^n_1}{k^n_{Nx,1}}\left(T^n_{Nx,1} - Tf^n_1\right) + T^n_{Nx-1,1}$

$$\therefore \quad T^{n+1}_{Nx,1} = Fo^n_{Nx,1}\left\{2\left(\frac{\Delta y}{\Delta x}\right)^2\left[Bi^n_1\ Tf^n_1 + T^n_{Nx-1,1}\right] + 2T^n_{Nx,2}\right.$$

$$+\left[\frac{1}{Fo^n_{Nx,1}} - 2\left(\left(\frac{\Delta y}{\Delta x}\right)^2 + \left(\frac{\Delta y}{\Delta x}\right)^2 Bi^n_1 + 1\right)\right]T^n_{Nx,1}\Bigg\} \quad (7.17)$$

provided $\quad Fo^n_{Nx,1} \le \dfrac{1}{2\left(\left(\dfrac{\Delta y}{\Delta x}\right)^2 + \left(\dfrac{\Delta y}{\Delta x}\right)^2 Bi^n_1 + 1\right)}$

where $Bi^n_1 = \dfrac{(\Delta x)h^n_1}{k^n_{Nx,1}} \equiv$ the Biot number at mesh point j = 1 at time step n.

<u>i = 1, j = 2 to Ny–1</u>

$\dfrac{\partial T^n_{1,j}}{\partial x} = 0$ gives $T^n_{0,j} = T^n_{2,j}$.

$$\therefore \quad T^{n+1}_{1,j} = Fo^n_{1,j}\Bigg\{2\left(\frac{\Delta y}{\Delta x}\right)^2 T^n_{2,j} + T^n_{1,j+1} + T^n_{1,j-1} + \left[\frac{1}{Fo^n_{1,j}} - 2\left(\left(\frac{\Delta y}{\Delta x}\right)^2 + 1\right)\right]T^n_{1,j}\Bigg\} \quad (7.18)$$

provided $\quad Fo^n_{1,j} \le \dfrac{1}{2\left(\left(\dfrac{\Delta y}{\Delta x}\right)^2 + 1\right)}$.

<u>i = 2 to Nx–1, j = 2 to Ny–1</u>

$$T^{n+1}_{i,j} = Fo^n_{i,j}\Bigg\{\left(\frac{\Delta y}{\Delta x}\right)^2\left(T^n_{i+1,j} + T^n_{i-1,j}\right) + T^n_{i,j+1} + T^n_{i,j-1} + \left[\frac{1}{Fo^n_{i,j}} - 2\left(\left(\frac{\Delta y}{\Delta x}\right)^2 + 1\right)\right]T^n_{i,j}\Bigg\} \quad (7.19)$$

provided $\quad Fo^n_{i,j} \le \dfrac{1}{2\left(\left(\dfrac{\Delta y}{\Delta x}\right)^2 + 1\right)}$.

i = Nx, j = 2 to Ny–1

This is very similar to the case i = Nx, j = 1 studied earlier. Using this earlier case as a guide gives:

$$T^{n+1}_{Nx,j} = Fo^{n}_{Nx,j}\left\{2\left(\frac{\Delta y}{\Delta x}\right)^2\left[Bi^{n}_{j}\ Tf^{n}_{j} + T^{n}_{Nx-1,j}\right] + T^{n}_{Nx,j+1} + T^{n}_{Nx,j-1} + \left[\frac{1}{Fo^{n}_{Nx,j}} - 2\left(\left(\frac{\Delta y}{\Delta x}\right)^2 + \left(\frac{\Delta y}{\Delta x}\right)^2 Bi^{n}_{j} + 1\right)\right]T^{n}_{Nx,j}\right\} \quad (7.20)$$

provided $Fo^{n}_{Nx,j} \le \dfrac{1}{2\left(\left(\frac{\Delta y}{\Delta x}\right)^2 + \left(\frac{\Delta y}{\Delta x}\right)^2 Bi^{n}_{j} + 1\right)}$.

i = 1, j = Ny

$\dfrac{\partial T^{n}_{1,j}}{\partial x} = 0$ and $\dfrac{\partial T^{n}_{1,Ny}}{\partial y} = 0$ give $T^{n}_{0,Ny} = T^{n}_{2,Ny}$ and $T^{n}_{1,Ny+1} = T^{n}_{1,Ny-1}$ respectively.

$$\therefore \quad T^{n+1}_{1,Ny} = Fo^{n}_{1,Ny}\left\{2\left(\frac{\Delta y}{\Delta x}\right)^2 T^{n}_{2,Ny} + 2T^{n}_{1,Ny-1} + \left[\frac{1}{Fo^{n}_{1,Ny}} - 2\left(\left(\frac{\Delta y}{\Delta x}\right)^2 + 1\right)\right]T^{n}_{1,Ny}\right\} \quad (7.21)$$

provided $Fo^{n}_{1,Ny} \le \dfrac{1}{2\left(\left(\frac{\Delta y}{\Delta x}\right)^2 + 1\right)}$.

i = 2 to Nx–1, j = Ny

$\dfrac{\partial T^{n}_{i,Ny}}{\partial y} = 0$ gives $T^{n}_{i,Ny+1} = T^{n}_{i,Ny-1}$.

$$\therefore \quad T^{n+1}_{i,Ny} = Fo^{n}_{i,Ny}\left\{\left(\frac{\Delta y}{\Delta x}\right)^2\left(T^{n}_{i+1,Ny} + T^{n}_{i-1,Ny}\right) + 2T^{n}_{i,Ny-1} + \left[\frac{1}{Fo^{n}_{i,Ny}} - 2\left(\left(\frac{\Delta y}{\Delta x}\right)^2 + 1\right)\right]T^{n}_{i,Ny}\right\} \quad (7.22)$$

provided $\quad Fo^n_{i,Ny} \le \dfrac{1}{2\left(\left(\dfrac{\Delta y}{\Delta x}\right)^2 + 1\right)}$.

<u>i = Nx, j = Ny</u>

This is very similar to the case i = Nx, j = 1 studied earlier. Using this earlier case as a guide gives:

$$T^{n+1}_{Nx,Ny} = Fo^n_{Nx,Ny}\left\{2\left(\frac{\Delta y}{\Delta x}\right)^2\left[Bi^n_{Ny}\ Tf^n_{Ny} + T^n_{Nx-1,Ny}\right] + 2T^n_{Nx,Ny-1} + \left[\frac{1}{Fo^n_{Nx,Ny}} - 2\left(\left(\frac{\Delta y}{\Delta x}\right)^2 + \left(\frac{\Delta y}{\Delta x}\right)^2 Bi^n_{Ny} + 1\right)\right]T^n_{Nx,Ny}\right\} \tag{7.23}$$

provided $\quad Fo^n_{Nx,Ny} \le \dfrac{1}{2\left(\left(\dfrac{\Delta y}{\Delta x}\right)^2 + \left(\dfrac{\Delta y}{\Delta x}\right)^2 Bi^n_{Ny} + 1\right)}$.

<u>Determining Δy</u>

Δy is obtained by specifying the number of spatial steps required in the y direction, Ny, and then the depth of the block is divided by Ny–1.

$$\Delta y = \frac{L_y}{Ny-1}\ m$$

<u>Determining $Fo^n_{i,j}$</u>

A very similar method to that discussed in §6.2 is used.

As in §6.2, the k_i (thermal conductivies) are calculated using the temperature midway between the initial and assumed final average temperature of the block. Suppose this final average block temperature is Tf^1_j , for any j between 2 and Ny, since all the Tf^1_j, $j \neq 1$, are chosen to be equal. Recall from §2.4, that Tf^n_1 = atmospheric temperature = 20 °C for all n.

<u>Determining Bi^n_j</u>

Similar to the method in §6.2, but here h = h(y, t), so

$$Bi_j^n = \frac{\Delta x \; h_j^n}{k_{Nx,j}^n} = \frac{\Delta xw \; h_j^n}{kw}$$

where $h_j^n = (hr_j^n + hc_j^n)$ W/m^{2}K

$hr_j^n \equiv$ the heat transfer coefficient for radiation of the flue wall at mesh point j at time step n, and

$hc_j^n \equiv$ the heat transfer coefficient for convection of the flue wall at mesh point j at time step n.

$$hr_j^n = \varepsilon\sigma\left(T_{Nx,j}^n - Tf_j^n\right)\left(\left(T_{Nx,j}^n\right)^2 - \left(Tf_j^n\right)^2\right)$$

and $hc_j^n = \dfrac{(kf_j^n)(Nu_j^n)}{\ell}$,

$kf_j^n \equiv$ the thermal conductivity of the fluid or air at mesh point j in the flue at time step n, in W/mK,

$Nu_j^n \equiv$ the Nusselt number at mesh point j in the flue at time step n and is dimensionless,

$\ell \equiv$ the characteristic length in m, see §6.2.

Determining Δt

A similar method to that used in §6.2 is followed.

(a) Obtaining Δta

$$Foa_{i,j}^n \le \frac{1}{2\left(\left(\frac{\Delta y}{\Delta xa}\right)^2 + 1\right)}$$

($Foa_{i,j}^n$ is the Fourier number of the anode at mesh point (i, j) at time step n)

i.e. $$\frac{\alpha a_{i,j}^n(\Delta ta)}{(\Delta y)^2} \le \frac{1}{2\left(\left(\frac{\Delta y}{\Delta xa}\right)^2 + 1\right)}$$

($\alpha a_{i,j}^n$ is the thermal diffusivity of the anode at mesh point (i, j) at time step n)

$$\therefore \quad \Delta ta \le \frac{(\Delta y)^2}{2\alpha a_{i,j}^n\left(\left(\frac{\Delta y}{\Delta xa}\right)^2 + 1\right)}.$$

The upper bound on Δta is obtained by calculating the maximum value that $\alpha a_{i,j}^n$ can take.

max. $\alpha a_{i,j}^n = \dfrac{ka}{(\rho a)(\min.(ca_p)_{i,j}^n)}$, see §6.2 for this calculation. As in §6.2, the minimum block temperature is taken to be the assumed final average block temperature which equals Tf_j^1 for any j between 2 and Ny (see the discussion earlier in this section).

(b) Obtaining Δtp

Similarly $$\Delta tp \le \frac{(\Delta y)^2}{2\alpha p_{i,j}^n \left(\left(\frac{\Delta y}{\Delta xp} \right)^2 + 1 \right)}$$

(c) Obtaining Δtw

$$Fow_{i,j}^n \le \min. \left(\frac{1}{2\left(\left(\frac{\Delta y}{\Delta xw} \right)^2 + 1 \right)}, \frac{1}{2\left(\left(\frac{\Delta y}{\Delta xw} \right)^2 + \left(\frac{\Delta y}{\Delta xw} \right)^2 Bi_j^n + 1 \right)} \right)$$

$$= \frac{1}{2\left(\left(\frac{\Delta y}{\Delta xw} \right)^2 + \left(\frac{\Delta y}{\Delta xw} \right)^2 Bi_j^n + 1 \right)}, \text{ since } Bi_j^n > 0, \forall \text{ j and n.}$$

i.e. $$\frac{\alpha w_{i,j}^n (\Delta tw)}{(\Delta y)^2} \le \frac{1}{2\left(\left(\frac{\Delta y}{\Delta xw} \right)^2 + \left(\frac{\Delta y}{\Delta xw} \right)^2 Bi_j^n + 1 \right)}$$

$\therefore$ $$\Delta tw \le \frac{(\Delta y)^2}{2\alpha w_{i,j}^n \left(\left(\frac{\Delta y}{\Delta xw} \right)^2 + \left(\frac{\Delta y}{\Delta xw} \right)^2 Bi_j^n + 1 \right)}$$

The upper bound on Δtw that satisfies the above inequality is obtained by calculating the maximum value that $\alpha w_{i,j}^n$ and Bi_j^n can take. See §6.2 for the calculation of max. $\alpha w_{i,j}^n$.

Since $$Bi_j^n = \frac{\Delta xw \; h_j^n}{kw},$$

the maximum value of Bi_j^n is obtained by calculating the maximum value of h_j^n.

$$\text{max. } h_j^n = \text{max. } hr_j^n + \text{max. } hc_j^n$$

$$\text{max. } hr_j^n = \varepsilon\sigma[\text{max. } T_{Nxw,j}^n - \text{min. } Tf_j^n] \; [(\text{max. } T_{Nxw,j}^n)^2 - (\text{min. } Tf_j^n)^2]$$

$$= \varepsilon\sigma[\text{initial } T_{Nxw,j} - \text{min } Tf_j^n] \; [(\text{initial } T_{Nxw,j})^2 - (\text{min. } Tf_j^n)^2]$$

$$= \varepsilon\sigma \; [T_{Nxw,j}^1 - \text{min. } Tf_j^n] \; [(T_{Nxw,j}^1)^2 - (\text{min. } Tf_j^n)^2]$$

Assume that min. Tf_j^n, the minimum fluid temperature at mesh point j at time step n, is 293 K (atmospheric temperature) for all n.

$$\text{max. } hc_j^n = \frac{(\text{max. } kf_j^n)(\text{max. } Nu_j^n)}{\ell}$$

$$\text{max. } kf_j^n = (5.65 \times 10^{-5}) \text{ max. } Tf_j^n + 1.02 \times 10^{-2},$$

see Equation (6.9).

Assume that max. Tf_j^n, the maximum fluid temperature at mesh point j at time step n, is 773 K for all n.

$$\text{max. } Nu_j^n = 0.023 \; (\text{max. } Re_j^n)^{0.8} \; (\text{max. } Pr_j^n)^{0.4},$$

see Equation (6.6)

$$\text{max. } Re_j^n = \frac{4\dot{m}}{(\text{min. } \mu_j^n)(\text{perimeter})},$$ see Equation (6.7)

$$\text{min. } \mu_j^n = \frac{(\text{min. } kf_j^n)(\text{min. } Pr_j^n)}{\text{max. } (cf_p)_j^n},$$ see Equation (6.8)

$$\text{max. } Pr_j^n = (1.89 \times 10^{-7}) \; (773)^2 - (2.20 \times 10^{-4}) \; 773 + 7.54 \times 10^{-1},$$

see Equation (6.11)

$$\text{min. } kf_j^n = (5.65 \times 10^{-5}) \; 293 + 1.02 \times 10^{-2}$$

$$\text{min. } Pr_j^n = (1.89 \times 10^{-7})(293)^2 - (2.20 \times 10^{-4}) \; 293 + 7.54 \times 10^{-1}$$

$$\text{max. } (cf_p)_j^n = (1.38 \times 10^{-1})773 + 9.92 \times 10^2, \text{ see Equation (6.10).}$$

(d) Obtaining the overall Δt.

The upper bound on the overall Δt = minimum (max. Δta, max. Δtp, max. Δtw).

Temperature on the anode/packing coke boundary

$Ta^n_{q,j}$ and $Foa^n_{q,j}$ are defined as the carbon anode temperature (in Kelvin) and Fourier number respectively at mesh point (q, j) at time step n, q is defined as in §6.2. j runs from 1 to N_y.

Similarly $Tp^n_{r,j}$ and $Fop^n_{r,j}$ are defined as the packing coke temperature (in Kelvin) and Fourier number respectively at mesh point (r, j), at time step n. r is defined as in §6.2.

At q = Nxa.

From Equation (7.16)

$$T^{n+1}_{Nxa,1} = Foa^n_{Nxa,1}\left\{\left(\frac{\Delta y}{\Delta xa}\right)^2\left(Ta^n_{Nxa+1,1} + Ta^n_{Nxa-1,1}\right) + 2Ta^n_{Nxa,2} + \left[\frac{1}{Foa^n_{Nxa,1}} - 2\left(\left(\frac{\Delta y}{\Delta xa}\right)^2 + 1\right)\right]Ta^n_{Nxa,1}\right\} \quad (7.24)$$

and from Equation (7.19), for j = 2 to Ny – 1,

$$Ta^n_{Nxa,j} = Foa^n_{Nxa,j}\left\{\left(\frac{\Delta y}{\Delta xa}\right)^2\left(Ta^n_{Nxa+1,j} + Ta^n_{Nxa-1,j}\right) + Ta^n_{Nxa,j+1} + Ta^n_{Nxa,j-1} + \left[\frac{1}{Foa^n_{Nxa,j}} - 2\left(\left(\frac{\Delta y}{\Delta xa}\right)^2 + 1\right)\right]Ta^n_{Nxa,j}\right\} \quad (7.25)$$

and from Equation (7.22)

$$Ta^{n+1}_{Nxa,Ny} = Foa^n_{Nxa,Ny}\left\{\left(\frac{\Delta y}{\Delta xa}\right)^2\left(Ta^n_{Nxa+1,Ny} + Ta^n_{Nxa-1,Ny}\right)\right.$$

$$+ 2Ta^{n}_{Nxa,Ny-1} + \left[\frac{1}{Foa^{n}_{Nxa,Ny}} - 2\left(\left(\frac{\Delta y}{\Delta xa}\right)^2 + 1\right)\right]Ta^{n}_{Nxa,Ny}\Bigg\} \qquad (7.26)$$

$Ta^{n}_{Nxa+1,j}$, j = 1 to Ny, is an imaginary mesh point outside the anode, which coincides with $Tp^{n}_{2,j}$ only if $\Delta xa = \Delta xp$.

At r = 1.

From Equation (7.16)

$$Tp^{n+1}_{1,1} = Fop^{n}_{1,1}\left\{\left(\frac{\Delta y}{\Delta xp}\right)^2\left(Tp^{n}_{2,1} + Tp^{n}_{0,1}\right) + 2Tp^{n}_{1,2} + \left[\frac{1}{Fop^{n}_{1,1}}\right] - 2\left(\left(\frac{\Delta y}{\Delta xp}\right)^2 + 1\right)Tp^{n}_{1,1}\right\} \qquad (7.27)$$

and from Equation (7.19), for j = 2 to Ny – 1,

$$Tp^{n+1}_{1,j} = Fop^{n}_{1,j}\left\{\left(\frac{\Delta y}{\Delta xp}\right)^2\left(Tp^{n}_{2,j} + Tp^{n}_{0,j}\right) + Tp^{n}_{1,j+1} + Tp^{n}_{1,j-1} + \left[\frac{1}{Fop^{n}_{1,j}} - 2\left(\left(\frac{\Delta y}{\Delta xp}\right)^2 + 1\right)\right]Tp^{n}_{1,j}\right\} \qquad (7.28)$$

and from Equation (7.22)

$$Tp^{n+1}_{1,Ny} = Fop^{n}_{1,Ny}\left\{\left(\frac{\Delta y}{\Delta xp}\right)^2\left(Tp^{n}_{2,Ny} + Tp^{n}_{0,Ny}\right) + 2Tp^{n}_{1,Ny-1} + \left[\frac{1}{Fop^{n}_{1,Ny}} - 2\left(\left(\frac{\Delta y}{\Delta xp}\right)^2 + 1\right)\right]Tp^{n}_{1,Ny}\right\} \qquad (7.29)$$

$Tp^{n}_{0,j}$, j = 1 to Ny, is an imaginary mesh point outside the packing coke which coincides with $Ta^{n}_{Nxa-1,j}$ only if $\Delta xa = \Delta xp$.

As was done in §6.2 , a heat balance is done on the anode/packing coke boundary using Fourier's Law to give:

$$-\,ka\left(\frac{Ta^{n}_{Nxa+1,j}\;-\;Ta^{n}_{Nxa-1,j}}{2\Delta xa}\right)\;=\;-\;kp\left(\frac{Tp^{n}_{2,j}\;-\;Tp^{n}_{0,j}}{2\Delta xp}\right),\;j=1\text{ to Ny},\quad(7.30)$$

$j = 1$.

Equations (7.24), (7.27) and (7.30) involve three unknowns: $Ta^{n}_{Nxa+1,1}$, $Tp^{n}_{0,1}$ and $Ta^{n+1}_{Nxa,1} = Tp^{n+1}_{1,1}$. These equations are solved for $Tp^{n+1}_{1,1}$, using the fact that $Ta^{n}_{Nxa,1} = Tp^{n}_{1,1}$ and $Ta^{n}_{Nxa,2} = Tp^{n}_{1,2}$.

$$\begin{aligned}Tp^{n+1}_{1,1} \;=\; \frac{Fop^{n}_{1,1}}{\Lambda_1}\Bigg\{&2\left(\frac{\Delta y}{\Delta xp}\right)^{2}Tp^{n}_{2,1}\;+\;2\left[\left(\frac{\Delta y}{\Delta xp}\right)^{2}\frac{ka}{kp}\frac{\Delta xp}{\Delta xa}\right]Ta^{n}_{Nxa-1,1}\\&+\;2\left[\frac{ka}{kp}\frac{\Delta xa}{\Delta xp}\;+\;1\right]Tp^{n}_{1,2}\\&+\left[\frac{ka}{kp}\frac{\Delta xa}{\Delta xp}\left(\frac{1}{Foa^{n}_{Nxa,1}}\;-\;2\left(\left(\frac{\Delta y}{\Delta xa}\right)^{2}\;+\;1\right)\right)\right.\\&\left.+\left(\frac{1}{Fop^{n}_{1,1}}\;-\;2\left(\left(\frac{\Delta y}{\Delta xp}\right)^{2}\;+\;1\right)\right)\right]Tp^{n}_{1,1}\Bigg\}\end{aligned}\qquad(7.31)$$

where $\Lambda_1 \;=\; 1 + \dfrac{Fop^{n}_{1,1}}{Foa^{n}_{Nxa,1}}\dfrac{ka}{kp}\dfrac{\Delta xa}{\Delta xp}$.

In order to satisfy the Law of Conservation of Energy it is required that the coefficients of $Tp^{n}_{2,1}$, $Ta^{n}_{Nxa-1,1}$, $Tp^{n}_{1,2}$ and $Tp^{n}_{1,1} \geq 0$.

ka and $kp > 0$.

$\alpha a^{n}_{Nxa,1}$ and $\alpha p^{n}_{1,1} > 0$ and hence $Foa^{n}_{Nxa,1}$ and $Fop^{n}_{1,1} > 0$.

$Foa^{n}_{Nxa,1} \leq \dfrac{1}{2\left(\left(\dfrac{\Delta y}{\Delta xa}\right)^{2}+1\right)}$ and $Fop^{n}_{1,1} \leq \dfrac{1}{2\left(\left(\dfrac{\Delta y}{\Delta xp}\right)^{2}+1\right)}$ are the restrictions determined earlier.

Therefore the coefficients ≥ 0.

j = 2 to Ny – 1

Similarly

$$Tp_{1,j}^{n+1} = \frac{Fop_{1,j}^{n}}{\Lambda_2}\left\{2\left(\frac{\Delta y}{\Delta xp}\right)^2 Tp_{2,j}^{n} + 2\left[\left(\frac{\Delta y}{\Delta xp}\right)^2 \frac{ka}{kp}\frac{\Delta xp}{\Delta xa}\right]Ta_{Nxa-1,j}^{n}\right.$$

$$+\left[\frac{ka}{kp}\frac{\Delta xa}{\Delta xp} + 1\right]Tp_{1,j+1}^{n} + \left[\frac{ka}{kp}\frac{\Delta xa}{\Delta xp} + 1\right]Tp_{1,j-1}^{n}$$

$$+\left[\frac{ka}{kp}\frac{\Delta xa}{\Delta xp}\left(\frac{1}{Foa_{Nxa,j}^{n}} - 2\left(\left(\frac{\Delta y}{\Delta xa}\right)^2 + 1\right)\right)\right.$$

$$\left.\left.+\left(\frac{1}{Fop_{1,j}^{n}} - 2\left(\left(\frac{\Delta y}{\Delta xp}\right)^2 + 1\right)\right)\right]Tp_{1,j}^{n}\right\} \quad (7.32)$$

where $\Lambda_2 = 1 + \dfrac{Fop_{1,j}^{n}}{Foa_{Nxa,j}^{n}}\dfrac{ka}{kp}\dfrac{\Delta xa}{\Delta xp}$.

j = Ny

Similarly

$$Tp_{1,Ny}^{n+1} = \frac{Fop_{1,Ny}^{n}}{\Lambda_3}\left\{2\left(\frac{\Delta y}{\Delta xp}\right)^2 Tp_{2,Ny}^{n} + 2\left[\left(\frac{\Delta y}{\Delta xp}\right)^2 \frac{ka}{kp}\frac{\Delta xp}{\Delta xa}\right]Ta_{Nxa-1,Ny}^{n}\right.$$

$$+ 2\left[\frac{ka}{kp}\frac{\Delta xa}{\Delta xp} + 1\right]Tp_{1,Ny-1}^{n}$$

$$+\left[\frac{ka}{kp}\frac{\Delta xa}{\Delta xp}\left(\frac{1}{Foa_{Nxa,Ny}^{n}} - 2\left(\left(\frac{\Delta y}{\Delta xa}\right)^2 + 1\right)\right)\right.$$

$$\left.\left.+\left(\frac{1}{Fop_{1,Ny}^{n}} - 2\left(\left(\frac{\Delta y}{\Delta xp}\right)^2 + 1\right)\right)\right]Tp_{1,Ny}^{n}\right\} \quad (7.33)$$

where $\Lambda_3 = 1 + \dfrac{Fop_{1,Ny}^{n}}{Foa_{Nxa,Ny}^{n}}\dfrac{ka}{kp}\dfrac{\Delta xa}{\Delta xp}$.

Temperature on the packing coke/flue wall boundary

This case is similar to the anode/packing coke boundary one.

$Tw^n_{s,j}$ and $Fow^n_{s,j}$ are defined as the flue wall temperature (in Kelvin) and Fourier number respectively at mesh point (s, j), at time step n. s is defined as in §6.2.

j = 1

$$Tw^{n+1}_{1,1} = \frac{Fow^n_{1,1}}{\Theta_1}\left\{2\left(\frac{\Delta y}{\Delta xw}\right)^2 Tw^n_{2,1} + 2\left[\left(\frac{\Delta y}{\Delta xw}\right)^2 \frac{kp}{kw}\frac{\Delta xw}{\Delta xp}\right]Tp^n_{Nxp-1,1} + 2\left[\frac{kp}{kw}\frac{\Delta xp}{\Delta xw} + 1\right]Tw^n_{1,2} + \left[\frac{kp}{kw}\frac{\Delta xp}{\Delta xw}\left(\frac{1}{Fop^n_{Nxp,1}} - 2\left(\left(\frac{\Delta y}{\Delta xp}\right)^2 + 1\right)\right) + \left(\frac{1}{Fow^n_{1,1}} - 2\left(\left(\frac{\Delta y}{\Delta xw}\right)^2 + 1\right)\right)\right]Tw^n_{1,1}\right\} \quad (7.34)$$

where $\Theta_1 = 1 + \frac{Fow^n_{1,1}}{Fop^n_{Nxp,1}}\frac{kp}{kw}\frac{\Delta xp}{\Delta xw}$.

j = 2 to Ny – 1

$$Tw^{n+1}_{1,j} = \frac{Fow^n_{1,j}}{\Theta_2}\left\{2\left(\frac{\Delta y}{\Delta xw}\right)^2 Tw^n_{2,j} + 2\left[\left(\frac{\Delta y}{\Delta xw}\right)^2 \frac{kp}{kw}\frac{\Delta xw}{\Delta xp}\right]Tp^n_{Nxp-1,j} + \left[\frac{kp}{kw}\frac{\Delta xp}{\Delta xw} + 1\right]Tw^n_{1,j+1} + \left[\frac{kp}{kw}\frac{\Delta xp}{\Delta xw} + 1\right]Tw^n_{1,j-1} + \left[\frac{kp}{kw}\frac{\Delta xp}{\Delta xw}\left(\frac{1}{Fop^n_{Nxp,j}} - 2\left(\left(\frac{\Delta y}{\Delta xp}\right)^2 + 1\right)\right) + \left(\frac{1}{Fow^n_{i,j}} - 2\left(\left(\frac{\Delta y}{\Delta xw}\right)^2 + 1\right)\right)\right]Tw^n_{1,j}\right\} \quad (7.35)$$

where $\Theta_2 = 1 + \frac{Fow^n_{1,j}}{Fop^n_{Nxp,j}}\frac{kp}{kw}\frac{\Delta xp}{\Delta xw}$.

j = Ny

$$Tw_{Ny}^{n+1} = \frac{Fow_{1,Ny}^{n}}{\Theta_3}\left\{2\left(\frac{\Delta y}{\Delta xw}\right)^2 Tw_{2,Ny}^{n} + 2\left[\left(\frac{\Delta y}{\Delta xw}\right)^2 \frac{kp}{kw}\frac{\Delta xw}{\Delta xp}\right]Tp_{Nxp-1,Ny}^{n}\right.$$

$$+ 2\left[\frac{kp}{kw}\frac{\Delta xp}{\Delta xw} + 1\right]Tw_{1,Ny-1}^{n}$$

$$+ \left[\frac{kp}{kw}\frac{\Delta xp}{\Delta xw}\left(\frac{1}{Fop_{Nxp,Ny}^{n}} - 2\left(\left(\frac{\Delta y}{\Delta xp}\right)^2 + 1\right)\right)\right.$$

$$\left.\left. + \left(\frac{1}{Fow_{1,Ny}^{n}} - 2\left(\left(\frac{\Delta y}{\Delta xw}\right)^2 + 1\right)\right)\right]Tw_{1,Ny}^{n}\right\} \quad (7.36)$$

where $\Theta_3 = 1 + \dfrac{Fow_{1,Ny}^{n}}{Fop_{Nxp,Ny}^{n}}\dfrac{kp}{kw}\dfrac{\Delta xp}{\Delta xw}$.

For the same reasons as before, the coefficients of the various mesh points in Equations (7.34) – (7.36) ≥ 0, so the Law of Conservation of Energy is satisfied.

Summary

The numerical solution of (7.13) requires the solution of:

(1) $$Ta_{1,1}^{n+1} = Foa_{1,1}^{n}\left\{2\left(\frac{\Delta y}{\Delta xa}\right)^2 Ta_{2,1}^{n} + 2Ta_{1,2}^{n}\right.$$

$$\left. + \left[\frac{1}{Foa_{1,1}^{n}} - 2\left(\left(\frac{\Delta y}{\Delta xa}\right)^2 + 1\right)\right]Ta_{1,1}^{n}\right\},$$

(2) $$Ta_{q,1}^{n+1} = Foa_{q,1}^{n}\left\{\left(\frac{\Delta y}{\Delta xa}\right)^2\left(Ta_{q+1,1}^{n} + Ta_{q-1,1}^{n}\right) + 2Ta_{q,2}^{n}\right.$$

$$\left. + \left[\frac{1}{Foa_{q,1}^{n}} - 2\left(\left(\frac{\Delta y}{\Delta xa}\right)^2 + 1\right)\right]Ta_{q,1}^{n}\right\}, \quad q = 2 \text{ to } Nxa - 1,$$

(3) $Ta_{Nxa,1}^{n+1} = Tp_{1,1}^{n+1}$, see Equation (7.31),

(4) $$Tp_{r,1}^{n+1} = Fop_{r,1}^{n}\left\{\left(\frac{\Delta y}{\Delta xp}\right)^2\left(Tp_{r+1,1}^{n} + Tp_{r-1,1}^{n}\right) + 2Tp_{r,2}^{n} + \left[\frac{1}{Fop_{r,1}^{n}} - 2\left(\left(\frac{\Delta y}{\Delta xp}\right)^2 + 1\right)\right]Tp_{r,1}^{n}\right\}, \quad r = 2 \text{ to } Nxp - 1,$$

(5) $$Tp_{Nxp,1}^{n+1} = Tw_{1,1}^{n+1}, \text{ see Equation (7.34),}$$

(6) $$Tw_{s,1}^{n+1} = Fow_{s,1}^{n}\left\{\left(\frac{\Delta y}{\Delta xw}\right)^2\left(Tw_{s+1,1}^{n} + Tw_{s-1,1}^{n}\right) + 2Tw_{s,2}^{n} + \left[\frac{1}{Fow_{s,1}^{n}} - 2\left(\left(\frac{\Delta y}{\Delta xw}\right)^2 + 1\right)\right]Tw_{s,1}^{n}\right\}, \quad s = 2 \text{ to } Nxw - 1,$$

(7) $$Tw_{Nxw,1}^{n+1} = Fow_{Nxw,1}^{n}\left\{2\left(\frac{\Delta y}{\Delta xw}\right)^2\left[Bi_1^{n}\, Tf_1^{n} + Tw_{Nxw-1,1}^{n}\right] + 2Tw_{Nxw,2}^{n} + \left[\frac{1}{Fow_{Nxw,1}^{n}} - 2\left(\left(\frac{\Delta y}{\Delta xw}\right)^2 + \left(\frac{\Delta y}{\Delta xw}\right)^2 Bi_1^{n} + 1\right)\right]T_{Nxw,1}^{n}\right\},$$

(8) $$Ta_{1,j}^{n+1} = Foa_{1,j}^{n}\left\{2\left(\frac{\Delta y}{\Delta xa}\right)^2 Ta_{2,j}^{n} + Ta_{1,j+1}^{n} + Ta_{1,j-1}^{n} + \left[\frac{1}{Foa_{1,j}^{n}} - 2\left(\left(\frac{\Delta y}{\Delta xa}\right)^2 + 1\right)\right]Ta_{1,j}^{n}\right\}, \quad j = 2 \text{ to } Ny - 1,$$

(9) $$Ta_{q,j}^{n+1} = Foa_{q,j}^{n}\left\{\left(\frac{\Delta y}{\Delta xa}\right)^2\left(Ta_{q+1,j}^{n} + Ta_{q-1,j}^{n}\right) + Ta_{q,j+1}^{n} + Ta_{q,j-1}^{n} + \left[\frac{1}{Foa_{q,j}^{n}} - 2\left(\left(\frac{\Delta y}{\Delta xa}\right)^2 + 1\right)\right]Ta_{q,j}^{n}\right\}, \quad q = 2 \text{ to } Nxa - 1, \quad j = 2 \text{ to } Ny - 1,$$

(10) $$Ta_{Nxa,j}^{n+1} = Tp_{1,j}^{n+1}, \text{ see Equation (7.32),}$$

$$(11)\quad Tp_{r,j}^{n+1} = Fop_{r,j}^{n}\left\{\left(\frac{\Delta y}{\Delta xp}\right)^2\left(Tp_{r+1,j}^{n} + Tp_{r-1,j}^{n}\right) + Tp_{r,j+1}^{n} + Tp_{r,j-1}^{n} + \left[\frac{1}{Fop_{r,j}^{n}} - 2\left(\left(\frac{\Delta y}{\Delta xp}\right)^2 + 1\right)\right]Tp_{r,j}^{n}\right\},\quad r = 2 \text{ to } Nxp-1,\quad j = 2 \text{ to } Ny-1,$$

$$(12)\quad Tp_{Nxp,j}^{n+1} = Tw_{1,j}^{n+1}\text{ , see Equation (7.35),}$$

$$(13)\quad Tw_{s,j}^{n+1} = Fow_{s,j}^{n}\left\{\left(\frac{\Delta y}{\Delta xw}\right)^2\left(Tw_{s+1,j}^{n} + Tw_{s-1,j}^{n}\right) + Tw_{s,j+1}^{n} + Tw_{s,j-1}^{n} + \left[\frac{1}{Fow_{s,j}^{n}} - 2\left(\left(\frac{\Delta y}{\Delta xw}\right)^2 + 1\right)\right]Tw_{s,j}^{n}\right\},\quad s = 2 \text{ to } Nxw-1,\quad j = 2 \text{ to } Ny-1,$$

$$(14)\quad Tw_{Nxw,j}^{n+1} = Fow_{Nxw,j}^{n}\left\{2\left(\frac{\Delta y}{\Delta xw}\right)^2\left[Bi_j^{n}\ Tf_j^{n} + Tw_{Nxw-1,j}^{n}\right] + Tw_{Nxw,j+1}^{n} + Tw_{Nxw,j-1}^{n} + \left[\frac{1}{Fow_{Nxw,j}^{n}} - 2\left(\left(\frac{\Delta y}{\Delta xw}\right)^2 + \left(\frac{\Delta y}{\Delta xw}\right)^2 Bi_j^{n} + 1\right)\right]Tw_{Nxw,j}^{n}\right\},$$

$$j = 2 \text{ to } Ny-1,$$

$$(15)\quad Ta_{1,Ny}^{n+1} = Foa_{1,Ny}^{n}\left\{2\left(\frac{\Delta y}{\Delta xa}\right)^2 Ta_{2,Ny}^{n} + 2Ta_{1,Ny-1}^{n} + \left[\frac{1}{Foa_{1,Ny}^{n}} - 2\left(\left(\frac{\Delta y}{\Delta xa}\right)^2 + 1\right)\right]Ta_{1,Ny}^{n}\right\},$$

(16) $$Ta^{n+1}_{q,Ny} = Foa^{n}_{q,Ny}\left\{\left(\frac{\Delta y}{\Delta xa}\right)^2\left(Ta^{n}_{q+1,Ny} + Ta^{n}_{q-1,Ny}\right) + 2Ta^{n}_{q,Ny-1} + \left[\frac{1}{Foa^{n}_{q,Ny}} - 2\left(\left(\frac{\Delta y}{\Delta xa}\right)^2 + 1\right)\right]Ta^{n}_{q,Ny}\right\},$$

$$q = 2 \text{ to } Nxa - 1,$$

(17) $$Ta^{n+1}_{Nxa,Ny} = Tp^{n+1}_{1,Ny}, \text{ see Equation (7.33),}$$

(18) $$Tp^{n+1}_{r,Ny} = Fop^{n}_{r,Ny}\left\{\left(\frac{\Delta y}{\Delta xp}\right)^2\left(Tp^{n}_{r+1,Ny} + Tp^{n}_{r-1,Ny}\right) + 2Tp^{n}_{r,Ny} + \left[\frac{1}{Fop^{1}_{r,Ny}} - 2\left(\left(\frac{\Delta y}{\Delta xp}\right)^2 + 1\right)\right]Tp^{n}_{r,Ny}\right\},$$

$$r = 2 \text{ to } Nxp - 1,$$

(19) $$Tp^{n+1}_{Nxp,Ny} = Tw^{n+1}_{1,Ny}, \text{ see Equation (7.36),}$$

(20) $$Tw^{n+1}_{s,Ny} = Fow^{n}_{s,Ny}\left\{\left(\frac{\Delta y}{\Delta xw}\right)^2\left(T^{n}_{s+1,Ny} + Tw^{n}_{s-1,Ny}\right) + 2Tw^{n}_{s,Ny-1} + \left[\frac{1}{Fow^{n}_{s,Ny}} - 2\left(\left(\frac{\Delta y}{\Delta xw}\right)^2 + 1\right)\right]Tw^{n}_{s,Ny}\right\},$$

$$s = 2 \text{ to } Nxw - 1,$$

(21) $$Tw^{n+1}_{Nxw,Ny} = Fow^{n}_{Nxw,Ny}\left\{2\left(\frac{\Delta y}{\Delta xw}\right)^2\left[\left[Bi^{n}_{Ny}\ Tf^{n}_{Ny} + Tw^{n}_{Nxw-1,Ny}\right] + 2Tw^{n}_{Nxw,Ny-1} + \left[\frac{1}{Fow^{n}_{Nxw,Ny}} - 2\left(\left(\frac{\Delta y}{\Delta xw}\right)^2 + \left(\frac{\Delta y}{\Delta xw}\right)^2 Bi^{n}_{Ny} + 1\right)\right]Tw^{n}_{Nxw,Ny}\right\},$$

provided $$Foa^{n}_{q,j} \le \frac{1}{2\left(\left(\frac{\Delta y}{\Delta xa}\right)^2 + 1\right)}, \qquad q = 1 \text{ to } Nxa,$$

$$Fop^{n}_{r,j} \leq \frac{1}{2\left(\left(\frac{\Delta y}{\Delta xp}\right)^2 + 1\right)}, \qquad r = 1 \text{ to } Nxp$$

$$Fow^{n}_{s,j} \leq \frac{1}{2\left(\left(\frac{\Delta y}{\Delta xw}\right)^2 + 1\right)}, \qquad s = 1 \text{ to } Nxw - 1$$

$$Fow^{n}_{Nxw,j} \leq \frac{1}{2\left(\left(\frac{\Delta y}{\Delta xw}\right)^2 + \left(\frac{\Delta y}{\Delta xw}\right)^2 Bi^{n}_{j} + 1\right)}, \quad j = 1 \text{ to } Ny, \; n > 1.$$

7.4 Heat balance at the flue wall

Since there is no heat flow across the boundaries $x = 0$, $y = 0$ and $y = L_y$, then all the heat flow from the block occurs along the boundary $x = L_x$, i.e. the flue wall. The heat transferred from the block across this boundary should equal the heat gained by the air in the flue, i.e. $\Delta Q + \Delta Qf = 0$, where

$\Delta Qf \equiv$ the heat gained by the fluid or air in time Δt and
$\Delta Q \equiv$ the heat transferred from the block in time Δt.

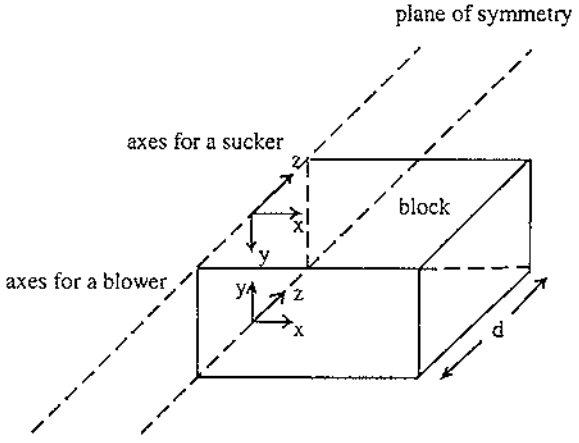

Figure 7.3
Schematic three-dimensional view of the block showing axes

Calculation of ΔQf

Consider the block, where the z direction is as shown in Figure 7.3. Let Q(t) be the heat in the block at time t. Then

$$\frac{dQ}{dt} = \frac{d}{dt}\left(\iiint_V \rho e \, dV\right) \qquad \text{see §3.1,}$$

$$= \frac{d}{dt}\left(\int_0^{L_x}\int_0^{L_y}\int_0^{d} \rho e \, dz \, dy \, dx\right)$$

where $dV = dx\, dy\, dz$ and d is as shown in Figure 7.3,

$$\frac{dQ}{dt} = d\int_0^{L_x}\int_0^{L_y}\frac{\partial}{\partial t}(\rho e)\, dy\, dx \qquad (\rho e \text{ is independent of } z)$$

$$= d\int_0^{L_x}\int_0^{L_y}\left(\rho c_p \frac{\partial T}{\partial t}\right) dy\, dx \qquad \text{see §3.1,}$$

$$= d\int_0^{L_x}\int_0^{L_y} \nabla\cdot(k\nabla T)\, dy\, dx \qquad \text{see §3.1,}$$

$$= d\int_0^{L_x}\int_0^{L_y}\left[\frac{\partial}{\partial x}\left(k\frac{\partial T}{\partial x}\right) + \frac{\partial}{\partial y}\left(k\frac{\partial T}{\partial y}\right)\right] dy\, dx$$

$$= d\int_0^{L_y}\int_0^{L_x}\frac{\partial}{\partial x}\left(k\frac{\partial T}{\partial x}\right) dx\, dy + d\int_0^{L_x}\int_0^{L_y}\frac{\partial}{\partial y}\left(k\frac{\partial T}{\partial y}\right) dy\, dx$$

$$= d\int_0^{L_y}\left[k\frac{\partial T}{\partial x}\right]_0^{L_x} dy + d\int_0^{L_x}\left[k\frac{\partial T}{\partial y}\right]_0^{L_y} dx$$

$$\therefore \qquad \frac{dQ}{dt} = d\int_0^{L_y} -\dot{Q}w \, dy \qquad (7.37)$$

since $\frac{\partial T}{\partial x} = 0$ on $x = 0$, $\frac{\partial T}{\partial y} = 0$ on $y = 0, L_y$ and the rate of heat flow per unit area of the flue wall $\equiv \dot{Q}w = -k\frac{\partial T}{\partial x}$ on $x = L_x$, see §6.2.

Now consider the air. Recall Equation (7.2) that is,

$$\rho f \frac{\partial}{\partial t}(cf_p Tf) + \frac{\dot{m}}{dW}\frac{\partial}{\partial y}(cf_p Tf) = \frac{1}{W}(\dot{Q}w)$$

$$\Rightarrow \qquad \rho f\left(Tf\frac{\partial(cf_p)}{\partial t} + cf_p\frac{\partial Tf}{\partial t}\right) + \frac{\dot{m}}{dW}\frac{\partial}{\partial y}(cf_p Tf) = \frac{1}{W}(\dot{Q}w)$$

$$\Rightarrow \qquad \rho f\left(Tf\frac{d(cf_p)}{dTf}\frac{\partial Tf}{\partial t} + cf_p\frac{\partial Tf}{\partial t}\right) + \frac{\dot{m}}{dW}\frac{\partial}{\partial y}(cf_pTf) = \frac{1}{W}(\dot{Q}w)$$

$$\Rightarrow \qquad \frac{\partial Tf}{\partial t} + \frac{\dot{m}}{dWF(pf)}\frac{\partial}{\partial y}(cf_pTf) = \frac{1}{WF(pf)}(\dot{Q}w) \qquad (7.38)$$

where $F = Tf\frac{d(cf_p)}{dTf} + cf_p$.

As discussed in §7.2, the transient term $\frac{\partial Tf}{\partial t}$ is neglected. Therefore Equation (7.38) becomes

$$\dot{m}\frac{d}{dy}(cf_pTf) = d(\dot{Q}w).$$

Integrating with respect to y gives:

$$\dot{m}\left((cf_pTf)\Big|_{y=Ly} - (cf_pTf)\Big|_{y=0}\right) = d\int_0^{L_y}\dot{Q}w\,dy$$

$$= -\frac{dQ}{dt} \text{ from Equation (7.37)}$$

Therefore $\Delta Qf \approx -\dot{m}\left((cf_pTf)\Big|_{y=L_y} - (cf_pTf)\Big|_{y=0}\right)\Delta t$

$$= -\dot{m}\left((cf_pTf)_{Ny} - (cf_pTf)_1\right)\Delta t \text{ J.}$$

Calculation of ΔQ

Consider an elemental volume V of block, as illustrated in Figure 7.4, centred at mesh point $(i+\frac{1}{2}, j+\frac{1}{2})$, $i = 1$ to $Nx-1$, $j = 1$ to $Ny-1$.

Then $$\Delta Q = \sum_{j=1}^{Ny-1}\sum_{i=1}^{Nx-1} V_{i+\frac{1}{2},j+\frac{1}{2}}\left[(\rho e)^{n+1}_{i+\frac{1}{2},j+\frac{1}{2}} - (\rho e)^{n}_{i+\frac{1}{2},j+\frac{1}{2}}\right]$$

where $V_{i+\frac{1}{2},j+\frac{1}{2}} = \Delta x\,\Delta y\,d\ m^3$ for all i and j, see Figure 7.4,

and $e \equiv$ internal energy per unit mass in J/kg - see §3.1.

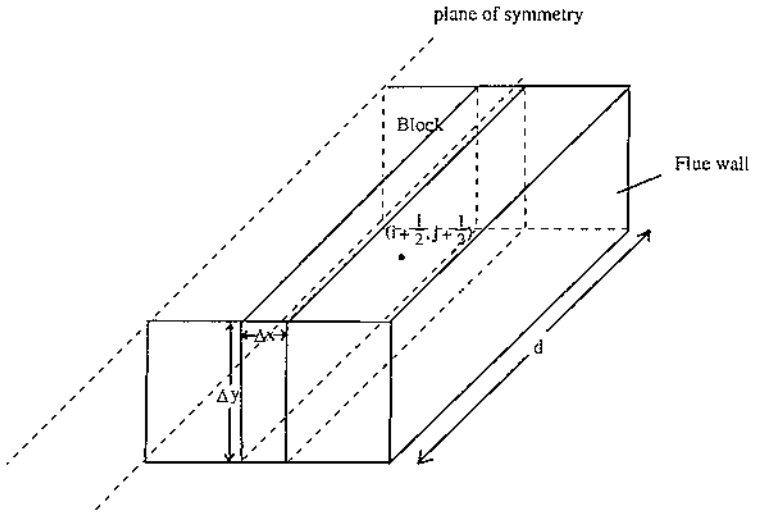

Figure 7.4
Schematic three-dimensional view of the block showing elemental volume V centred at mesh point $(i+\frac{1}{2}, j+\frac{1}{2})$

$\rho = \rho a, \rho p$ or ρw and $e = ea, ep$ or ew depending on whether the calculations are occurring in the anode, packing coke or flue wall. ea, ep and ew are the internal energies per unit mass of the anode, packing coke and flue wall respectively.

Recall from §3.1, that $c_p(T, p) = \frac{\partial h}{\partial T} = \frac{\partial e}{\partial T}$ at constant pressure.

Therefore $e(T, p) = \int_0^T c_p(\tau, p)d\tau + f(p)$ where $f(p)$ is some function of pressure.

If $c_p(0, p)$ is assumed to be zero, then $e(0, p) = f(p)$. Then assuming that $e(0, p) = 0$, gives

$$e(T, p) = \int_0^T c_p(\tau, p)d\tau .$$

Now consider $ca_p = (1.31)\tau + 4.55 \times 10^2$, see Equation (4.3)

Therefore
$$ea = \int_0^T [(1.31)\tau + 4.55 \times 10^2]d\tau$$
$$= \left(\frac{1.31}{2}\right)T^2 + (4.55 \times 10^2)T \text{ J/kg}$$

Similarly $ep = \left(\frac{1.28}{2}\right)T^2 + (5.27 \times 10^2)T$ J/kg

and $ew = 1250\,T$ J/kg

$\Delta Q = \Delta Qa + \Delta Qp + \Delta Qw$

where $\Delta Qa \equiv$ the heat transferred from the anode in time Δt in J,

$\Delta Qp \equiv$ the heat transferred from the packing coke in time Δt in J,

and $\Delta Qw \equiv$ the heat transferred from the flue in time Δt in J.

Consider ΔQa

$$\Delta Qa = (\Delta xa)(\Delta y)d(\rho a)\sum_{j=1}^{Ny-1}\sum_{i=1}^{Nx-1}\left(ea^{n+1}_{q+\frac{1}{2},j+\frac{1}{2}} - ea^{n}_{q+\frac{1}{2},j+\frac{1}{2}}\right)$$

$ea^{n+1}_{q+\frac{1}{2},j+\frac{1}{2}}$ and $ea^{n}_{q+\frac{1}{2},j+\frac{1}{2}}$ can not be easily calculated. They are approximated using the average of ea^{n+1} and ea^{n} calculated at mesh points (q, j), $(q + 1, j)$, $(q, j + 1)$ and $(q + 1, j + 1)$ - see Figure 7.5.

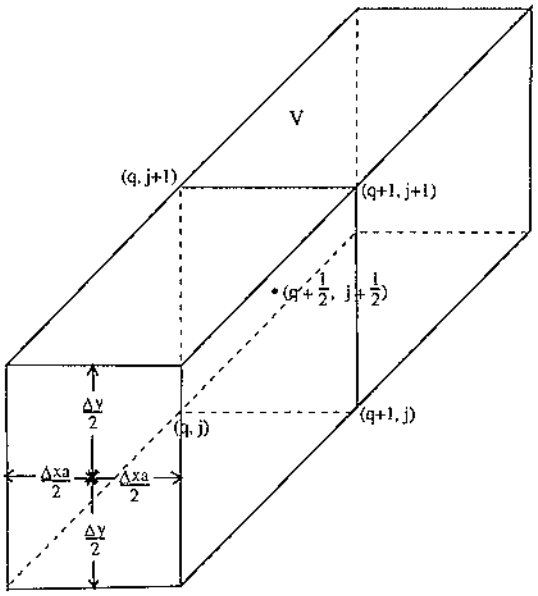

Figure 7.5
A more detailed view of V in the anode showing mesh points
assuming that a blower is operating

$$ea^{n+1}_{q+\frac{1}{2},j+\frac{1}{2}} - ea^{n}_{q+\frac{1}{2},j+\frac{1}{2}} \approx 0.25\left[\left(ea^{n+1}_{q,j} - ea^{n}_{q,j}\right) + \left(ea^{n+1}_{q+1,j} - ea^{n}_{q+1,j}\right) + \left(ea^{n+1}_{q,j+1} - ea^{n}_{q,j+1}\right) + \left(ea^{n+1}_{q+1,j+1} - ea^{n}_{q+1,j+1}\right)\right]$$

$$\text{Therefore } \Delta Qa \approx (\Delta xa)(\Delta y)d(\rho a)(0.25)\left\{\left(ea^{n+1}_{1,1} - ea^{n}_{1,1}\right) + \left(ea^{n+1}_{Nxa,1} - ea^{n}_{Nxa,1}\right) + \left(ea^{n+1}_{1,Ny} - ea^{n}_{1,Ny}\right) + \left(ea^{n+1}_{Nxa,Ny} - ea^{n}_{Nxa,Ny}\right) + 2\left[\sum_{q=2}^{Nxa-1}\left((ea^{n+1}_{q,1} - ea^{n}_{q,1}) + (ea^{n+1}_{q,Ny} - ea^{n}_{q,Ny})\right) + \sum_{j=2}^{Ny-1}\left((ea^{n+1}_{1,j} - ea^{n}_{1,j}) + (ea^{n+1}_{Nxa,j} - ea^{n}_{Nxa,j})\right)\right] + 4\left[\sum_{j=2}^{Ny-1}\sum_{q=2}^{Nxa-1}\left(ea^{n+1}_{q,j} - ea^{n}_{q,j}\right)\right]\right\}$$

Similarly for ΔQp and ΔQw.

7.5 Results

The program requires similar input to the one for the one-dimensional case, but here the air temperature required to be entered is the initial air temperature (for the one-dimensional case, the air temperature was assumed to be constant). As discussed before (see §7.3), the Tf^1_j are chosen to be equal for all j = 2 to Ny, with Tf^n_1 = atmospheric temperature = 20 °C for all n. Also the number of mesh points in the y direction (Ny) has to be entered. The program's output is the transient temperature distribution of the block and of the air in the flue.

The initial block temperatures ($Ta^1_{q,j}$, $Tp^1_{r,j}$, $Tw^1_{s,j}$) are chosen to be 600 °C. The initial air temperatures (Tf^1_j , j = 2 to Ny) are chosen to be 100 °C. Nxa = 15, Nxp = 4, Nxw = 4 and Ny = 160. Mesh point (1, 1) corresponds to x = 0, y = 0; mesh point (1, 160) corresponds to x = 0, y = L_y ; mesh point (21, 1) corresponds to x = L_x , y = 0 and mesh point (21, 160) corresponds to x = L_x, y = L_y . The total number of mesh points is 3360. The computer used for the calculations could not handle too many more than this number of mesh

points. Δxa, Δxp, Δxw and Δy are approximately the same - 0.028 to 0.032 m. The length of the overall time step (Δt) is 20 seconds, as in the one-dimensional case.

Either a blowing or sucking fan is operating, since as has been discussed before (see §2.4), it makes no difference to the temperature profile calculated by this model, as to whether a blower or a sucker is used.

Figures 7.6 and 7.7 show the temperature profile of the block in the x direction at $y = 0$ and $y = L_y$ respectively at 32 hours for various mass flows. Figure 7.8 shows the corresponding temperature profile of the air in the flue at 32 hours for the same mass flows. Similarly for Figures 7.9 - 7.11, except that time is at 64 hours, and for Figures 7.12 - 7.14 except that time is at 96 hours.

The arrows in the figures indicate the mesh points on the anode/packing coke and packing coke/flue wall boundaries.

Heat balance at the flue wall

The percentage difference between ΔQ and ΔQf relative to ΔQ is calculated at the end of each time step. Percentage difference $= \frac{\Delta Q - \Delta Qf}{\Delta Q} \times 100.$

The percentage difference between total ΔQ and total ΔQf relative to total ΔQ is also calculated at the end of each time step. Total ΔQ (in J) is the total heat transferred from the block from $n = 1$ up to the present time. Similarly total ΔQf (in J) is the total heat transferred into the fluid or air from $n = 1$ up to the present time.

Total percentage difference $= \frac{\text{total } \Delta Q - \text{total } \Delta Qf}{\text{total } \Delta Q} \times 100.$ In all cases, even at 96 hours, both the percentage difference and total percentage difference $< 0.5\%$.

7.6 Discussion of results

The temperature profile of the block and of the air in the flue

The results here are very similar to those of the one-dimensional model. As the mass flows increase, the block cools more quickly, and as time goes on and the temperature difference between the block and the air decreases, then so does the

rate of cooling of the block. As before, these results confirm that the set-up of the model and the calculations are correct. For this particular set of initial temperatures, it takes a mass flow of 15 kg/s in order for the anodes to reach approximately 200 $^{\circ}$C at 96 hours. This mass flow compares well with the experimental ones (5.6 kg/s for a blower, 11.3 kg/s for a sucker - see §6.2).

As expected, the temperature of the block in the y direction increases as y goes from 0 to L_y - compare Figures 7.6 and 7.7, Figures 7.9 and 7.10, and Figures 7.12 and 7.13. This is because the air temperature in the flue is also increasing as y goes from 0 to L_y (see Figures 7.8, 7.11 and 7.14). However this vertical (or y) temperature variation of the block is quite small, even for the smallest mass flow of 5 kg/s. This is because the air temperature does not increase greatly above the inlet air temperature (20 $^{\circ}$C), even as the air flows along the flue and gains heat from the block. See Figures 7.8, 7.11 and 7.14. This is even more so as time goes on and less heat is being transferred from the block, due to the block cooling that has already occurred. This is due to the fact that the air is being sucked or blown through the flue at a rate that enables a rapid replacement (especially with larger mass flows) of the air in the flue. Hence, a particular quantity of air is not remaining in the flue long enough for it to gain much heat, and therefore increase in temperature.

The transient variation of the air temperature is quite small and as time goes on, becomes smaller. See Figures 7.8, 7.11 and 7.14. This is consistent with the assumption made in §7.2, that the transient or $\frac{\partial T}{\partial t}$ term in the partial differential equation for the air temperature can be ignored (since the thermal inertia of the air is so much less than that of the block).

Heat balance at the flue wall

The small discrepancy, especially between the cumulative heat given out by the block and the cumulative heat transferred into the fluid, indicates that the calculations in the block and air are correctly related and quite accurate.

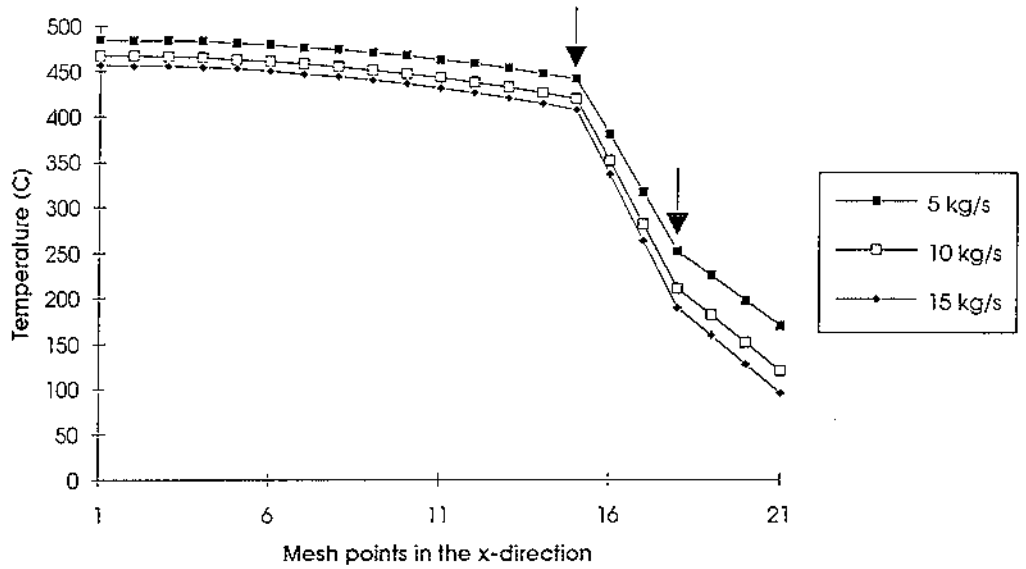

Figure 7.6
Temperature profile of the block (y = 0) at 32 hours (1 fire cycle)

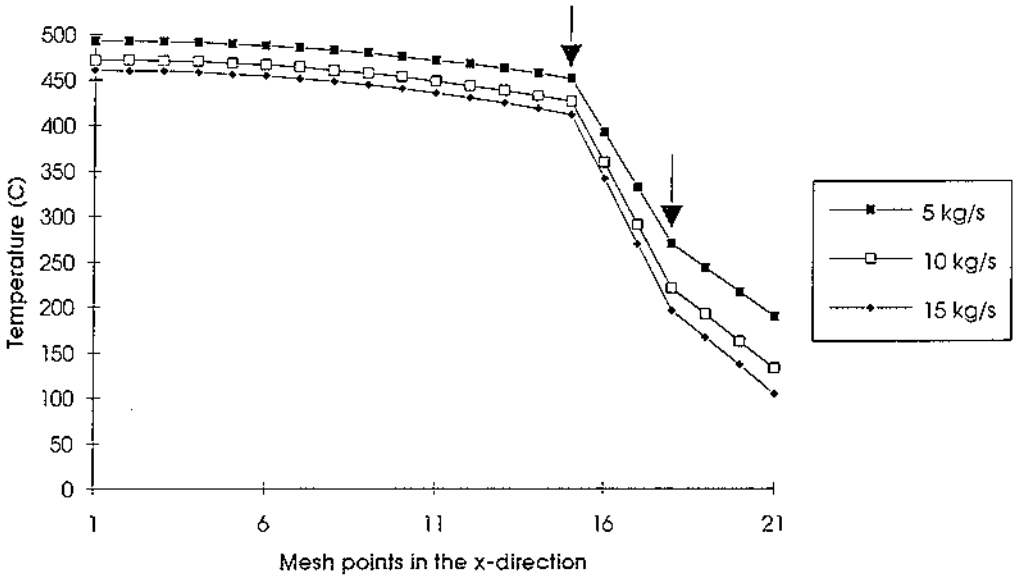

Figure 7.7
Temperature profile of the block ($y = L_y$) at 32 hours

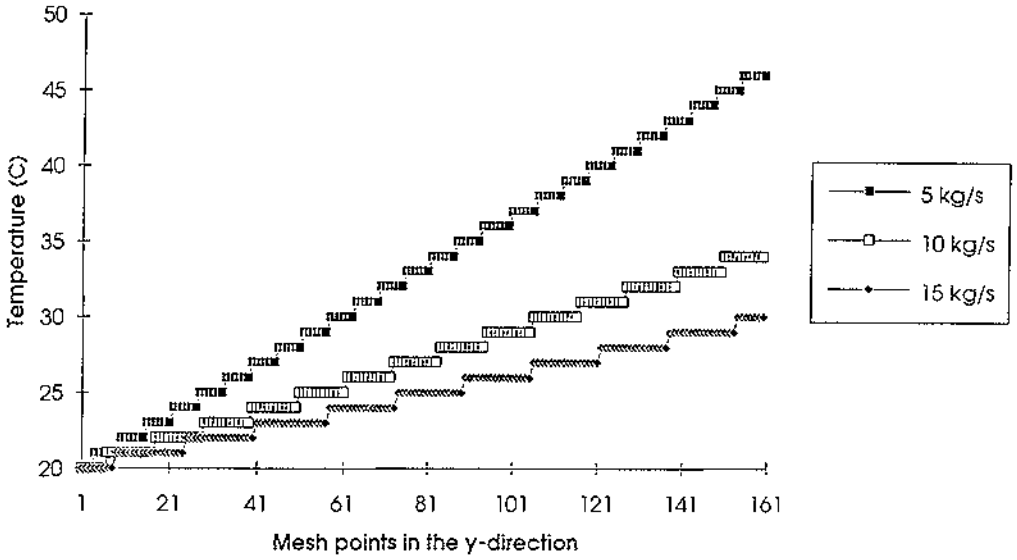

Figure 7.8

Temperature profile of the air in the flue at 32 hours

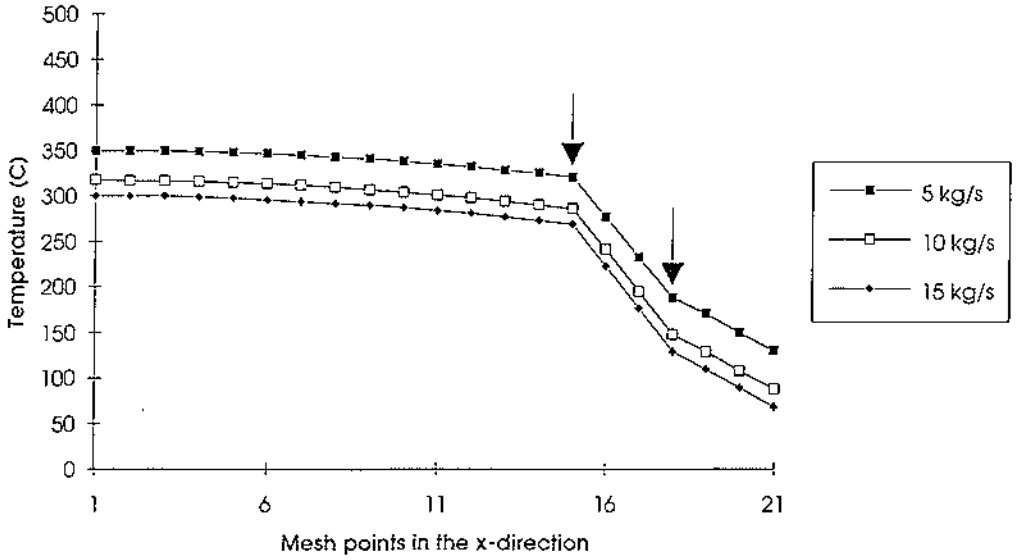

Figure 7.9

Temperature profile of the block (y = 0) at 64 hours (2 fire cycles)

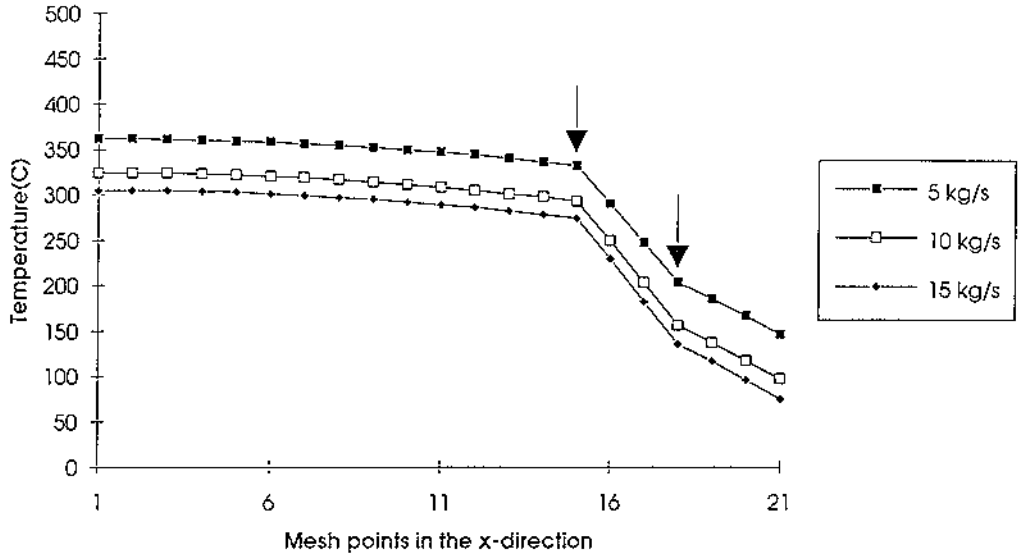

Figure 7.10
Temperature profile of the block ($y = L_y$) at 64 hours

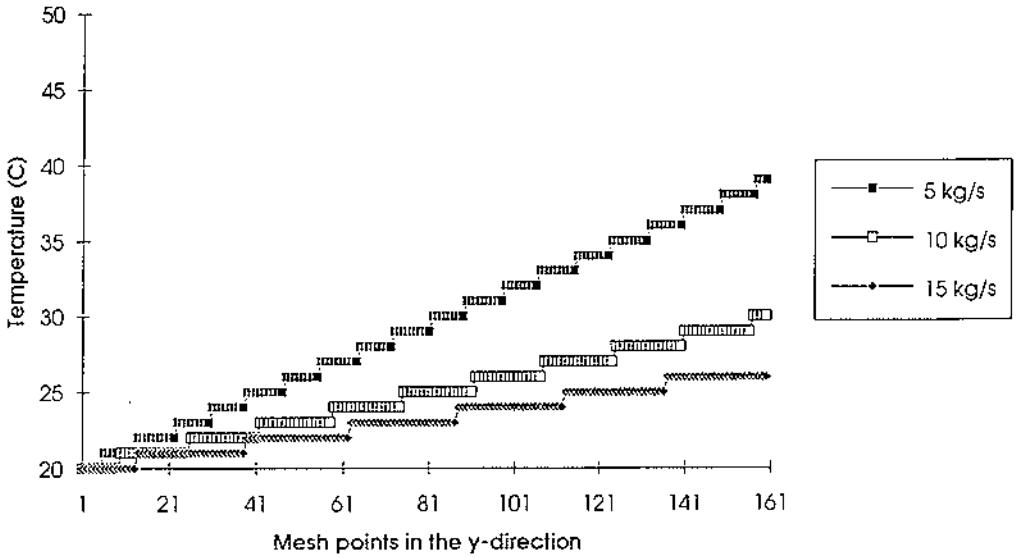

Figure 7.11
Temperature profile of the air in the flue at 64 hours

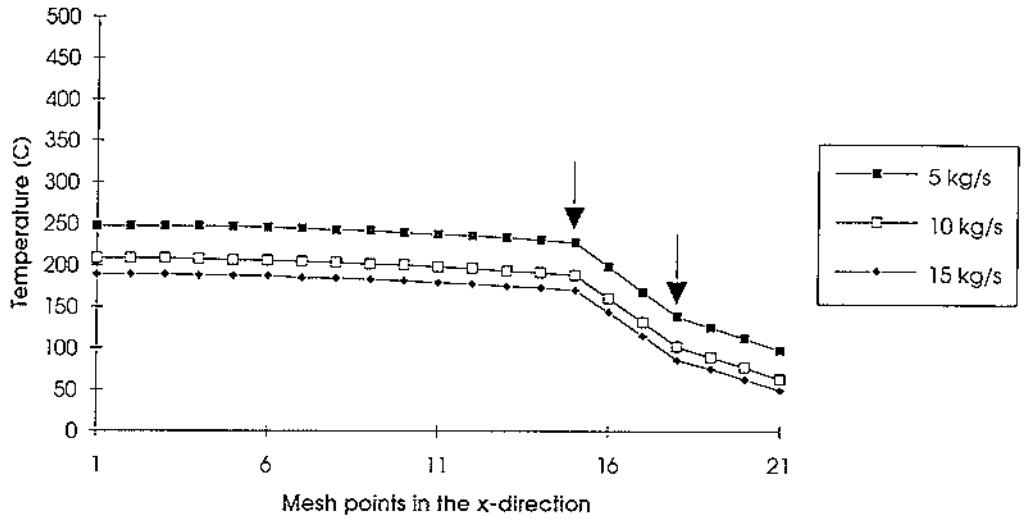

Figure 7.12
Temperature profile of the block (y = 0) at 96 hours (3 fire cycles)

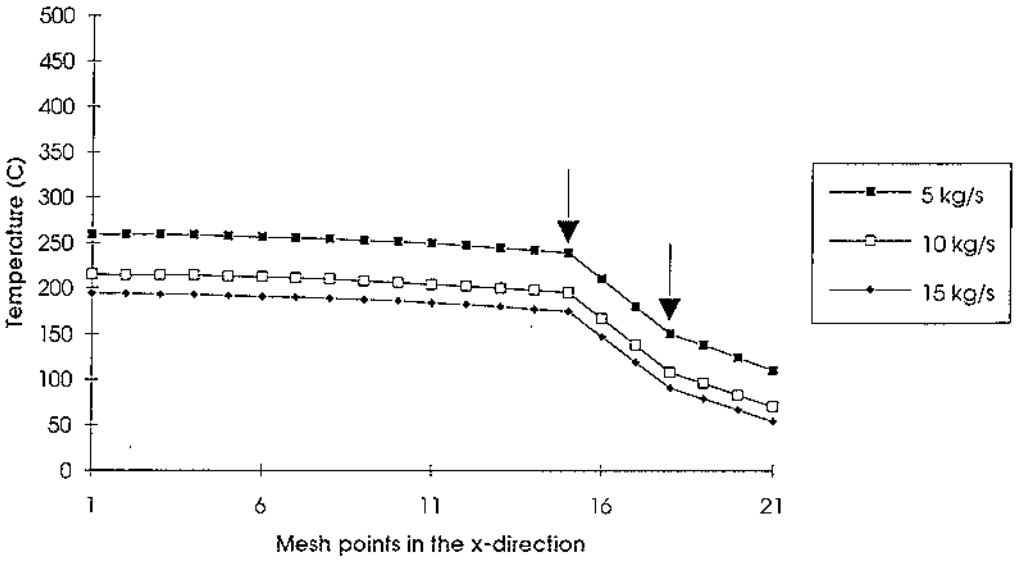

Figure 7.13
Temperature profile of the block (y = L_y) at 96 hours

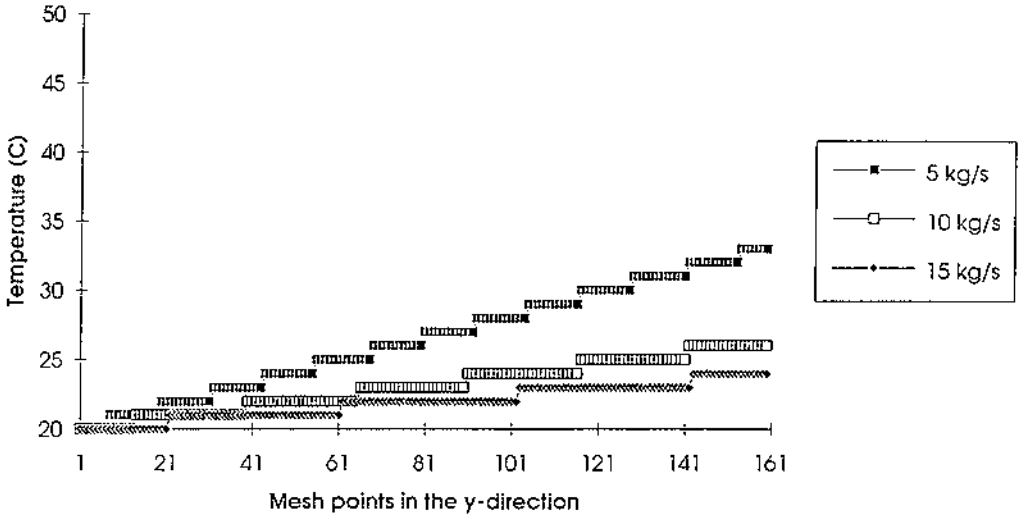

Figure 7.14

Temperature profile of the air in the flue at 96 hours

CHAPTER 8 THE AIR PRESSURE IN A SECTION

8.1 Introduction

The pressure in the flues and fire shafts is investigated. It is assumed that the spaces between the bottom of the anode/flue walls and the foundation, and in the gallery are so large, that the air flowing through them does not experience any change in pressure.

8.2 Calculation of the pressure

From McKibbin (private communication, 1993)

$$\Delta p = -\lambda \frac{\Delta y\,(\rho f)v^2}{2\ell} \qquad (8.1)$$

where $\Delta p \equiv$ the change in pressure of the air in N/m^2

and $\lambda \equiv$ the friction factor (dimensionless).

Since $(\rho f)v = \frac{\dot{m}}{\text{area}}$, then $v^2 = \left(\frac{\dot{m}}{\rho f \times \text{area}}\right)^2$

So Equation (8.1) becomes $\frac{\Delta p}{\Delta y} = \frac{-\lambda \times \text{perimeter} \times \dot{m}^2}{8 \times (\text{area})^3 \times \rho f}$ (8.2)

If $\frac{\Delta p}{\Delta y}$ is approximated by $\frac{\partial p}{\partial y}$ and $\frac{\partial p}{\partial y}$ is approximated by using a forward difference formula, then

$$\frac{\Delta p}{\Delta y} \approx \frac{\partial p}{\partial y} \approx \frac{p(y+\Delta y,\, t) - p(y,\, t)}{\Delta y}$$

$$= \frac{p^n_{j+1} - p^n_j}{\Delta y} \text{ in subscript/superscript notation.}$$

j and n are defined as before, $j = 1$ to Ny, $j, n \in \mathbb{Z}^+$ and the error of the left hand side is of order Δy.

$\lambda = \lambda(\mathrm{Re}, \frac{\varepsilon}{\ell})$ is the friction factor.

$\mathrm{Re} = \mathrm{Re}(y, t)$ is the Reynolds number.

ε is the roughness of the bricks used in the flue and fire shaft walls and is estimated as 1.65×10^{-3} m.

$\rho f = \rho f(Tf)$ and using values obtained from Haywood (1968), a linear approximation for ρf is obtained, using the points $(373, 9.46 \times 10^{-1})$ and $(973, 3.63 \times 10^{-1})$ - see Figure 8.1.

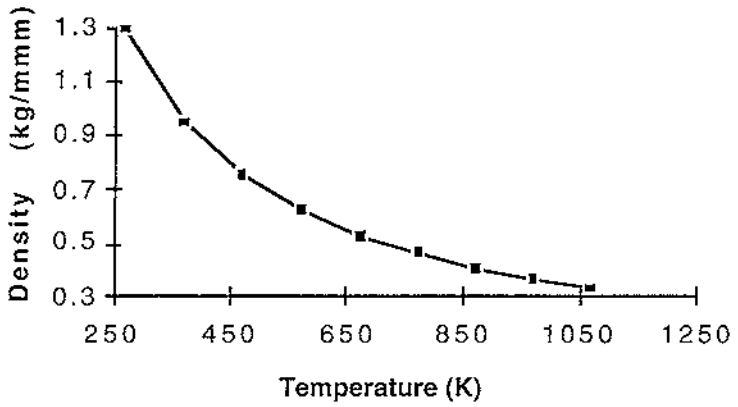

Figure 8.1
Density of air at 1 atmosphere [interpolated from data from Haywood (1968)]

$$\rho f = (-9.72 \times 10^{-4})\, Tf + 1.31 \text{ kg/m}^3$$

So Equation (8.2) becomes

$$p_{j+1}^{n} = \frac{-\lambda_j^n \times \Delta y \times \text{perimeter} \times \dot{m}^2}{8 \times (\text{area})^3 \times \rho f_j^n} + p_j^n$$

λ_j^n is given by the Churchill equation,

$$\lambda_j^n = 8\left[\left(\frac{8}{Re_j^n}\right)^{12} + \left(A_j^n + B_j^n\right)^{-3/2}\right]^{\frac{1}{12}},$$

$$A_j^n = \left\{2.457\ \ell n\left[\left(\frac{7}{Re_j^n}\right)^{0.9} + 0.27\ \frac{\varepsilon}{\ell}\right]\right\}^{16}$$

$$= \left\{2.457\ \ell n\left[\left(\frac{7}{Re_j^n}\right)^{0.9} + \frac{0.27 \times 1.65 \times 10^{-3} \times \text{perimeter}}{4 \times \text{area}}\right]\right\}^{16},$$

$$B_j^n = \left(\frac{37530}{Re_j^n}\right)^{16}$$

The mass flow, perimeter and area are different depending on whether the calculations are occurring in the fire shaft or flue. See §6.2 for the discussion on mass flows, and Figures 2.1 and 2.3 respectively for fire shaft and flue dimensions.

Blower

In this case, the inlet pressure at time step n is at the top of the fire shaft - see Figure 8.2. If pfs_j^n is defined to be the air pressure in the fire shaft at mesh point j (j = 1 to Ny) at time step n, then pfs_1^n is the inlet pressure at time step n. Since the pressure difference across a blower is 200 N/m^2 then

$$pfs_1^n = (\text{atmospheric pressure} + 200)\ \text{N/m}^2$$
$$= (101325 + 200)\ \text{N/m}^2$$
$$= 101525\ \text{N/m}^2\ (\text{or Pa})$$

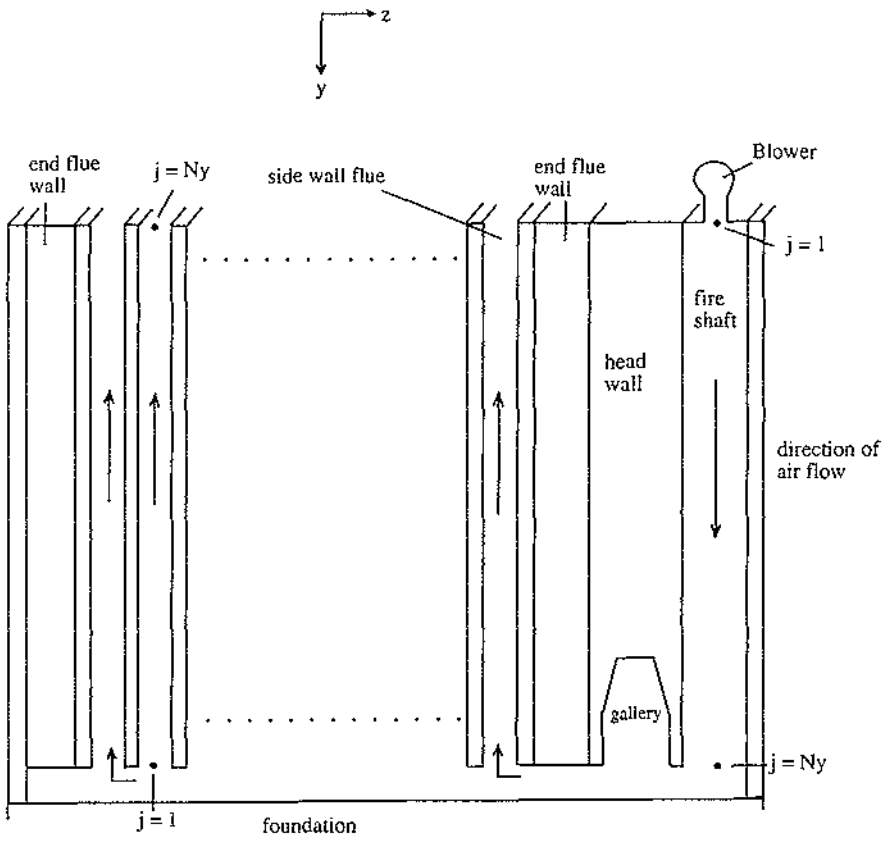

Figure 8.2
Schematic longitudinal view of a flue wall showing air flow direction for a blower and the layout of mesh points

The pressure at the bottom of the fire shaft at time step n, pfs^n_{Ny}, is used as the inlet pressure for the flue, since it is being assumed that there are no pressure changes occurring in the gallery or in the area between the foundation and the bottom of the anode/flue walls. That is, $pfl^n_1 = pfs^n_{Ny}$, where pfl^n_1 is the air pressure in the flue at mesh point 1 at time step n.

The temperature of the air along the fire shaft (j = 1 to Ny) is assumed to be the same as the inlet air temperature for the flue, Tf^n_1 (20 °C for all n, see §2.4). The density of air and the friction factor are functions of temperature.

Sucker

This case is the reverse of the previous one. The inlet air pressure at time step n is at the top of the flue - see Figure 8.3. pfl_j^n is defined to be the air pressure in the flue at mesh point j (j = 1 to Ny) at time step n. pfl_1^n = atmospheric pressure = 101325 N/m^2.

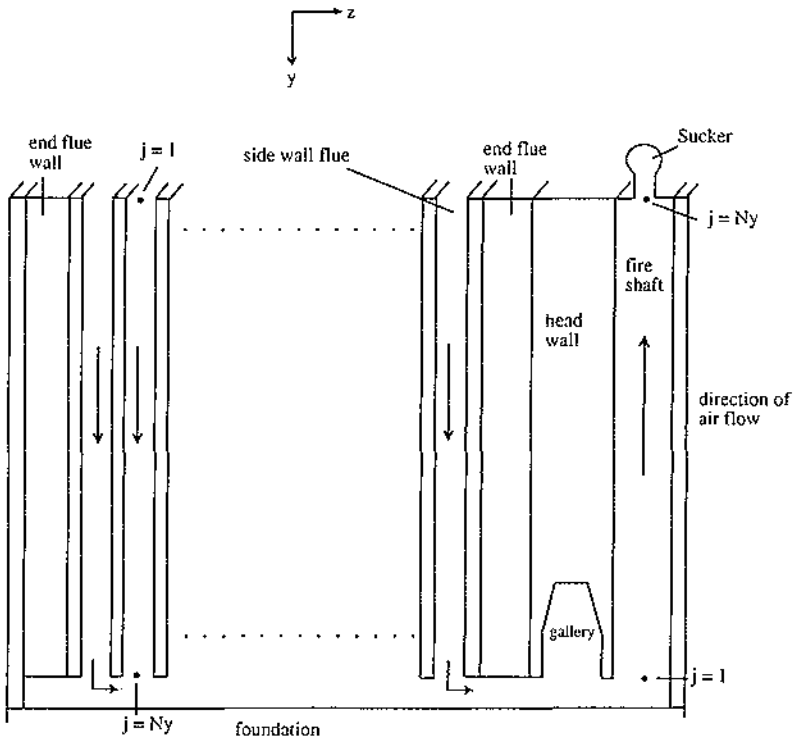

Figure 8.3
Schematic longitudinal view of a flue wall showing air flow direction for a sucker and the layout of mesh points.

The pressure at the bottom of the flue, pfl_{Ny}^n, is used as the inlet pressure for the fire shaft, since it is being assumed that there are no pressure changes occurring in the area between the foundation and the bottom of the anode/flue walls or in the gallery. That is, $pfs_1^n = pfl_{Ny}^n$.

In this case the temperature of the air along the fire shaft (j = 1 to Ny) is assumed to be the same as the outlet air temperature for the flue, Tf_{Ny}^n. This outlet air temperature varies with time, so the air temperature along the fire

shaft also varies with time. This contrasts with the blower case, where the air temperature along the fire shaft remains constant with respect to time.

8.3 Results

The program has exactly the same input as the one that outputs the two-dimensional temperature distribution of the block and the temperature distribution of the air in the flue - see §7.5. The output for here is the one-dimensional transient pressure distribution in the fire shaft and flue.

Figures 8.4 and 8.5 show the pressure distribution at 32 and 96 hours respectively for various mass flows when a blower is operating. Similarly Figures 8.6 and 8.7 show the pressure distribution at 32 and 96 hours respectively for various mass flows when a sucker is operating. The arrows in the figures indicate where the flue ends and the fire shaft begins. The flue mesh points are to the left of the arrow and the fire shaft mesh points are to the right of the arrow. The blower and sucker are positioned as shown.

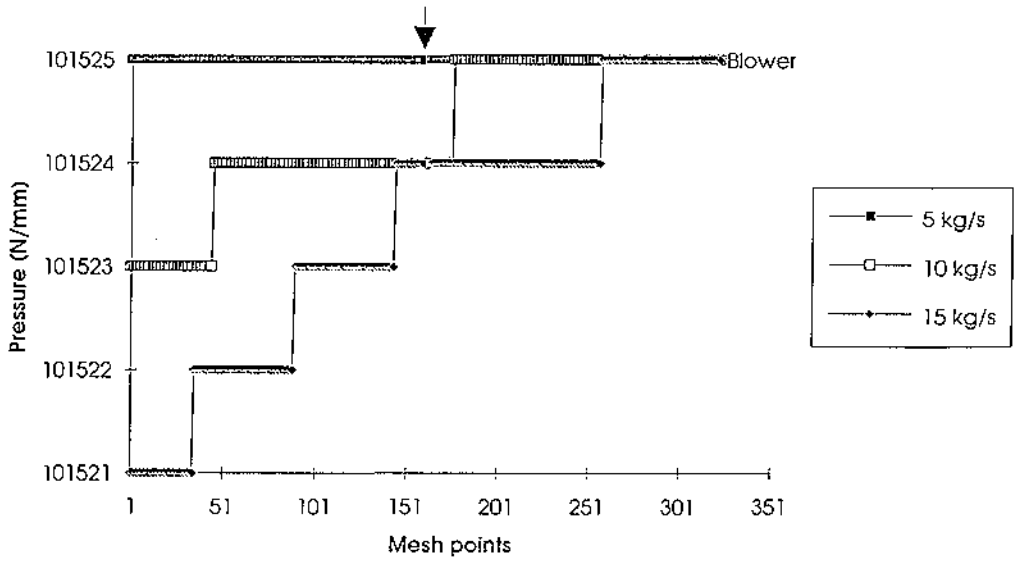

Figure 8.4
Air pressure profile for a blower at 32 hours (1 fire cycle)

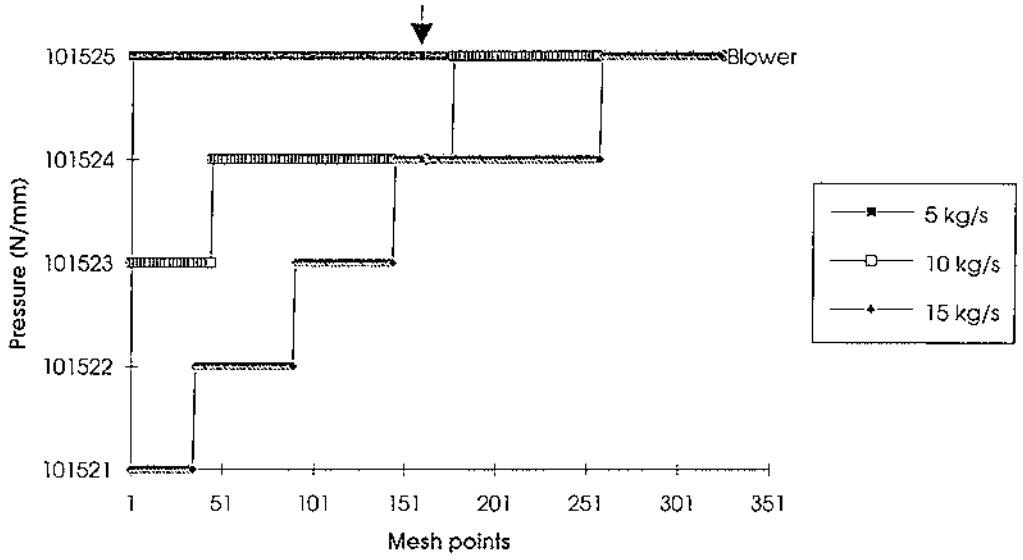

Figure 8.5
Air pressure profile for a blower at 96 hours (3 fire cycles)

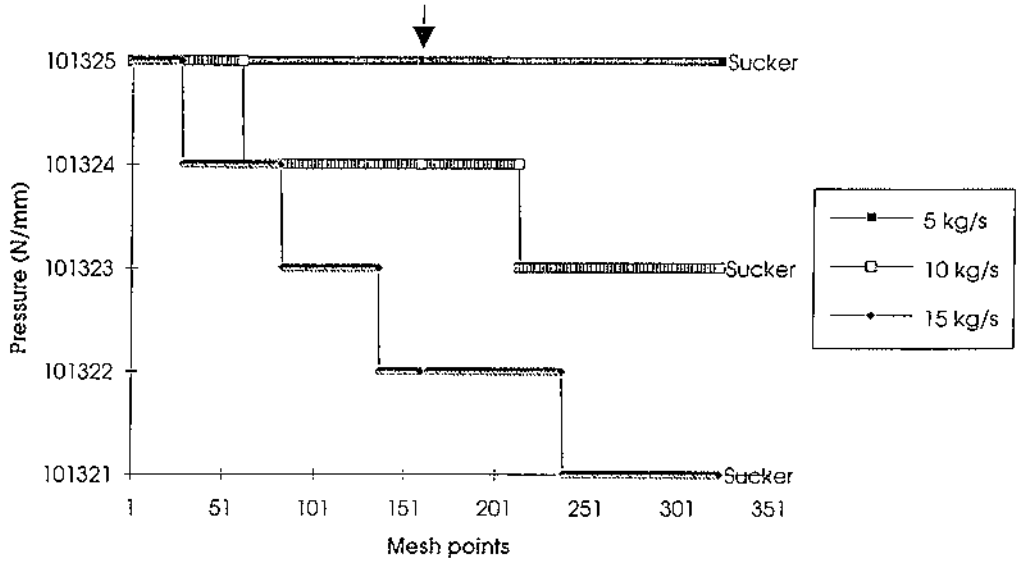

Figure 8.6
Air pressure profile for a sucker at 32 hours

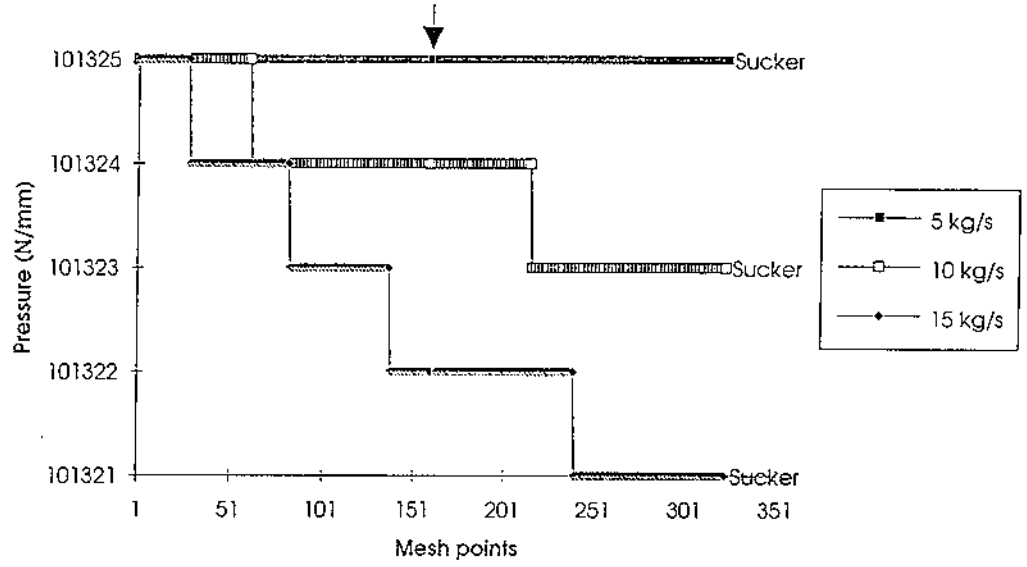

Figure 8.7
Air pressure profile for a sucker at 96 hours

Figures 8.8, 8.9 and 8.10 compare the pressure distribution for a blower versus a sucker at 96 hours, for mass flows of 5, 10 and 15 kg/s respectively.

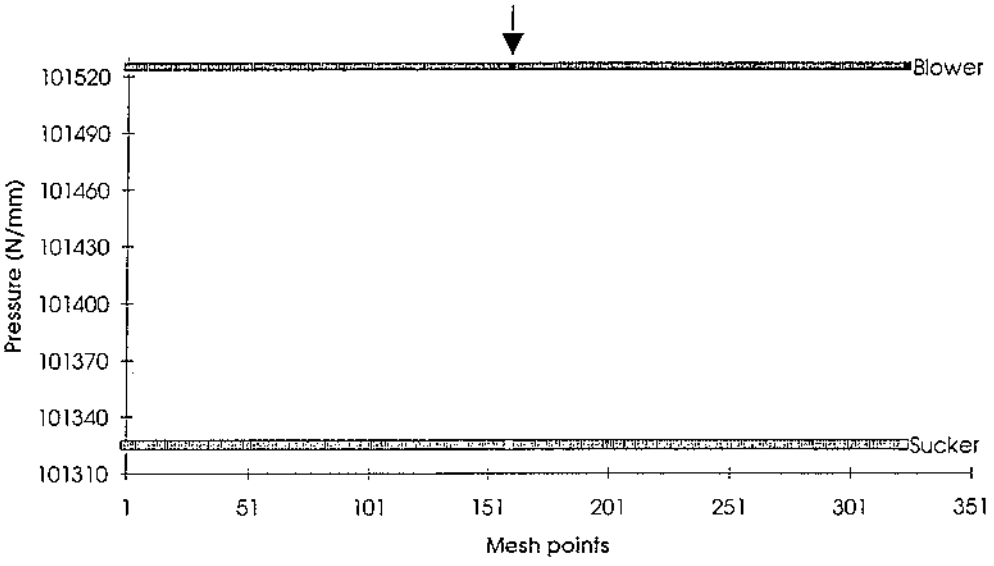

Figure 8.8
Air pressure profile for a blower versus a sucker at 96 hours
for $\dot{m} = 5$ kg/s

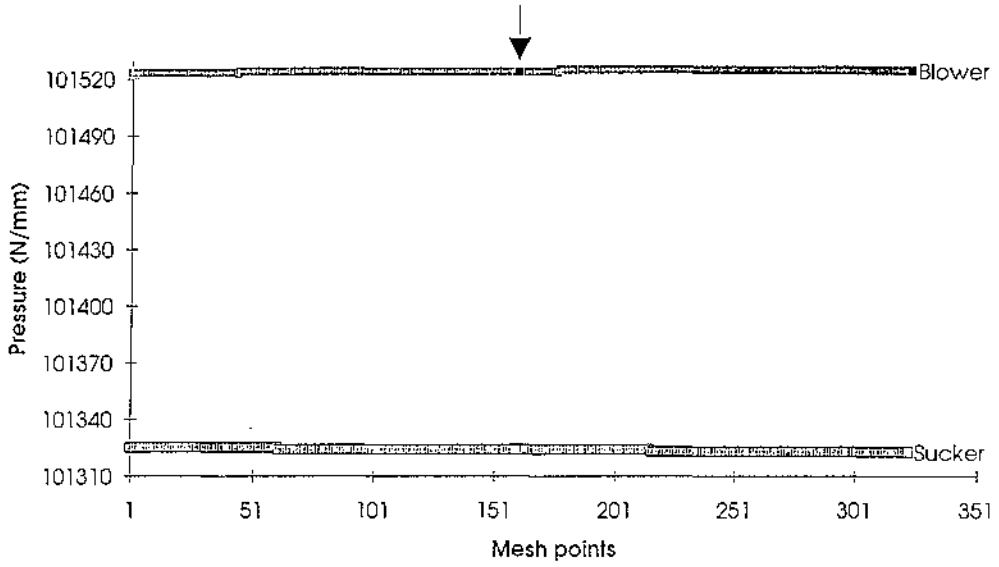

Figure 8.9
Air pressure profile for a blower versus a sucker at 96 hours
for $\dot{m}$=10 kg/s

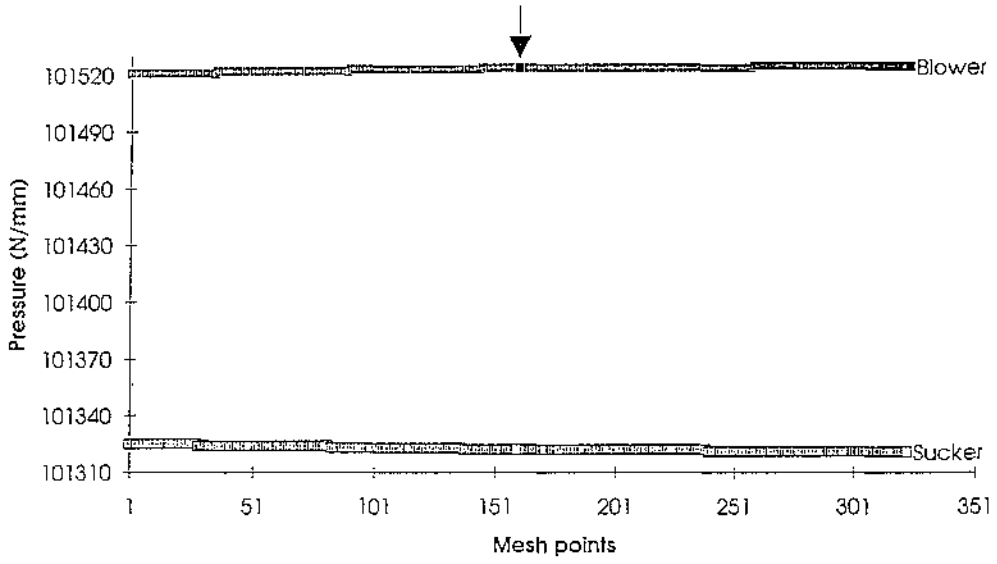

Figure 8.10
Air pressure profile for a blower versus a sucker at 96 hours for
$\dot{m}$ = 15 kg/s

8.4 Discussion of results

As expected, the air pressure decreases as the distance from the blower increases or as the distance from the sucker decreases. These results confirm that the set-up of the model and the calculations are correct. For both sucker and blower, the larger the mass flows are, then the larger the pressure drop along the flue and fire shaft. For $\dot{m} = 5$ kg/s there is no pressure drop for all cases. The pressure difference along the flue is larger than that along the fire shaft for both sucker and blower.

The spatial and transient air temperature changes in the flue are small, see §7.5 - Figures 7.8, 7.11 and 7.14, and in particular the changes in Tf^{n}_{Ny} are small for all n. Since in the case of a sucker, the air temperature along the fire shaft is assumed to be Tf^{n}_{Ny}, then the air temperature in the fire shaft does not change much with time. (Recall that for a blower, the air temperature along the fire shaft is assumed to be 20 °C for all time.) Hence it would be expected that the spatial and transient pressure changes would be small for a given mass flow for both a sucker and a blower, since in this model the pressure is a function of temperature as well as mass flow. This is the case - compare Figures 8.4, 8.5 and Figures 8.6, 8.7.

Note the symmetry between the pressure distribution for a blower versus a sucker in Figures 8.8, 8.9 and 8.10. This is due to the fact that for the two-dimensional model, the air temperature distribution in the flue for a blower is the reverse of that for a sucker. Also the assumed air temperatures in the fire shaft for a blower and a sucker are approximately equal, especially as n gets bigger (that is, as time goes on).

CHAPTER 9 SUMMARY AND CONCLUSION

9.1 Introduction

This thesis has been concerned with the mathematical modelling of the cooling of carbon anodes used in the aluminium industry. The effects of different mass flows of air on the block temperature, the air temperature in the flues and the air pressure in the flues and fire shafts have been studied. The three-dimensional problem was modelled by simplifying it to one and two dimensions. These simplifications were made by using the fact that the flues, flue walls and anodes zone of a section is the most important one for anode cooling, and by assuming that the only heat transfer from the block is into the air in the flues. All other boundaries were assumed to be adiabatic. These assumptions were justified by dimensional considerations. The problem, therefore, was to solve the heat equation with the appropriate boundary conditions.

The one-dimension heat equation was solved analytically, but determining the exact form of the boundary condition on the flue wall was a problem. Numerical methods were then used to successfully calculate the one- and two-dimensional temperature distributions in the block and the one-dimensional temperature distribution of the air in the flue. The thermal conductivities within the anode, packing coke and flue wall were assumed to be constant for all time. All other thermal properties, which were assumed to be dependent on temperature, varied over time as the temperature distribution changed. Having non-constant thermal conductivities results in non-linear terms in the equations. This would have proved difficult, even in the one-dimensional case, when solving for the temperatures of the mesh points on the anode/packing coke, packing coke/flue wall and flue wall/flue boundaries.

9.2 One-dimensional model

A forward difference (explicit) method was used to calculate the transient temperature distribution in the block. The air temperature in the flue was assumed to be constant. Heat balances were done at the anode/packing coke, packing coke/flue wall and flue wall/flue boundaries in order to calculate the temperatures at the mesh points on these boundaries. It was found that as the mass flows increased, the rate of cooling of the block increased. The results

also showed that as time went on and the temperature difference between the block and the air decreased, then the rate of cooling of the block also decreased. These results confirmed that the set-up of the model and the calculations were correct. For the particular chosen initial block and air temperatures (600 ^{o} C and 20 ^{o}C respectively), a mass flow that was similar to the experimental ones was required, in order to cool the anodes so that they could be safely removed from the pits after 96 hours (3 fire cycles).

9.3 Two-dimensional model

This case was very similar to the one-dimensional case, except that here the air temperature in the flues was not constant, but changing with time and space as heat was transferred into the air from the block. The air temperature along the flue was calculated using relaxation - an implicit numerical method. The two-dimensional heat equation for the block was solved using a forward difference method similar to that used for the one-dimensional case. The results were similar to those obtained in the one-dimensional case.

As a check on the working, the heat transferred from the block was equated with the heat transferred into the air in the flue. A small discrepancy ($< 0.5\%$) was found, even cumulatively after 96 hours, which showed that the calculations in the block and air were correctly related and quite accurate.

9.4 Air pressure

The transient one-dimensional air pressure distributions in the flue and fire shaft were calculated using a forward difference method. The spaces in the gallery and between the bottom of the anode/flue walls and the foundation were assumed to be sufficiently large, so that air flowing through them did not change in pressure. This enabled the pressure distribution in the flue to be linked with that in the fire shaft. The temperature in the fire shaft was assumed to be atmospheric temperature in the case of a blower, and the flue outlet air temperature in the case of a sucker.

The results gave pressure distributions that were appropriate for a blower and a sucker. For both a sucker and a blower, the pressure drop along the flue and fire shaft increased as the mass flows increased. Also the larger pressure drop occurred in the flues for both sucker and blower.

9.5 Conclusion

The models presented in this thesis enable the transient one- and two-dimensional temperature distributions in the anodes, packing coke and flue wall part of a forced cooling section to be calculated for various mass flows of air in the flues. The transient one-dimensional air temperature distribution in the flues, and the transient one-dimensional air pressure distribution in the flues and fire shafts are also calculated for various mass flows. It would have been good to have some experimental temperature data to compare with the results obtained from the models. However for the chosen initial temperatures, the mass flow used by the models to cool the anodes to the appropriate temperature, is very close to the experimental mass flows. The next step in improving the models would be to solve the heat equation with non-constant thermal conductivities, that is, allowing the thermal conductivities of the anode, packing coke and flue wall to vary with temperature, as was done for the other thermal properties. Other improvements might include having boundary conditions at the bottom and top of the pits that allow for the fact that heat is also lost from the block across these boundaries.

REFERENCES

Bajpai, A.C., Calus, I.M. and Fairley, J.A. (1977) Numerical methods for engineers and scientists. John Wiley and Sons, Great Britain.

Bourgeois, T., Bui, R.T., Charette, A., Sadler, B.A. and Tomsett, A.D. (1990) Computer simulation of a vertical ring furnace. *Light Metals*, 547 - 552.

Bui, R.T., Charette, A., Bourgeois, T. and Dernedde, E. (1987) Performance analysis of the ring furnace used for baking industrial carbon electrodes. *Canadian Journal of Chemical Engineering*, 65, 96 - 101.

Bui, R.T., Peter, S., Charette, A., Tomsett, A.D. and Potocnik, V. (1992) Reidhammer furnace : Underlid heat transfer analysis. *Light Metals*, 731 - 738.

Burden, R.L. and Faires, J.D. (1989) Numerical analysis. Fourth edition. PWS-Kent Publishing Co., Massachusetts.

Currie, I.G. (1993) Fundamental mechanics of fluids. Second edition. McGraw-Hill Inc., Toronto.

de Fernández, M.E., Marletto, J. and Martirena, H. (1983) Combined mathematical simulation and experimental studies on a closed baking furnace. *Light Metals*, 805-817.

Furman, A. and Martirena, H. (1980) A mathematical model simulating an anode baking furnace. *Light Metals*, 545 - 552.

Haywood, R.W. (1968) Thermodynamic tables in SI (metric) units. Cambridge University Press, Cambridge.

Holman, J.P. (1986) Heat transfer. Sixth edition. McGraw-Hill Book Co., U.S.A.

Log, T. and Oye, H.A. (1990) Thermal conductivity of prebaked anodes. *Light Metals*.

O'Neil, P.V. (1991) Advanced engineering mathematics. Third edition. Wadsworth Publishing Co., California.

Perry, R.H., Green, D.W. and Maloney, J.O. (editors) (1984) Perry's chemical engineers' handbook. McGraw-Hill Book Co., U.S.A.

Rogers, G.F.C. and Mayhew, Y. (1992) Engineering thermodynamics, work and heat transfer. Fourth edition. Longman Group, United Kingdom.

Thibault, M.A., Bui, R.T. Charette, A. and Dernedde, E. (1985) Simulating the dynamics of the anode baking ring furnace. *Light Metals*, 1141 - 1151.